



**Alasmariya Islamic University
Faculty of Science
Department of Chemistry**

The Green synthesis of gold nanoparticles of papaya leaf extract as a cytotoxic agent in breast cancer

Submitted by: Salima Mohammed Ahmed Farhat

**Supervised by: Prof. Adel Mohamed Mlitan
Professor of Biochemistry at Misurata University**

**Co-Supervised by: Dr. Ali Mohammed ALhalib
Assistant Professor of Organic Chemistry at Alasmariya University**

**This thesis serves as a partial completion of the criteria needed to
earn a Master of Science in Chemistry, specialty of biochemistry.**

Academic year (2025)



الجامعة الإسلامية
كلية العلوم
قسم الكيمياء

التوليف الأخضر لجسيمات الذهب النانوية لمستخلص أوراق البابايا كعامل سمي لموت الخلايا في سرطان الثدي

إعداد الطالبة: سليمة محمد أحمد فرحات

تحت إشراف: عادل محمد مليطان
أستاذ كيمياء حيوية جامعة مصراتة
مشرف مشارك: د. علي محمد الهليب
أستاذ مساعد كيمياء عضوية بالجامعة الإسلامية

قدمت الرسالة استكمالاً لمتطلبات الإجازة العلمية (ماجستير) في علوم الكيمياء

العام الجامعي (2025)



قرار لجنة مناقشة رسالة الإجازة العالية (الماجستير)

عملا بقرار السيد/ رئيس الجامعة رقم (570) لسنة 2025 م، الصادر في 06 / 08 / 2025م، القاضي بتشكيل لجنة لمناقشة رسالة علمية للحصول على درجة الإجازة العالية (الماجستير) في تخصص الكيمياء المقدمة من الطالبة : سليمة محمد فرحات ، كلية العلوم وعنوانها:

(التوليف الأخضر لجسيمات الذهب النانوية لمستخلص أوراق البابايا كعامل سمي لموت الخلايا في سرطان الثدي)

وتتكون اللجنة من الاساتذة:

- | | | |
|---------------|-----------------------------|----------------------------|
| مشرفا ومقررا. | الجامعة: مصراتة | 1. أ.د. عادل محمد مليطان |
| مشرفا ثانيا | الجامعة: الاسمرية الاسلامية | 2. د. علي محمد الهليب |
| عضوا داخليا. | الجامعة: الاسمرية الاسلامية | 3. د. سليمة علي المبروك |
| عضوا خارجيا. | الجامعة: مصراتة | 4. ا.د. حنان الصادق الضراط |

عقدت اللجنة جلسة علنية علي تمام الساعة: العاشرة من صباح يوم: الخميس الموافق: 18 / 09 / 2025م، بقاعة الاجتماعات بالكلية لمناقشة الرسالة و تقويم مستواها العلمي و المنهج الذي اتبعته الباحثة و المصادر التي استخدمتها في دراستها، وقررت ما يلي:

بعد اتمام الطالبة: سليمة محمد فرحات لمتطلبات الدراسات العليا واجتياز امتحاناتها ومناقشة رسالتها و تقويمها تقرر: اجتيازها بدون ملاحظات

توقيعات أعضاء لجنة المناقشة:

- | | | |
|----------------|-----------------------------|----------------------------|
| التوقيع: | الجامعة: مصراتة | 1. أ.د. عادل محمد مليطان |
| التوقيع: | الجامعة: الاسمرية الاسلامية | 2. د. علي محمد الهليب |
| التوقيع: | الجامعة: الاسمرية الاسلامية | 3. د. سليمة علي المبروك |
| التوقيع: | الجامعة: مصراتة | 4. ا.د. حنان الصادق الضراط |

يعتمد:

رئيس الجامعة



بعد من عشرة (10) نسخ



Declaration

I Salima Mohammed Ahmed Farhat confirm that work contained in this thesis / dissertation, unless otherwise referenced is the researcher is own work, and has not been previously submitted to meet requirements of an award at this University or any other higher education or research institution, I furthermore, cede copyright of this thesis / dissertation iv favour of University of Tripoli.

Student's name:.....

Signature:.....

Date: / / 20

الإقرار

أقر أنا سليمة محمد أحمد فرحات بأن ما اشتملت عليه الرسالة إنما هو نتاج جهدي الخاص، باستثناء ما تمت الإشارة إليه حيثما ورد، وأن هذه الرسالة ككل أو أي جزء منها لم يقدم من قبل لنيل درجة علمية، أو بحث علمي لدى أي مؤسسة تعليمية أو بحثية أخرى، وللجامعة حق توظيف الرسالة أو الأطروحة والاستفادة منها مصدرا مرجعيا للمعلومات، لأغراض الاطلاع أو الإعارة أو النشر بما لا يتعارض وحقوق الملكية الفكرية المقررة بالتشريعات النافذة.

التوقيع:-----

التاريخ:-----/-----/20م

Abstract

This study investigates the green synthesis of gold nanoparticles (AuNPs) using *Carica papaya* leaf extract and evaluates their anticancer potential against MCF-7 breast cancer cells. The AuNPs were characterized using UV-visible spectroscopy, X-ray diffraction (XRD), transmission electron microscopy (TEM), atomic force microscopy (AFM), dynamic light scattering (DLS), zeta potential analysis, scanning electron microscopy (SEM), and Fourier transform infrared spectroscopy (FTIR) and the *Carica papaya* leaf extract was analyzed using chromatography-mass spectrometry (GC-MS). The synthesized AuNPs exhibited a characteristic surface plasmon resonance peak at 558.6 nm, with predominantly spherical morphology and sizes ranging from 20.3 to 61.0 nm. FTIR analysis confirmed the presence of phytochemicals from *C. papaya* leaf extract as capping agents, Gas chromatography-mass spectrometry analysis of the papaya leaf extract revealed a complex phytochemical profile with isopropyl tetradecanoate as a major component, which is likely to play a key role in the green synthesis of gold nanoparticles. The AuNPs demonstrated potent cytotoxicity against MCF-7 cells with an IC₅₀ value of 22.09 ± 0.33 $\mu\text{g/mL}$. Flow cytometry analysis revealed that the AuNPs induced cell cycle arrest at the G1/S phase and significantly increased apoptosis. Molecular docking studies suggested strong interactions between the AuNPs and the HER2-HER3-NRG1 beta complex. Additionally, the AuNPs exhibited notable antioxidant activity in the DPPH radical scavenging assay. These findings highlight the potential of green-synthesized AuNPs using *C. papaya* leaf extract as a promising Nanotherapeutic agent for breast cancer treatment, warranting further investigation into their molecular mechanisms and in vivo efficacy.

Keywords: Green synthesis; Gold nanoparticles; *Carica papaya*; MCF-7 breast cancer; Anticancer activity; Antioxidant properties; Apoptosis; Cell cycle arrest; Phytochemicals; Nanotechnology.

Dedication

To my beloved parents, who sowed the seeds of aspiration in my heart and showered me with unending love and care, whose presence was a beacon of light that lighted my path and whose support kept me upright at every turn...

To my beloved brothers, the joyous lights that illuminated my life, and my traveling companions who were there for me at every turn.

I want to express my gratitude to my beloved hubby, who has always been there for me and supported me through every trial and tribulation. I appreciate your unwavering encouragement and belief in me, even at the most trying times.

To my darling kid, the source of my happiness, I dedicate this letter to let you know that you were the driving force behind my progress and this achievement.

The greatest teachers and mentors I ever had were my esteemed professors, who never skimmed on their expertise or counsel.

To my friends, partners in challenges and dreams, who helped to make my academic journey filled with love and wonderful memories.

Acknowledgments

Al Praise be to Allah, by whose grace good deeds are accomplished, and by whose grace difficulties are overcome.

I would like to extend my sincere thanks and appreciation to my first supervisor, Dr. Adel Mohammed Mlitan, who helped me during my scientific journey by sharing his expertise and experience and being a wonderful guide and support.

I would also like to express my deep gratitude to Dr. Ali Mohammed Al-Hulaib, my second supervisor, whose assistance and guidance greatly enhanced this effort. I owe him my sincere gratitude and admiration because his experience and useful criticism greatly influenced the development and quality of the research.

I would also like to express my gratitude to Dr. Wissam Al-Kallab and Dr. Mukhtar Abu Rizeza, who inspired and taught me during my studies and worked to greatly enhance my knowledge and skills.

I would also like to express my deep gratitude to my family who have always been by my side, supporting me with prayers and encouragement. I can never express how grateful I am to my husband, child, mother, father and siblings; you have been and continue to be a wonderful source of love, support and encouragement.

I would also like to express my gratitude to my friends Amina Al-Fulus and Salima Wali, who supported me during my research journey. Finally, I would like to thank everyone who contributed to the success of this work, whether with a word, advice or encouragement, asking God Almighty to reward them with the best reward.

Salima

Table of contents

No	Content	Page
	Declaration	I
	Abstract	II
	Dedication	III
	Acknowledgments	IV
	Table of Contents	V
	List of Tables	IX
	List of Figures	X
	List of Abbreviations	XII
	المخلص	I
Chapter One: Introduction & Literature Review		
1.1	Green synthesis of nanoparticles	1
1.1.1	Definition of green synthesis and its importance?	1
1.1.2	Green synthesis's benefits for medicinal applications	1
1.2	Nanoparticles: Characteristics and Uses	2
1.2.1	What Nanoparticles Are?	2
1.2.2	Historical overview	4
1.2.3	Synthesis of nanoparticles	6
1.2.4	Methods for producing nanomaterials	6
1.2.5	Classification of Nanoparticles	8
1.2.6	Properties of Nanoparticles	9
1.2.6.1	Mechanical Characteristics	9
1.2.6.2	Electrical Characteristics	10
1.2.6.3	Characteristics of Biology	10
1.3	Gold molecules	10
1.3.1	Gold nanoparticles	11
1.3.2	Gold nanoparticle shapes	12
1.3.3	Nanoparticle Characterization	12

1.3.4	Gold nanoparticle applications in the medical domain	13
1.4	Chemical makeup and biological activities of <i>Carica papaya</i> leaf extract	14
1.4.1	Vitamin content in papaya fruit	17
1.4.2	The chemical makeup of leaves (enzymes, flavonoids, and phenolics).	17
1.4.2.1	Phenolic substances	17
1.4.2.2	Flavonoid chemicals	17
1.4.2.3	Enzymatic activity	18
1.4.3	<i>Carica papaya</i> leaf extract's bioactivity	18
1.4.3.1	Anthelmintic action	18
1.4.3.2	Antiangiogenic characteristics	19
1.4.3.3	Antimicrobial and antioxidant properties	19
1.4.3.4	Fungicidal activity	19
1.5	Phenolic Compounds	19
1.6	Flavonoids	21
1.6.1	Flavonoid classification	22
1.7	Cancer	24
1.7.1	benign tumors	25
1.7.2	Cancerous Growths	25
1.8	Definition, biological processes, and current therapies for breast cancer	26
1.8.1	definition	26
1.8.2	The study of epidemiology	26
1.8.3	Risk variables	26
1.8.3.1	Genetic variables	26
1.8.3.2	Factors related to reproduction	26
1.8.3.3	Hormonal variables	27
1.8.3.4	Aspects of lifestyle	27
1.8.4	Clinical characteristics	28
1.8.5	Pathophysiology	29
1.8.6	Treatment for Breast Cancer	29

1.8.7	Mechanisms of biology	32
1.8.8	The biological processes that lead to breast cancer.	32
1.9	Using Nanotechnology to Treat Breast Cancer	32
1.9.1	Mechanism of cancer cell suppression by gold nanoparticles.	34
1.10	Literature Review	36
1.1	Objectives	38
Chapter Two: Experimental Work		
2.1	Materials	39
2.2	Equipment	39
2.3	Methods	39
2.3.1	Green Synthesis of Gold Nanoparticles (AuNPs)	39
2.3.1.1	Plant Material Preparation	39
2.3.1.2	Extract Preparation	40
2.1.1.3	AuNP Synthesis	40
2.3.2	Characterization of AuNPs	40
2.3.2.1	UV-Visible Spectroscopy	40
2.3.2.2	X-Ray Diffraction (XRD)	40
2.3.2.3	Fourier Transform Infrared Spectroscopy (FTIR)	40
2.3.2.4	Transmission Electron Microscopy (TEM)	41
2.3.2.5	Atomic Force Microscopy (AFM)	41
2.3.2.6	Scanning Electron Microscope (SEM)	41
2.3.2.7	Dynamic Light Scattering (DLS) and Zeta Potential	41
2.3.2.8	Gas Chromatography-Mass Spectrometry (GC-MS) Equipment	42
2.3.2.9	Molecular Docking	42
2.3.3	Antioxidant Activity Assessment	43
2.3.3.1	DPPH Radical Scavenging Assay	43
2.3.4	In Vitro Anticancer Activity	43
2.3.4.1	Cell Culture	43
2.3.4.2	MTT Assay	43
2.3.5	Flow Cytometry Analysis	44

2.3.5.1	Cell Cycle Analysis	44
2.3.5.2	Apoptosis Assay	44
2.3.6	Statistical Analysis	44
Chapter Three: Results and Discussion		
3.1	Characterization of Gold Nanoparticles	45
3.1.1	X-Ray Diffraction (XRD) Analysis	45
3.1.2	UV-Visible Spectroscopy	46
3.1.3	Fourier Transform Infrared Spectroscopy (FTIR)	48
3.1.4	Transmission Electron Microscopy (TEM) Analysis	51
3.1.5	Atomic Force Microscopy (AFM) Analysis	52
3.1.6	Scanning Electron Microscopy (SEM)	54
3.1.7	Dynamic Light Scattering (DLS) and Zeta Potential Analysis	55
3.1.8	Gas Chromatography-Mass Spectrometry (GC-MS) Analysis of <i>Carica papaya</i> Leaf Extract	57
3.1.9	Molecular Docking Study	62
3.1.9.1	Molecular Dynamics Simulation	62
3.2	Antioxidant Activity	64
3.2.1	DPPH Radical Scavenging Activity Results and Discussion	64
3.3	Anticancer Activity Against MCF-7 Breast Cancer Cells	66
3.4	Flow Cytometry Analysis	67
3.4.1	Cell Cycle Analysis	67
3.4.2	Apoptosis Analysis	69
Chapter Four: Conclusions and Recommendations		
4.1	Conclusions	72
4.2	Recommendations	73
	References	74
	Appendices	83

List of Tables

No	Table	Page
1	Shows the chemical and physical properties of gold	11
2	Flavonoids with some plant species and their biological sources	23
3	Major compounds identified in <i>Carica papaya</i> leaf extract by GC-MS analysis	59
4	Docking Scores and hydrogen bonding of the 3 isopropyl tetradecanoate molecules conjugated with gold NP (IPTD- GnP) on specific selected breast cancer marker proteins	63
5	DPPH radical scavenging activity of green-synthesized gold nanoparticles at different concentrations	64
6	Cytotoxicity of AuNPs against MCF-7 breast cancer cells	66
7	DNA Content Analysis of MCF-7-positive breast cancer cells treated with green-synthesized AuNPs	68
8	Apoptosis Stages in MCF-7-positive breast cancer cells treated with green-synthesized AuNPs	69

List of Figures

No	Figure	Page
1	Types of nanoparticles.	3
2	Nanoparticles have clinical relevance. Numerous therapeutic indications (black text) have been authorized for organic and inorganic nanoparticles, and more indications (red text) are being explored in ongoing clinical research.	4
3	Different methods for NPs synthesizing	6
4	Methods for preparing nanoparticles Top - Bottom, Bottom – Top	7
5	Different types of AuNPs	12
6	Shows a cartoon showing several techniques for adding and removing medicinal compounds from gold nanoparticles	13
7	Shows the shape of the leaves of the papaya <i>Carica</i>	15
8	Shows a papaya fruit	16
9	Structural formula of salicylic acid	17
10	Papain enzyme structure	18
11	Structural formula of phenols	19
12	Types of immunotherapies for breast cancer	31
13	Mechanism of action of nanoparticles against cancer cells	35
14	XRD pattern of green-synthesized AuNPs	45
15	UV-Visible absorption spectrum of green-synthesized gold nanoparticles	46
16a	Illustrated FTIR pattern before gold nanoparticles	49
16b	Illustrated FTIR of AuNPs green synthesis	50
17	TEM micrographs of green-synthesized AuNPs high magnification	51
18	AFM (a) 3D topographic image of green-synthesized AuNPs	52
18	AFM (b) 2D rendered image of green-synthesized AuNPs	53
19	Illustrated SEM images of AuNPs	55
20	DLS curve of green-synthesized AuNPs high magnification	56
21	Zeta potential distribution of green-synthesized AuNPs	57
22	Total Ion Chromatogram (TIC) of <i>Carica papaya</i> leaf extract	58
23	(a)Mass spectrum of the peak at retention time 44.09 minutes	59
23	(b)Mass spectrum of the peak at retention time 44.09 minutes, identified as isopropyl tetradecanoate	60

24	The molecule's lengthy hydrocarbon chain adheres to the surface of freshly generated gold nanoparticles.	60
25	Illustrated meocluer docking of AuNPs green synthesis	63
26	Illustrated 3 isopropyl tetradecanoate molecules conjugated with gold NP (IPTD-GnP) on specific selected breast cancer marker protein complex	64
27	Dose-response curve of AuNPs against MCF-7 breast cancer cells	67
28	Cell cycle distribution of control and AuNP-treated MCF-7-positive breast cancer cells	69
29	Apoptosis stages in control and AuNP-treated MCF-7-positive breast cancer cells	70

List of Abbreviation

Symbol	Abbreviation
Abraxane	Paclitaxel Nanoparticle
AD	Anno Domini
AFM	Atomic Force Microscopy
AHRS	Aryl Hydrocarbon Receptor
Annexin V-FITC/PI	Annexin Violet-Fluorescein Isothiocyanate/ Propidium Iodide
ANOVA	Analysis of Variance
ATCC	America Type Culture Collection
AuNPs	Gold Nanoparticles
Å	Angstrom
BC	Breast Cancer
BCT	Breast Conserving Therapy
BRC1	Breast Cancer Gene1
BRC2	Breast Cancer Gene2
BRC3	Breast Cancer Gene3
BRIP1	BRCA1-Interacting Protein 1
C°	Celsius
CCNB1	Cyclin B1
CDK1	Cyclin-Dependent Kinase 1
CHEK2	Checkpoint Kinase 2
CPLE	<i>Carica Papaya</i> leaf Extract
CRLX101	Camptothecin Nanoparticle
DLS	Dynamic Light Scattering
DMEM	Dulbecco's Modified Eagle's Medium
DMSO	Dimethyl Sulfoxide
DNA	Deoxyribonucleic Acid
Doxil	Doxorubicin Liposomal

DPPH	1,1-Diphenyl-2-picrylhydrazyl
EV	Electron Volt
FBS	Fetal Bovine Serum
Feraheme	Ferumoxytol
FTIR	Fourier Transform Infrared
G1/S	GAP1/ Synthesis
GAE/Kg	Grams of Gallic Acid Equivalent per Kilogram).
GC-MS	Gas Chromatography-Mass Spectrometry
GNPs	Gold Nanoparticles
GSH/GSSG	Glutathione disulfide
g/cm³	Grams/Centimeter
g/mol	Grams/mol
HAuCl₄	Hydrogen Tetrachloroaurate OR Chloroauric Acid
HER2	Human Epidermal Growth Factor Receptor 2
HER3	Human Epidermal Growth Factor Receptor 3
HR	Human Resources
HRTEM	High-Resolution Transmission Electron Microscopy
IBM	International Business Machines
IC50	Inhibitory Concentration
IPTD	Isopropyl Tetra Decanoate
IV	Intravenous
Kcal	Kilocalorie
Kg	Kilograms
IPTD-GnP	Isopropyl Tetra Decanoate Conjugated with Gold Nanoparticles
KV	Kilovolt
MA	MilliAmpere
MCF-7	Michigan Cancer Foundation-7
MD	Molecular Dynamics
Min	Minute
µg/ ml	Microgram/Millimeter

MM	MilliMoles
Mol	Mole
MTOP	Mechanistic Target of Rapamycin).
MTT	(3-(4,5-Dimethylthiazol-2-yl)-2,5-diphenyltetrazolium bromide)
MV	Megavolt
NF1	Neurofibromatosis
NF-KB.11	Nuclear Factor kappa-light-chain-enhancer of activated B cells
NM	NanoMeter
NMs	Nanomaterials
NNI	National Nanotechnology Initiative
NRG1	Neuregulin1
PALB2	partner and localizer of BRCA2
PBS	Phosphate-Buffered Saline
PDB	Protein Data Bank
PDB ID	Protein Data Bank Identifier
PH	Potential Hydrogen
PI	Propidium Iodide
PI3K	Phosphatidylinositol 3-kinase
PKM2	Pyruvate Kinase M2
PTEN	Phosphatase and Tensin Homolog
RNA	Ribonucleic Acid
RNase A	Ribonuclease A
ROS	Reactive Oxygen Species
SD	Standard Deviation
SEER	Surveillance, Epidemiology, and End Results
SEM	Scanning Electron Microscope
SKBR3	Stanford, Karyotype, Breast, Radiation 3
SPR	Surface Plasmon Resonance
STK11	Serine/Threonine Kinase 11
TEM	Transmission Electron Microscopy

TIC	Total Ion Chromatogram
TNBC	Triple Negative Breast Cancer
TOP2A	Topoisomerase II Alpha
UCSF	University of California San Francisco
UV-Visible	Ultraviolet- Visible
VEGFR1-2	Vascular Endothelial Growth Factor Receptor 1-2
X-ray	X-Ray Radiation
XRD	X-Ray Diffraction
λ	Wavelength

Chapter One

Introduction

1.1 Green synthesis of nanoparticles

1.1.1 Definition of green synthesis and its importance

Because it is less expensive, produces less pollution, and enhances human health and environmental safety, green synthesis is superior to conventional chemical synthesis. Various techniques, including physical, chemical, and biological processes, are used to create metallic nanoparticles in both top-down and bottom-up approaches. The properties of nanoparticles are verified by a variety of instrumental analyses, including atomic force microscopy (AFM) scanning electron microscopy (SEM), transmission electron microscopy (TEM) Fourier transform infrared spectroscopy (FTIR), ultraviolet-visible (UV-Vis) spectroscopy, and X-ray diffraction (XRD). The main conclusions highlight the complexity of plant composition and regional and seasonal distribution, where green synthesis is constrained by production location and time, as well as issues with low yield and purity, green synthesis, however, presents different growth opportunities and possible uses in light of the pollution and environmental issues currently linked to chemical synthesis. (1)

1.1.2 Green synthesis's benefits for medicinal applications

Utilizing eco-friendly and sustainable processes, green synthesis techniques employ biomolecules, microbes, and plant extracts as stabilizing and reducing agents. In addition to being a safer and more environmentally friendly option than traditional synthesis techniques, these techniques also provide researchers the chance to change the characteristics of nanomaterials to improve their ability to treat cancer.

By using green technology, environmental pollution may be decreased and time-consuming, complicated processes can be eliminated. The diagnosis and treatment of illnesses like cancer are greatly aided by techniques based on the encapsulation of medications or other agents and their targeted delivery to cancer cells. These techniques are utilized as highly effective diagnostic probes, tissue engineering, catalytic applications, intercellular biosensors, enzyme immobilization, etc. The creation of safe and efficient anticancer nanomaterials is greatly promising when green synthesis techniques are combined with cutting-edge nanotechnology.

(2)

1.2 Nanoparticles: Characteristics and Uses

1.2.1 Nanoparticles

Because of their potential and adaptability to solve worldwide research issues in energy, water and sanitation, medicine, agriculture, materials science, and cosmetics, nanomaterials (NMs) have acquired significance in the twenty-first century. Richard Feynman's adage, "There's plenty of room at the bottom," first appeared in 1959 as a flexible and adaptable framework that may offer economical and ecologically responsible answers to the sustainability problems confronting humanity. Materials with sizes between one and one hundred nanometers are referred to as nanomaterials. Nanomaterials have special qualities that may be adjusted to fit their needs because of their size and high surface area. Furthermore, a nanomaterial's reactivity, endurance, and other characteristics are influenced by its size, shape, and unique structure. These characteristics make these materials attractive options for a variety of commercial and household applications, including as energy, medicinal, environmental, imaging, cosmetics, and catalysis. (3)

According to its definition, nanotechnology is an advanced technology that is founded on the study and comprehension of basic sciences and nanoscience. It offers the technological capacity to produce nanomaterials and regulate their internal structure by reorganizing and rearranging atoms and molecules to guarantee the creation of unique and distinctive products. The lengths of extremely small objects that are only visible under an electron microscope are measured in nanometers. The sizes, measurements, complicated material molecules, and tiny particles like bacteria and viruses are all expressed in this unit.

The manipulation of matter at the atomic, molecular, and supramolecular scales is known as nanotechnology. The technical objective of accurately modifying atoms and molecules to create macroscale products—also known as molecular nanotechnology—is the oldest and most comprehensive definition of nanotechnology. The National Nanotechnology Initiative subsequently created a broader definition of nanotechnology, defining it as the manipulation of materials having at least one dimension between 1 and 100 nm.

The definition has evolved from a particular technological objective to a research category that encompasses all forms of research and techniques that address the unique properties of matter that occur below a certain size threshold, reflecting the importance of quantum mechanical effects in this range of the quantum world. As a result, the word "nanotechnology" is frequently

used to describe a broad variety of studies and applications that have similar size characteristics. (4)

When compared to materials made of big particles, nanostructured materials have special qualities. This is because they have intriguing chemical, electrical, and magnetic capabilities due to their composition of nanoscale components. One of the most prominent of these characteristics is that, as a result of quantum size effects, nanoparticles have a higher mechanical strength than their traditional solid-structure counterparts. It is also known that nanomaterials may take on a variety of forms, including spherical particles and carbon nanotubes. Low density, strong electrical resistance, and corrosion resistance are characteristics of these materials etc... as in the figure (1). (5)

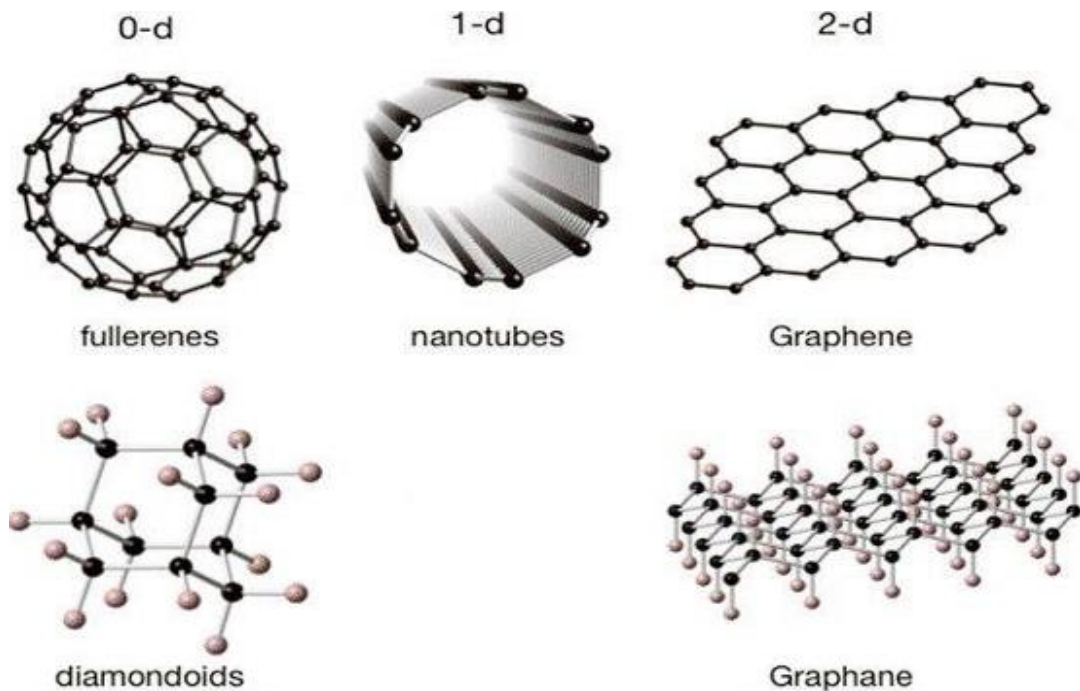


Figure 1: Types of nanoparticles.

Nanotechnology's fundamental units are nanoparticles. They exhibit distinct behavior from matter on a large scale. The many types of nanoparticles are as follows: inorganic (such as magnetic nanoparticles, noble metal nanoparticles like "silver"), organic (such as carbon nanoparticles like "fullerenes"), and semiconductor (such as "zinc oxide"). (6)

As seen in Figure (2), inorganic nanoparticles have already received approval for imaging applications and the treatment of anemia. They have also demonstrated success in preclinical

studies and are currently being developed in the clinic for a range of applications, such as thermal ablation of tumors and sentinel lymph node imaging during surgery. (7)

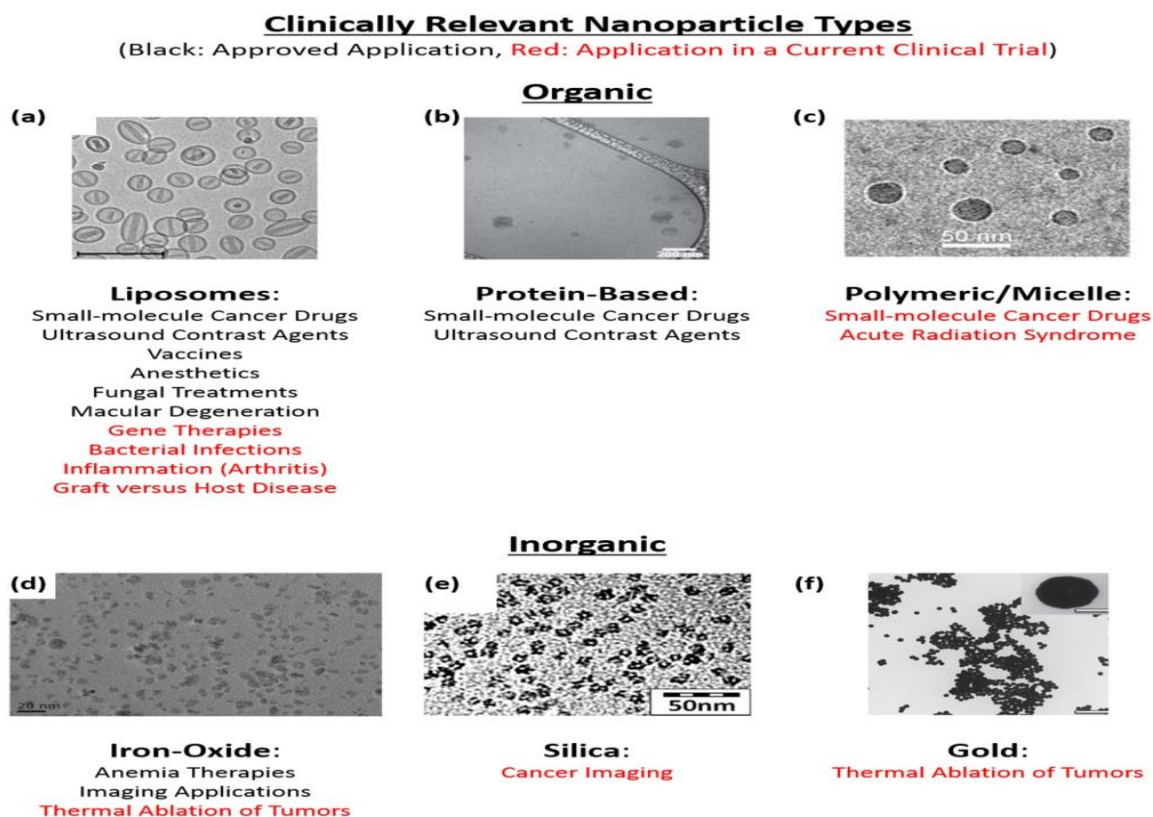


Figure 2: Nanoparticles have clinical relevance. Numerous therapeutic indications (black text) have been authorized for organic and inorganic nanoparticles, and more indications (red text) are being explored in ongoing clinical research. Among the examples are (a) Doxil (side bar 200 nm), (b) Abraxane (scale bar 200 nm), (c) CRLX101 (scale bar 50 nm), (d) Feraheme (scale bar 20 nm), and (e) an early version of Cornell Dots (scale bar 50 nm) and (f) are seen in Gold nanoshells (inset: 100 nm scale bar, main figure: 1000 nm scale bar) from Nano spectra, the company that makes AuroLase.

1.2.2 Historical overview:

In the Middle Ages, nanotechnology was employed without glassmakers realizing its significance. They painted wood, like the violin made by the "Astra Divari" family, which has been preserved to this day thanks to paints containing nanoparticles, and they used colloidal gold nanoparticles for coloring. This was in 1711 AD. (8)

The notion of manipulating atoms and molecules originated from a thought experiment called "Maxwell's Demon" that was carried out by "James Maxwell" in 1867AD.

AD 1959 Richard Feynman was the one who created the idea of nanotechnology.

1974 AD In a study submitted to the University of Tokyo, the word "nanotechnology" was first used. According to the research, technology is the process of employing a single atom or molecule to prepare, separate, and combine materials.

1976 AD The Arab scientist "Munir Yafeh" was able to provide an answer to "Richard's" query and make his vision a reality by founding a business that specialized in producing nanodevices and their extremely limited applications.

The technological business IBM was named after the invention of the scanning tunneling microscope in 1981 AD, which could work directly with atoms and molecules and take pictures of them.

In 1986 AD, the renowned mathematician "Eric Drexler" wrote a book named "Engines of Formation" that is regarded as the true beginning of nanotechnology research. In it, he discussed the fundamentals and workings of molecular nanotechnology.

The Japanese scientist "Sumiie Igami" made the discovery of what are now known as carbon nanotubes in 1991 AD, and this discovery was crucial to the production of nanotechnology and equipment. (8)

The tiniest letter in history, the letter "P" with a heart next to it, was written with atoms in 1992 AD by "Munir Yafeh" as a sign of love for Palestine (Plastin).

The National Nanotechnology Initiative (or "NNI") was launched by the United States of America government in 2000, making nanotechnology a national strategic technology and enabling extensive government support for it across all economic, scientific, and academic domains.

Japan created a dedicated center for nanotechnology researchers in 2002 AD by offering all required equipment, assisting and motivating researchers, and facilitating information sharing among them.

The mysteries of this technology and the realm of nanomaterials were revealed in 2003 AD.

When basic components of nanomaterials were added to the Malaysian rubber sector, the results of the technology quadrupled (from 12% to 20%) in 2004 AD, marking the beginning of the stage of industrial applications. (8)

1.2.3 Synthesis of nanoparticles

Synthesis occurred through two approaches: Bottom-Up and Top-Down showings figure (3). (9)

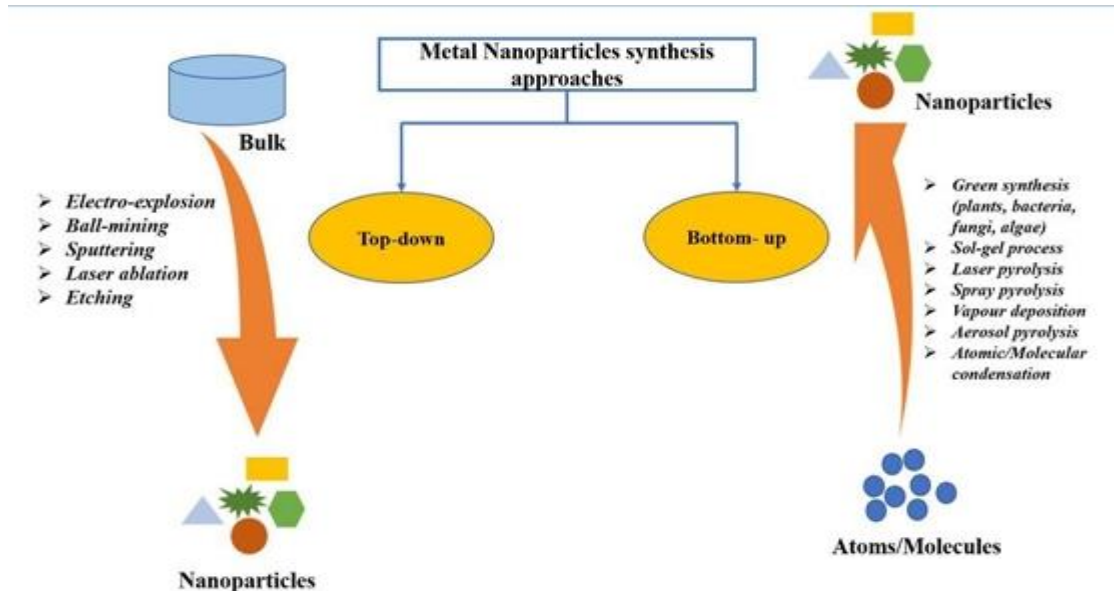


Figure 3: Different methods for NPs synthesizing

1.2.4 Methods for producing nanomaterials

There are two ways to create or transform any substance into a nano formula:

1. This process, known as the down-Top approach, involves turning large metal pieces into nanoparticles by crushing and grinding them, then adding materials that help to stabilize and fix them. This process yields nanoparticles that range in size from 10 to 100 nm.
2. Using the up-Bottom strategy, which relies on the process of assembling atom by atom or molecule by molecule, this procedure converts from a very small size to a bigger size. (4) The preparation method is shown in the figure (4).

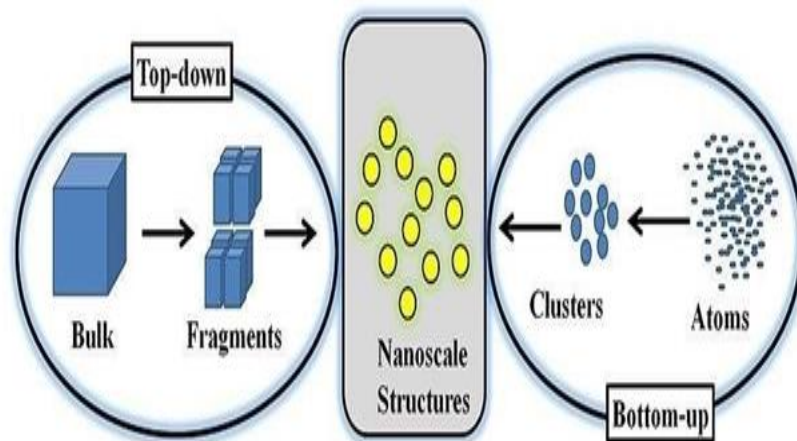


Figure 4: Methods for preparing nanoparticles Top - Bottom, Bottom – Top. (10)

There are three ways to use these ideas and methods:

1. Physical synthesis technique: Using a tubular furnace and the well-known evaporation-condensation process at atmospheric pressure, this method creates nanoparticles.
2. The biological synthesis method: This technique uses elements of living things as encapsulates and reducing agents for nanoparticles. Vitamins, carbohydrates, amino acids, and enzymes are a few examples. This approach is eco-friendly.
3. Chemical reduction method: This technique relies on metal salts as reducing agents in addition to stabilizers and encapsulates, such as elemental hydrogen and citrate borohydride, which are often utilized to create a stable colloidal silver solution. (4)

Many biological applications greatly benefit from the use of metallic nanoparticles especially those made of gold and silver. Antimicrobial capabilities have been demonstrated using silver nanoparticles. As a result, they are now widely used in a variety of technologies, including toothpaste mouthwash, bath soap, water purification, infant bottles, and several public health applications.

Molecular microscopy, genomics, biosensors, precise drug delivery (by loading the drug onto nanoparticles for easy delivery to the target part of the body), thermal therapy of cancer cells, microorganism detection, imaging of biological tissues and cells (using magnetic resonance imaging techniques), and in vivo acoustic imaging techniques are just a few of the biomedical fields where gold nanoparticles have recently expanded their applications. (11)

1.2.5 Classification of Nanoparticles

There are two primary categories for nanoparticles:

Particles composed of carbon compounds, such as carbon nanotubes and fluorine, are referred to as organic nanoparticles.

Metallic and magnetic nanoparticles like silver and gold, metal oxides like zinc and titanium, and semiconductors like zinc oxide are examples of inorganic nanoparticles. Due to their special qualities, these particles are being used more and more in a variety of industrial, medicinal, and agricultural domains.

Additionally, nanoparticles can be categorized based on their size:

Materials with just one dimension in the nanoscale (less than 100 nm) range are known as one-dimensional nanoparticles. Thin films, which are utilized in electronics, coatings, and medicine for a variety of applications, are examples of this category. They are distinguished by their thickness at the nanoscale.

Two-Dimensional and Three-Dimensional Nanoparticle Classification:

The two dimensions of two-dimensional nanoparticles are between 1 and 100 nanometers, whereas the third dimension is bigger. Carbon nanotubes, nanosheets, and nanowires are a few examples.

Three-dimensional nanoparticles, whose three dimensions fall inside the nanoscale (less than 100 nanometers), make up the third category. Examples include dendrimers, which are branching nano polymers utilized in the delivery of drugs and pesticides, fullerenes, which include 60 carbon atoms, and nanospheres. Because of their unique electrical and thermal characteristics, quantum dots—tiny materials with quantum properties—find application in a variety of industries, such as medication delivery, semiconductors, and lasers. They are between two and ten nanometers in size.

Because of these materials' many uses and contemporary applications in cutting-edge nanotechnology, their manufacturing has expanded around the world. (12)

1.2.6 Properties of Nanoparticles

nanoparticles exhibit special physical, chemical, and biological features because of their tiny size and large surface area. Because of their high surface-to-volume ratio, nanoparticles have highly active atoms and molecules on their surface.

The surface area and particle size are inversely correlated. The relative surface area increases with decreasing size. Because of this, nanoparticles are more efficient than bigger particles. The material's efficacy as a chemical catalyst is raised by the improved chemical reactions brought about by this larger surface area.

Additionally, nanoparticles are known to have novel chemical and physical characteristics that might not be noticeable in their bigger (micrometric) state. A substance can acquire previously unknown features, especially biological ones, as it reaches the nanoscale.

Among the characteristics that set nanomaterials apart are:

1. special mechanical qualities.
2. alterations in magnetic, electrical, and thermal characteristics.
3. increased chemical reactivity and surface activity.

1.2.6.1 Mechanical Characteristics

Metallic materials become more resilient to loads and can tolerate a wider range of pressures. This is brought about by their cohesive strength and hardness, as well as by adjusting the size of the material's grains and regulating the atoms' arrangement.

1. Point of Melting

The size of a material's grains affects its melting point. For instance, the temperature at which gold transitions from a solid to a liquid is known as its melting point, and it is believed to be 1064°C when it is in its crystalline form. (12)

However, it has been discovered that when gold's grain sizes fall into the nanometer range (1.35 nm), the metal's melting point drops to around 500°C. This decline is explained by variations in the surrounding environment and the arrangement of its atoms, as well as the fact that the exterior surface area of its gold increases as the grain diameters decrease.

2. Properties of Optics

Nanomaterials and non-nanomaterials have quite different optical characteristics. The size of the grains affects how light is refracted or scattered at the material's surface. For instance, when the grain sizes of pure gold are more than 200 nanometers, the well-known hue yellow emerges.

However, these grains' color darkens and turns opaque when they are shrunk to fewer than 20 nanometers. Depending on their size at the nanoscale, the grains might be green, orange, or red in appearance.

1.2.6.2 Electrical Characteristics

The electrical characteristics of materials are enhanced as their size is reduced to the nanoscale. Effective electrical current conduction is made possible by the conversion of non-conductive materials into conductive nanoparticles.

1.2.6.3 characteristics of Biology

When metals like gold and silver are turned into nanoparticles, they have special biological properties that include the capacity to eradicate a variety of parasites and infections. In medicine, they have shown efficacy. (12)

1.3 Gold molecules:

The radioactive isotope is one of the twenty known isotopes of gold. Moreover, gold is the least reactive of all metals, has excellent electrical and conductive qualities, is unaffected by oxygen at room temperature, and is unaffected by air and the majority of chemicals. Gold is a single-crystal, face-centered cubic system that appears black in finely split portions and yellow in dense bulk. Furthermore, gold may be dissolved in any solvent system other than water, including sulfuric acid and potassium cyanide. Like copper and silver, gold, the 79th element in the periodic table, contains one electron outside the full shell. To maximize its utility, gold is either plated with the base metal or alloyed with additional metallic components. Because of this, metal characteristics are significant and have been well studied. (13)

The physical and chemical characteristics of gold are listed in table (1) below. (13)

Table 1: shows the chemical and physical properties of gold.

	The physical and chemical characteristics of gold	
1	Chemical symbol	Au
2	color	Vibrant yellow
3	The number of atoms	79
4	Density	19.3g/cm ³
5	Atomic weight	197g/mol
6	Melting temperature	1064.4°C
7	Boiling temperature	2807°C
8	Specific gravity	18.88
9	Isotopes	7

1.3.1 Gold nanoparticles

These metal nanoparticles are employed in nanobiotechnology to identify big biomolecules attached to their surface by physical adsorption or coupling via Au-S bonds. The binding of big biomolecules to the surface of nanoparticles is commonly referred to as "functionalization," whilst these nanostructures are known as bio composites. Therefore, the metal core serves as an optical marker, and a probe molecule is employed for a special connection to the target.

Making multifunctional nanobiocomposites with various modular conjugates, including active biosensing, improved imaging contrast, drug delivery, and tumor targeting, is the goal of using gold nanoparticles (GNPs) with surface molecules. Currently, one may think of bioconjugation chemistry as a distinct subfield of nanobiotechnology. (13)

Adsorption and chemisorption are the two primary methods for functionalizing gold nanoparticles. The adsorption technique relies on the passive adsorption of polymers onto the particle surface via disulfide bonding or hydrophobic and electrostatic interactions. In particular, proteins attach to gold colloids by hydrophobic attraction (tryptophan), charge-charge attraction (lysine), and disulfide bonding (cysteine and methionine). The advantage of

the adsorption method is that the functional characteristics of the attached macromolecule are maintained since there are little changes to the macromolecule's molecular structure. Potential adsorption and competition with target molecule binding sites are the drawbacks.

The classical chemistry of thiols and thiolate bonds or macromolecules serves as the basis for the chemical binding of biomolecules to gold nanoparticles. The ability of sulfur and gold atoms to create a covalent connection is well recognized. In bioconjugation chemistry, this characteristic is frequently employed to try and create alkanethiol bonds for the covalent binding of various biomolecules to gold nanoparticles. (13)

1.3.2 Gold nanoparticle shapes

Depending on the manufacturing technique, AuNPs can be made in a range of sizes and shapes, such as nanorods (rod-shaped AuNPs),

nanocages (hollow porous AuNPs) and nanoshells (Au-coated objects, such silica beads). (9) as seen in Figure (5)

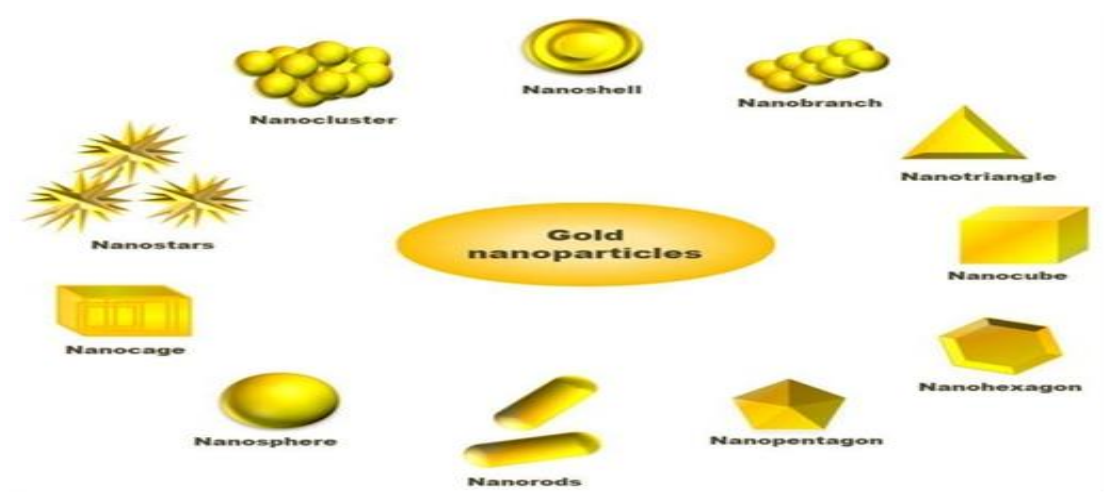


Figure 5: Different types of AuNPs.

1.3.3 Nanoparticle Characterization.

Many analytical techniques have been created in order to pinpoint the unique thermal electrical, chemical, and optical properties of noble metal nanoparticles and to verify their average particle size, shape, distribution, surface morphology, surface charge, and surface area. On the basis of their characteristic and adjustable SPR band, AuNPs are distinguished by a visible color shift. Indirect methods (spectroscopic approach) are used to study the composition, structure, and crystal phase of AuNPs. They have amazing optical properties due

to their SPR, which is observed using UV-visible spectroscopy (UV vis). Functional atoms or groups connected to the surface of AuNPs can be identified by surface chemistry analysis using Fourier transform infrared spectroscopy (FTIR). The morphology of AuNPs is now better characterized because to new developments in sophisticated microscopic methods. Atomic force microscopy (AFM), transmission electron microscopy (TEM), high-resolution transmission electron microscopy (HRTEM), and scanning electron microscopy (SEM) are a few techniques used to identify and characterize an object's size, shape, and surface morphology. (9)

1.3.4 Gold nanoparticle applications in the medical domain

Gold nanoparticles (GNPs) have started to be actively employed in a number of nanomedicine fields in recent years for both therapeutic and diagnostic applications. It is important to note that both humans and animals are increasingly receiving injections of gold nanoparticles. Specifically, they act as carriers for the transfer of medications, genetic materials, and antigens. They are also utilized as independent medicinal or diagnostic agents to treat cancers and other illnesses. AurImmune (CYT-6091) and AuroLase are two intravenous (IV) preparations that have previously undergone clinical testing. (14)

A summary panel of the various techniques for loading and releasing therapeutic ingredients into and out of gold nanoparticles is shown in Figure (6). (15)

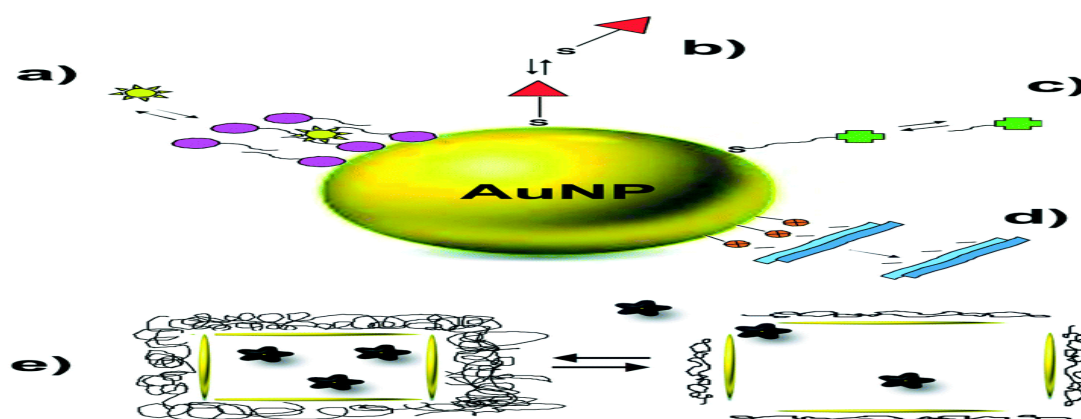


Figure 6: shows a cartoon showing several techniques for adding and removing medicinal compounds from gold nanoparticles. (a): Hydrophobic molecule partitioning and diffusion in a surfactant bilayer; (b): Drugs are immobilized by Au-S (or Au-N) bonds, forming complexes on the surface. (c): Drug complexation to capping agent functional groups; (d): Electrostatic aggregation and coupling for loading; (e): Hollow cubes with porous walls that are gold nanocages. The medications trapped within the

particle are released when the sensitive polymers are broken down by the heat produced by exposure to a near-infrared laser.

1.4 Chemical makeup and biological activities of *Carica papaya* leaf extract

The family Caricaceae, which includes the six genera *Carica*, *Jarella*, *Horovitzia*, *Jacaratia*, *Vasconcela*, and *Silicomorpha*, includes the *Carica papaya*, often referred to as pawpaw. Papaya is a member of the *Carica* genus, which has only one species *Carica papaya*. (16)

All parts of the papaya tree have been the subject of much research, but the leaves and fruits are the main emphasis since they are widely employed for a number of reasons, including food consumption, cosmetics, medicine, and pest control. Macromolecules like proteins, lipids carbohydrates, and vital minerals like potassium, phosphorus, magnesium, iron, calcium, and dietary fiber, along with vitamins like beta-carotene, vitamin C, vitamin B1, vitamin B2, and vitamin B3, make up the majority of the nutrients present in papaya leaf extracts. Papaya leaf extracts have been found to contain a wide range of phytochemicals, including phenolic compounds like gallic acid, protocatechuic acid, kaempferol, apigenin, catechin deoxykaempferol, and deoxyquercetin; flavonoid glycosides; quinones; cyanogenic glycosides; phenols; and alkaloids are among the phytochemicals. It has been noted that papaya leaf extract helps treat fever brought on by viral illnesses including chikungunya, dengue, and malaria. Moreover, papaya leaf extract has notable qualities including anti-inflammatory antiviral, anticancer, antidiabetic, and antiparasitic activities. According to recent research plants high in flavonoids may be useful in treating diseases including diabetes and hyperglycemia. (17) Ethanolic extract of papaya leaves also lowers the incidence of cancer and encourages apoptosis and cancer cell death in animal models of cervical cancer. The expression of the genes NF-kB.11 and 53P- may also be enhanced. (18) Figure (7) shows a close-up of a papaya leaf.



Figure 7: shows the shape of the leaves of the papaya Carica. (19)

Throughout the year, papaya is accessible and a nutrient-dense food. Three potent antioxidants are abundant in it: vitamin C, vitamin A and vitamin E; minerals, potassium and magnesium; fiber, folate, and the B vitamin pantothenic acid. In addition to all of this papain, a digestive enzyme, is a good treatment for sports injuries, allergies, and trauma. Together, papaya's nutrients strengthen the heart, guard against heart attacks, strokes, and disorders of the heart, and stop colon cancer. Beta-carotene, which is abundant in the fruit, guards against the harm that free radicals may do and can lead to some types of cancer. According to reports, it aids in preventing diabetic heart disease.

Papaya is a good source of fiber, which helps decrease elevated cholesterol levels. Papaya efficiently cures and improves all kinds of various illnesses of the abdomen and digestive system. It is a medication for constipation, dyspepsia, hyperacidity, and dysentery. Due to its abundance of proteolytic enzymes, papaya aids in the digestion of proteins. Papain, a digestive enzyme present in papayas, is also isolated, powdered, and used as a digestive aid. Regular consumption of ripe fruit relieves chronic constipation. Papaya is also said to delay the onset of aging. It could be effective because inadequate digestion deprives our bodies of enough nutrients. Figure (8) shows a papaya fruit.



Figure 8: shows a papaya fruit

The papaya's skin considered the finest medication for wounds, and the fruit is said to help with stomach issues. Even the pulp that remains after the papaya's juice is extracted can be used as apply a poultice to the injuries. Papaya's antioxidant components and papain and chymopapain enzymes have been shown to help reduce inflammation and cure burns. This is the reason why eating all these nutrients helps persons with inflammatory disorders (such osteoarthritis, rheumatoid arthritis, and asthma) as their condition becomes better.

Because papaya contains vitamins A and C, it helps maintain a healthy immune system by making you more resilient to colds and coughs. Including papaya in your diet guarantees a healthy intake of vitamins A and C, which are vital for keeping oneself healthy. *Carica papaya* constituents have an alkaline combination, similar to that of borax or potassium carbonate, and have demonstrated promising results in treating eczema, cutaneous tubercles, warts, corns sinuses, and other skin hardness. They can also be injected into indolent glandular tumors to encourage absorption. Papaya green fruits are used to stimulate the reproductive organs, cure dyspepsia, constipation, amenorrhea, high blood pressure, and general debility.

Papaya's nutritional benefits aid in halting cholesterol oxidation. Rich in calcium and iron, papaya is also a strong source of vitamins A, B, and G and a great source of ascorbic acid or vitamin C. Terpenoids, alkaloids, flavonoids, carbohydrates, glycosides, saponins, and steroids are all present in unripe *C. papaya* extracts. (20)

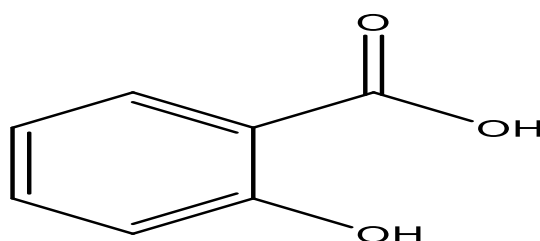
1.4.1 Vitamin content in papaya fruit

One medium papaya fruit offers 24% of the daily recommended consumption of vitamin C, making it a great and abundant source of the vitamin. About 120 calories, 30 grams of carbohydrates (including 5 grams of fiber), 18 grams of sugar, 2 grams of protein, and no cholesterol are found in a medium papaya. Additionally, papaya fruit is an excellent source of fiber, folate, vitamin A, copper, magnesium, and pantothenic acid. Alpha and beta carotene lutein and zeaxanthin, vitamin E, calcium, and B vitamins are also present in the fruit. potassium, vitamin K, and lycopene, the powerful antioxidant most commonly associated with tomatoes. (21)

1.4.2 The chemical makeup of leaves (enzymes, flavonoids, and phenolics).

1.4.2.1 Phenolic substances

1. Research has shown that the total phenolic content of *carica papaya* leaves is considerable, with values of about 15.0 grams of gallic acid equivalent (GAE)/kg of dried leaves.
2. The two most common phenolic chemicals found are rutin and salicylic acid, both of which have antioxidant qualities. (17) Figure (9) shows the structural formula of salicylic acid.



2-hydroxybenzoic acid

Figure 9: Structural formula of salicylic acid

1.4.2.2 Flavonoid chemicals

1. Studies have shown that flavonoids, which are abundant in papaya leaves, have a variety of pharmacological actions. (23,24)
2. Colorimetric techniques may be used to quantify the total flavonoid content, which indicates their concentration and possible health advantages. (24)

1.4.2.3 Enzymatic activity

1. Papain, an enzyme that is isolated from *Carica papaya*, is well-known for its use in industry and medicine, especially in wound healing and digestion. The structure of the papain enzyme is shown in Figure (10).
2. Papain's effectiveness in therapeutic settings depends on a number of variables including temperature and pH, which affect papain activity. (25)

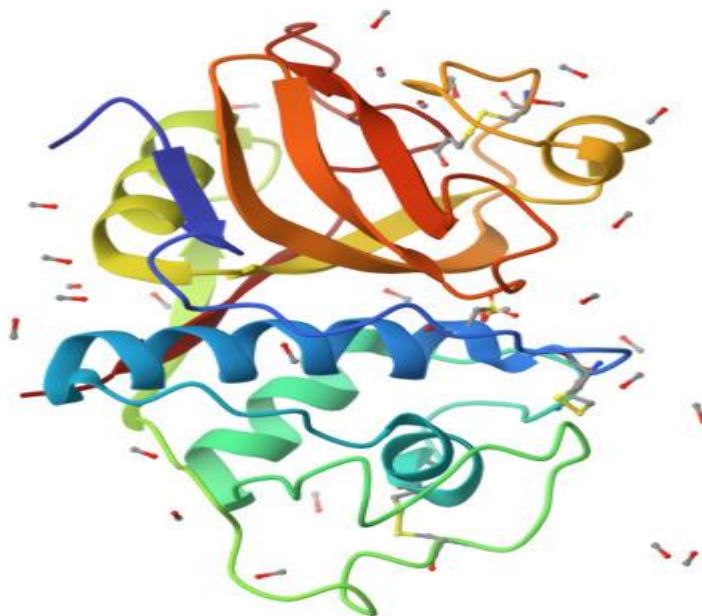


Figure10: Papain enzyme structure. (26)

1.4.3 *Carica papaya* leaf extract's bioactivity

A variety of medicinal qualities, including as anthelmintic antiangiogenic, antioxidant, antibacterial, and fungicidal actions, are included in the bioactivity of *Carica papaya* leaf extract. These varied endeavors demonstrate papaya leaf extract's promise as a natural cure for a range of medical conditions. (27)

1.4.3.1 Anthelmintic action

1. When compared to the synthetic medication albendazole, *Carica papaya* leaf extract (CPLE) had strong anthelmintic effects against *Allolobophora caliginosa*.
2. Worms exposed to *Carica papaya* Leaf Extract displayed structural alterations, including decreased size and thicker cuticles. (27)

1.4.3.2 Antiangiogenic characteristics

1. By altering vascular endothelial growth factor receptors (VEGFR1 and VEGFR2), the extract demonstrated the ability to suppress angiogenesis which is essential for the advancement of cancer.
2. Research conducted in vivo showed that the placental membrane model reduced capillary development. (28)

1.4.3.3 Antimicrobial and antioxidant properties

1. Ethanolic extracts of *Carica papaya* Leaf Extract had the best effectiveness in scavenging free radicals, demonstrating considerable antioxidant activity.
2. Significant antibacterial activity against a number of Gram-positive and Gram-negative bacteria was also demonstrated by the extract. (29)

1.4.3.4 Fungicidal activity

Carica papaya Leaf Extract showed promise as a natural fungicide by effectively combating *Phytophthora* species-induced black cocoa pod disease. (30)

1.5 Phenolic Compounds:

Phenols are aromatic compounds that have a hydroxyl group attached to one or more benzene rings. Derivatives with one or more hydroxyl groups are among the many different chemical structures and functional characteristics of phenolic substances. The structural formula is shown in Figure (11).

These substances' characteristics range from being extremely hydrophilic (quercetin-3-sulfate) to being extremely lipophilic (tangeretin).

The term "phenols" is used to refer to aromatic chemical compounds that include one or more rings and one or more hydroxyl groups, according to Walker (1975).

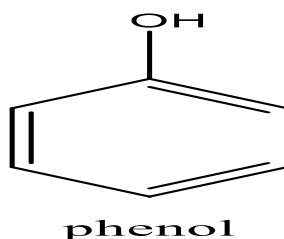


Figure 11: Structural formula of phenols

Particularly in regions where plant diseases are common, plant phenolic compounds have shown strong anticancer, antifungal, anti-inflammatory, and antioxidant properties.

In addition to their significant function in human health, phenolic compounds are persistent plant molecules that find wide use in sectors like leather tanning and dye manufacture.

Phenolics have several uses in the food, cosmetic, and pharmaceutical sectors and may be found in food crops in a variety of forms, both edible and inedible. (31)

There are many different types of phenols found in nature, from basic phenols to extremely complex compounds. Their categorization is therefore crucial, particularly when examining the connection between these compounds' chemical structure and biological action. Phenols have been categorized in a number of ways, the most common being:

Initially: Phenols are categorized in the first way as:

1. Flavonoids

Flavonoid types include:

1. flavones.

A-Flavones, including orientin, cosmosiin, luteolin, vitexin, apigenin, apiin, and baicalein

B-Flavonols like rutin, myricetin, myricitrin, kaempferol, and quercetin

2. Flavanones, including fustin, hesperetin, naringenin, and hesperidin the aromatendrin.

3. Chalcones, including phloretin, phlorizin, butein, carthamin, and dihydrochalcone.

4. Isoflavones, including puerarin, genistein, genistin, daidzein, daidzin, and 3-phenylchromone.

5. Anthocyanidins, including delphinidin, cyanidin, pelargonidin, and anthocyanin.

6. Aureusidin and other aurones.

7. Biflavones, including hinokiflavone and amenthoflavone.

8. Neoflavonoids, including flavonolignan. (31)

1.6 Flavonoids

Flavonoids are phenolic substances that are extensively distributed across the kingdom of plants. They come from malonate and aromatic amino acids like tyrosine and phenylalanine. The flavan nucleus, the fundamental building block of a flavonoid, is usually based on the common structure known as diphenyl propane. It is composed of a three-carbon carbon chain (C6-C3-C6) connecting two aromatic rings. Rings A, B, and C are the names of these rings. Ring C is a three-carbon ring that serves as a bridge between rings A and B, which are aromatic rings. Flavonoids vary from one another in terms of the degree of oxidation and the pattern of substitution on the C-ring.

The type of flavonoid also affects the substitution patterns on the A- and B-rings. A class of naturally occurring substances with varying phenolic contents includes flavonoids. The plant's leaves, blossoms, stems, peels, roots, seeds, fruits, and fluids like tea and wine are all home to them.

Before flavonoids were separated and thoroughly investigated, they were categorized as active substances with positive health benefits. Several of the more than 4,444 flavonoids that have been discovered so far have been linked to the appealing hues of fruits, leaves, and flowers. (31)

There are several types of flavonoids, such as methylated derivatives, sugar forms (glycosides), and unsweetened forms (aglycones).

A pyrano ring (C) with a phenyl ring (B) attached at the second position of the C-ring is joined to a benzene ring (A) to generate an aglycone, the unsweetened form of a flavonoid.

Plants produce flavonoids as glycosidic derivatives, which give flowers, foliage, and fruits their vibrant purple, red, blue, and dazzling hues. During pollination, flavonoids serve as visual signals for insects, among other significant and varied functions in the plant environment. Anthocyanins, flavonols, and flavones are a few examples. The composition of substances like catechins is responsible for their astringency. Other flavonoids work well against insects that harm plants. In the light phase of photosynthesis, flavonoids also function as catalysts, contributing to the electron transport system through the generation of reactive oxygen species (ROS), which aid in defending plant cells against stress. Because of their great absorption capacity, they also shield plants from UV rays. (31)

Flavonoids are essential dietary ingredients. They support vital physiological processes in plants even though they are not necessary nutrients for humans.

Flavonoids are examples of secondary chemicals, which make up 5–14% of known plant products.

1.6.1 Flavonoid classification:

Flavonoids are categorized according to the three-carbon chain's oxidation state (C6-C3-C6) and comprise:

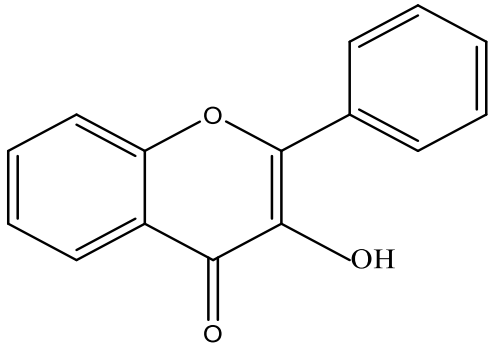
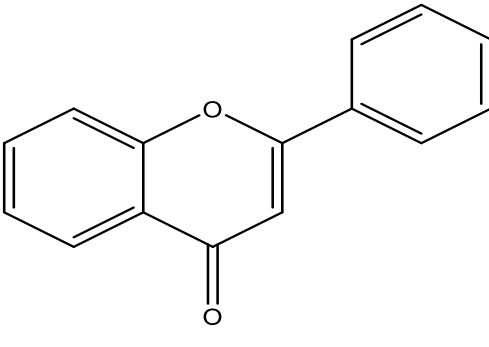
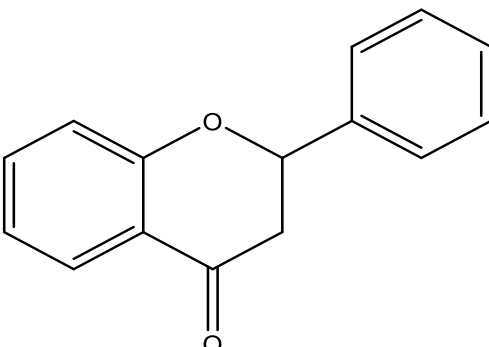
1. Anthocyanins
2. Flavanols, including catechins
3. Flavonols
4. Flavonoids
5. Isoflavones
6. Flavanones

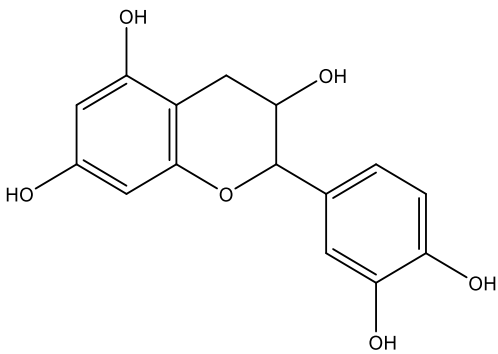
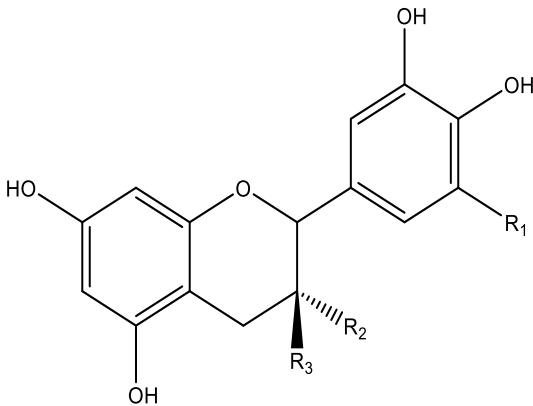
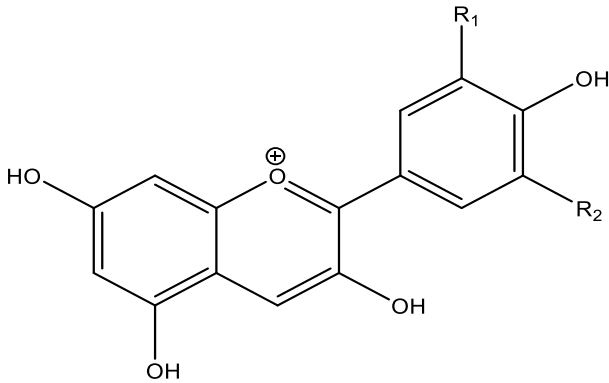
Table (2) lists the several kinds of flavonoids and their plant sources along with their derivatives.

The structure of the ring (C) may also be used to categorize flavonoids as follows:

1. Flavonols: have a double bond between carbons two and three, three hydroxyl (OH) groups, and a ketone (keto) group.
2. Flavones: Have four OH groups, a ketone group, and a double bond between carbons two and three.
3. Flavanonols: Have four OH groups and a ketone group.
4. Flavanones: Lack a double bond between C2 and C3, but have four OH groups and a ketone group.
5. Flavanols: Have no ketone groups and three OH groups. (31)

Table 2: Flavonoids with some plant species and their biological sources.

Groups	Composites	Food sources
<p>Flavonols</p>  <p>3-methyl-2-phenyl-4<i>H</i>-chromen-4-one</p>	<p>Quercetin, kaempferol, myricetin</p>	<p>Apples, green and black tea, and black grapes</p>
<p>Flavones</p>  <p>2-phenyl-4<i>H</i>-chromen-4-one</p>	<p>Tangeretin, nobiletin, apigenin</p>	<p>Celery, peppers</p>
<p>Flavonones</p>  <p>2-phenylchroman-4-one</p>	<p>Naringenin, hesperetin ,eriodictyol</p>	<p>Orange, lemon, and grape juice</p>

<p>Flavanols</p>  <p>2-(3,4-dihydroxyphenyl)chromane-3,5,7-triol</p>	<p>Silibinin, silymarin, taxifolin</p>	<p>Cocoa, cocoa liquor, and chocolate</p>
<p>Catechins</p> 	<p>(+) catechin, gallicocatechin, (-) epicatechin</p>	<p>Chocolate, grapes, peaches, and green tea</p>
<p>Anthocyanins</p> 	<p>Cyanidin, delphinidin, malvidin</p>	<p>Black grapes, strawberries, and red wine</p>

1.7 Cancer

A class of disorders known as cancer, or malignant tumor, is characterized by the unchecked proliferation of altered cells, as well as their capacity to invade nearby healthy tissues and spread to distant locations inside an organism's body. Sarcoma, lymphoma/leukemia, myeloma, adenocarcinoma, and carcinoma are the five subgroups into which it may be further subdivided based on various sources. Cardiovascular disease is the

world's largest cause of mortality, followed by cancer. Scientists often ascribe cancer to the suppression of cell differentiation, loss of control over cell proliferation, and chromosomal aneuploidy; inhibition of cellular death and senescence.

and hyperactive telomerase at the subcellular level; oncogenes that are overly activated and anti-oncogenes that are overly inhibited; gene mutation; and epigenetic alteration (DNA methylation, histone acetylation, etc.) at the molecular level. mutagens in an in vitro setting, such as physical carcinogens (such as UV and X-rays),

Biological carcinogens (DNA viruses, RNA retroviruses) and chemical carcinogens (benzopyrene, aflatoxin B1, etc.) can encourage the conversion of benign tumors into malignant tumors with the aid of in vivo environmental variables. environment (such as immune system malfunction, chronic inflammation, and hormone secretion disorders) and too much oxygen radicals. (32)

In order to choose the best course of treatment, cancer staging and classification are crucial. Generally speaking, there are two primary forms of cancer:

1.7.1 benign tumors:

These tumors typically develop in one place, do not spread to other areas of the body and are not life-threatening. They are generally not anticipated to reoccur and can be surgically removed. On the other hand, a benign tumor may put pressure on delicate regions, including blood vessels or brain nerves, resulting in functional consequences that need to be treated with surgery to alleviate symptoms. (32)

1.7.2 Cancerous Growths:

This variety, which is distinguished by erratic and uncontrolled growth and division, is more dangerous and can be fatal. Malignant tumors are distinguished by their high propensity to return even after excision, their quick dissemination to adjacent and distant organs, and the death of surrounding cells. Compared to benign tumors, they are thought to be far more hazardous. Substances released by cancer cells aid in their metastasis, or the formation of secondary tumors in other parts of the body. Moreover, they are made up of diverse cells that develop from a single cell that has had a genetic flaw that has changed its composition and characteristics. (33)

1.8 Definition, biological processes, and current therapies for breast cancer

1.8.1 Definition

Breast cancer is defined as a tumor that arises from breast tissue and is typified by unchecked aberrant cell growth in the breast's ducts and/or lobules, which produce milk.

The majority of the time, the tumor starts in the breast ducts (ductal malignancies). The most prevalent invasive malignancy in women globally is breast cancer.

1.8.2 The study of epidemiology

Every year, more than a million women worldwide receive a breast cancer diagnosis. Over 500,000 women lose their lives to this illness each year. Between 2017 and 2018, there were about 252,710 new cases of invasive breast cancer, 63,960 new cases of non-invasive breast cancer in women, and 2,470 new cases in males. According to the Surveillance, Epidemiology, and End Results (SEER) database, a woman's lifetime chance of having breast cancer is 1 in 8, 1 in 202 from birth to age 39, 1 in 26 from age 40 to age 59, and 1 in 28 from age 60 to age 69. At 27.2 per 100,000, breast cancer is the second-highest cancer death rate. (34)

1.8.3 Risk variables

1.8.3.1 Genetic variables

Between 20% and 25% of breast cancer patients have a favorable family history. High-risk Mutations in the TP53 gene, BRCA1, BRCA3, PTEN, STK11, neurofibromatosis (NF1) and CDH-1 are examples of risk alleles. A 40–85% lifetime risk of breast cancer is attributed to E-Cadherin. A 20%–40% lifetime risk of breast cancer is attributed to moderate risk genes such as homozygous ataxia-telangiectasia (ATM) mutations, somatic mutations in the tumor suppressor gene CHEK2, and BRCA1 and BRCA2 modifier genes BRIP1 and PALB2. The combination of these genetic risk variants and lifestyle variables leads to the development of breast cancer that is clustered in families. (34)

1.8.3.2 Factors related to reproduction

Early menarche: For both premenopausal and postmenopausal women, an early menarche (before the age of twelve) increases the risk of breast cancer. There is a preventive effect

against breast cancer when menarche is delayed. A ten percent reduction in risk is linked to a two-year delay.

Age at first pregnancy and parity: Compared to parous women, nulliparous women are more likely to acquire breast cancer. A lower risk of breast cancer is associated with a younger age at first pregnancy and more children born before the age of 35. A woman who is older at the time of her first preterm pregnancy may be more susceptible to breast cancer than a woman who is nulliparous.

Breastfeeding: There is a protective effect against breast cancer during breastfeeding. Generally speaking, breastfeeding postpones the beginning of ovulation and lowers normal sex hormone levels. It has been calculated that for every year of breastfeeding, the reduction is 4.3%.

Menopausal age: A higher risk of breast cancer is linked to a later start of menopause. The risk of breast cancer increases by 3% for every year that the menopause is delayed, and by 17% for every five years that the menopause is delayed. (34)

1.8.3.3 Hormonal variables

Compared to non-HRT users, HRT users (>5 years) had a higher risk of breast cancer. The Nurses' Health Study data, imply that women using unopposed postmenopausal estrogen have a 23% higher chance of developing breast cancer by the time they are 70 years old. For both premenopausal and postmenopausal women, elevated levels of endogenous sex hormones, primarily testosterone, raise the risk of breast cancer. (34)

1.8.3.4 Aspects of lifestyle

Alcohol consumption: A daily intake of between 5.0 and 9.9 grams of alcohol has been linked to an elevated risk of breast cancer.

Physical activity: Regular exercise has been demonstrated to have a preventative impact on breast cancer. When combined with other risk factors, physical inactivity is responsible for 21% of all fatalities from breast cancer globally.

Obesity: Particularly in postmenopausal women, obesity increases the risk of breast cancer. Compared to lean women, the incidence of postmenopausal breast cancer is approximately 1.5 times greater for overweight women and 2 times higher for obese women. The likelihood of

getting cancer is further increased by resistance and hyperinsulinemia. Human cancer cells have been shown to overexpress the insulin receptor, and insulin exerts anabolic effects on cellular metabolism.

Diet: There is a direct correlation between breast cancer and diet. Research indicates that the incidence of breast cancer is negatively correlated with soy consumption in Asian populations but not in Western ones. Consuming fruits and vegetables high in carotenoids and other micronutrients lower the incidence of HR breast cancers.

Smoking: There is a correlation between tobacco use and an increased risk of breast cancer. According to research by the American Cancer Society, women who started smoking before the birth of their first child were 21% more likely to get breast cancer than women who never smoked.

Radiation: Breast cancer risk is increased by radiation exposure from a variety of causes, such as nuclear explosions and the treatment of childhood cancer. (34)

Uncontrolled proliferation of mammary epithelial cells is the hallmark of breast cancer (BC), a diverse illness that has a major impact on women's health all over the world. With over 2.3 million diagnoses every year, it makes up 11.7% of all new cancer cases. (35)

1.8.4 Clinical characteristics

Women's symptoms

1. An enlarged breast
2. Pain in the breasts and a tender bulge region breast eczema, breast retraction, breast discharge, and breast swelling
3. A lump beneath the armpit Dimpling or irritation of the skin surrounding the breast
4. Skin fixation over the lump
5. Ulceration over the lump

Men's symptoms

1. include breast lumps.
2. Inversion of the breasts. (34)

1.8.5 Pathophysiology:

Breast cancer often starts as ductal hyperproliferation and, after ongoing stimulation by several carcinogenic agents, progresses to benign tumor or even metastatic carcinoma. The development and spread of breast cancer are significantly influenced by tumor microenvironments, such as macrophages or stromal effects. The only thing that can affect tumor development is stromal exposure to toxins. A mutagenic inflammatory milieu produced by macrophages can promote angiogenesis and help cancer cells evade immunological rejection.

The genesis and progression of breast cancer may be explained by two theories: the stochastic theory and the cancer stem cell hypothesis.

According to the cancer stem cell theory, the same stem cells or progenitor cells are the source of all tumor subtypes. Different tumor phenotypes are caused by acquired genetic and epigenetic alterations in the progenitor cells. According to the stochastic hypothesis, a single cell type gives rise to each tumor subtype. Any breast cell may eventually get random mutations that cause it to change into a tumor or neoplasm. (34)

1.8.6 Treatment for Breast Cancer

1. Among the treatment approaches are
2. Surgery (lumpectomy or mastectomy)
3. Radiation and chemotherapy
4. Endocrine and targeted treatments
5. Immunotherapy and gene therapy are examples. (36)

Tumor excision is one of the primary surgical techniques used to treat breast cancer in women. mastectomy; excision of the lymphatic system under the arms; and removal of the sentinel lymph node. Patients who are deemed ineligible for breast-sparing treatment or who refuse to undergo breast-sparing surgery because of the severity of their condition are given a breast amputation.

With the exception of subcutaneous amputation, breast amputation entails the removal of the whole breast as well as the skin that surrounds the mammary gland. It is feasible to create:

1. simple amputation, which is typically used as a palliative measure for patients who cannot get drastic therapy
2. subcutaneous amputation, which involves removing the tissue from the breast glands and the modified radical mastectomy in accordance with the Patey method, which involves removing the mammary gland, axillary fossa lymph nodes, pectoral muscle minor, and pectoral muscle major fascia in a single tissue block
3. modified radical mastectomy in accordance with the Madden method, which involves removing the mammary gland, pectoral muscle major fascia, and armpit lymph nodes
4. According to the Halsted approach, a radical mastectomy involves removing the mammary gland, axillary fossa lymph nodes, and other tissue in patients who have been identified with infiltration of the cancer process on the pectoral muscles. bigger pectoral muscle. Nowadays, this technique is seldom ever utilized. (37)

Breast conserving therapy (BCT), a treatment for early-stage cancer, is currently gaining popularity and using the same level of efficacy. According to the standards set forth by the Association of Breast Surgery, patients who fulfill the requirements for eligibility for sparing therapy ought to be given the choice between this treatment and mastectomy. Sparing therapy for breast cancer might include: - removing the tumor along with the surrounding healthy tissue; - doing a quadrantectomy operation inside the axillary fossa (all of the axillary fossa's lymph nodes—axillary lymphadenectomy or sentinel lymph node).

Oncological completeness is the primary goal of surgery for patients receiving treatment for breast cancer. The right cosmetic outcome is crucial for both breast conserving surgery and radical mastectomy. Adjuvant treatment for breast cancer includes hormone therapy immunotherapy, chemotherapy, radiation, and/or a combination of these techniques in addition to surgical surgery.

All patients treated with techniques that spare the mammary gland get radiation therapy which lowers the chance of the disease process returning. Additionally, metastases in at least four axillary lymph nodes and the presence of positive tissue margins are indications for adjuvant radiation treatment. Radiation is applied to the nodal fields and chest region. Chemotherapy with cytostatics is another kind of adjuvant treatment. When the illness process becomes more widespread, this approach is employed. It might be connected to radiation treatment. When additional radiation treatment is indicated for breast amputees, it should be administered following adjuvant chemotherapy.

Regardless of age or menopausal status, hormone therapy is utilized for patients with breast cancer who express the estrogen receptor. Reducing hormone secretion and easing cancer-related illnesses and symptoms are two further reasons to use hormone treatment. (37)

Immunotherapy is regarded as one of the most successful therapies for triple negative breast cancer that has spread. When used with chemotherapy, it works by boosting the body's defenses against as an immunotherapy for breast cancer, several techniques have been explored, including:

Anti-vaccine, tumor-lytic viral, and tumor-targeting immunotherapy Figure (12) The results of the treatments have been excellent. In addition to its impact on patients with severe autoimmune melanoma and poor response if used without chemotherapy, it proved effective against both primary tumors and advanced tumors (metastases). It also produced results by trapping the tumor, preventing its spread, and extending the patients' life expectancy. (38)

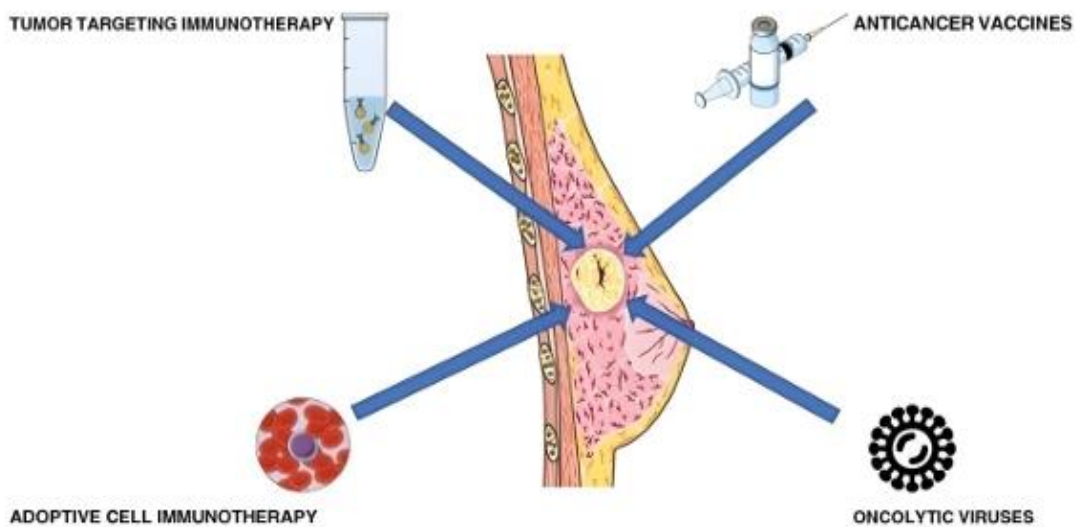


Figure 12: Types of immunotherapies for breast cancer

Modern oncology is able to provide a customized treatment plan that is tailored to the specifics of each cancer because of advancements in diagnosis. Multigene tests were made available to doctors, and they are an effective diagnostic tool when used to a well-chosen patient population. They assist in determining the best course of action for a particular patient and estimating the chance that the illness may reoccur. (37)

1.8.7 Mechanisms of biology

Among the primary molecular mechanisms at play are:

1. Through estrogen receptors, estrogen signaling affects the development of tumors. (39)
2. genetic alterations that impact pathways like PI3K/AKT/mTOR in BRCA1, BRCA2, and other genes. (35)
3. pathways of drug resistance, including modifications to immunological response and drug metabolism. (40)

1.8.8 The biological processes that lead to breast cancer.

The key elements of the development of breast cancer are explained in the sections that follow.

1. The role of genetics
 - mutated BRCA1 and BRCA2 genes These gene mutations greatly raise the risk of breast cancer by impairing DNA repair pathways, which in turn causes malignancy. (41)
 - Differential expression of genes: Important genes linked to cell cycle control that may be biomarkers for breast cancer include CDK1, CCNB1 and TOP2A, according to studies. (42)
2. Cell signaling pathways
 - The M2 Pyruvate Kinase (PKM2) Apoptosis, tumor-microenvironment interactions and cell proliferation are all impacted by this enzyme's dual roles in metabolism and cell signaling. (43)
 - AhRs, or aryl hydrocarbon receptors: Through processes like the epithelial-to-mesenchymal transition, environmental contaminants that activate AhR can interfere with endocrine processes and accelerate the development of cancer. (44)
3. Regulation of several atoms

Epigenetic modifications: Non-coding RNA and DNA methylation play a key role in controlling gene expression and advancing the pathophysiology of breast cancer. (45)

1.9 Using Nanotechnology to Treat Breast Cancer

The therapy of breast cancer is nearly always incurable, even with the recent successes and positive outcomes. Radiation and surgery are often reserved for palliative treatment in cases of severe illness. In order to lower the toxicity and adverse effects of traditional

medicines, lower treatment costs, and increase patient survival, additional and better treatments are thus required.

Because of its importance to human health and the battle against the deadliest diseases including cancer, nanotechnology research has started to spread into the domains of pharmacology and medicine. Because of their mechanical and thermal characteristics nanomaterials have emerged as a chemotherapeutic substitute. Technology advancements for implants have been beneficial. Since animal cell culture methods outside the body are regarded as one of the applications of biotechnology, tissue culture is used to examine the efficacy of nanoparticles on malignant tumors.

Because they contain the majority of the nutrients required for the proliferation of cancer cells outside the living body, this process involves introducing entire tissue pieces or a group of enzymatically differentiated cells into the body. This allows for the control and management of the conditions that lead to the growth of cancer cells, as well as the control of the duration of exposure of the various cancer cells cultured to the preparation.

For instance, breast cancer was treated with the chemotherapeutic medication calprotectin (CPT). When the two bind at the nucleophilic site, it prevents the DNA topoisomerase enzyme from doing its job, which causes CPT to dissociate and create lactone. Because lactone is extremely poisonous, unstable at the pH of the body, and poorly soluble in water, it has not been used in clinical cancer applications. By encapsulating CPT internally with solid, insoluble lipid nanoparticles, the toxicity of the drug was decreased and the efficacy of breast cancer treatment was increased. Compared to chemotherapy with free CPT, the therapeutic effect was less pronounced and more effective against breast cancer cells in organic solvents. (38)

Because of their high cell uptake, biocompatibility, and low toxicity, bio-synthesized gold nanoparticles are novel medications for the treatment of breast cancer. As a result, they have been extensively utilized in the medical profession, especially in the detection and treatment of cancer.

The aqueous extract of the endophytic fungus *Commiphora wightii*, which was isolated from the plant *Cladosporium* spp., was utilized to create gold nanoparticles, which were shown to be effective against 7-MCF breast cancer. The MTT assay (in vitro) demonstrated the efficacy of gold nanoparticles derived from the endophytic fungus *Fusarium solani* extract against 7-MCF breast cancer. (38)

1.9.1 Mechanism of cancer cell suppression by gold nanoparticles.

Numerous researchers have shown that gold nanoparticles effectively target cancer cells despite the fact that their exact impact on cancer cells is yet unknown. He noted that the generation of free cells, oxidation of glutathione, disruption of the cell cycle to activate the caspase 3 protein, necrosis of cancer cells, and programming of cell death are some of the ways that gold nanoparticles impact cancer cells as in the figure (13).

Apoptosis, or programmed cell death, is one of the most potent antitumor processes that gold nanoparticles may elicit because of their strong affinity for different biomolecules and ease of passage across cellular barriers. These cells exhibit morphological alterations that eventually result in cell death, such as cell shrinkage, nucleus fragmentation, and extensive diffusion of plasma molecules. The remaining dead cells are subsequently consumed by macrophages.

Additionally, he showed that two human kidney cancer cell lines experienced programmed cell death as a result of gold nanoparticles' permeability of the mitochondrial membrane, which caused malfunction and programmed cell death. Additionally, he stated that the Hep2 liver cancer cell line was poisoned by gold nanoparticles and that the death of infected liver cells was caused by programmed cell death.

The production of carcinogenic intracellular reactive oxygen species (ROS) is another hypothesized anticancer mechanism. As a result, the cancer cell experiences oxidative stress which damages its genetic material and biofilms and ultimately results in programmed cell death. Glutathione (GSH), an antioxidant that shields cells from free radicals, is oxidized by them. Glutathione disulfide is produced from GSH (GSSG). This causes the oxidized glutathione to be reduced by the enzyme glutathione reductase. The ratio of GSSG to GSH is one of the most significant markers of elevated oxidative stress. Gold nanoparticle-treated cancer cells have been shown to have lower GSH levels. Thus, among the anticancer properties of gold nanoparticles are enhanced glutathione oxidation and free radical production. (38)

According to one study, gold nanoparticles caused cytotoxicity in HeLa cervical cancer cells by producing reactive oxygen species, which harms the mitochondrial pathway and ultimately results in programmed cell death. Additionally, it showed how gold nanoparticles may cause cytotoxicity by producing reactive oxygen species, which damages biological components by causing oxidative stress in cancer cells. The accumulation of gold nanoparticles in cancer cells throughout the quiescent phase, the G1 phase (the first phase of the cell cycle), and the S phase

(the second phase of the cell cycle) following GO therapy was also suggested to have a potential involvement in cell cycle regulation.

The function of cells in causing planned cell death. When 7-McF breast cancer cells were exposed to gold nanoparticles, this was discovered. The findings show how effectively these nanoparticles may cause cell arrest at different phases of the cell cycle. One of the helices that breaks down cellular proteins is caspase, which also causes programmed cell death as a result of expansion, the removal of undesirable cells, or natural equilibrium. Additionally, gold nanoparticles increase caspase 3 activity, which results in a 40% reduction in cell viability. Because gold nanoparticles stimulate the activity of caspase 3 and caspase 9, they are also extremely toxic to human breast cancer cells and kill them. (38)

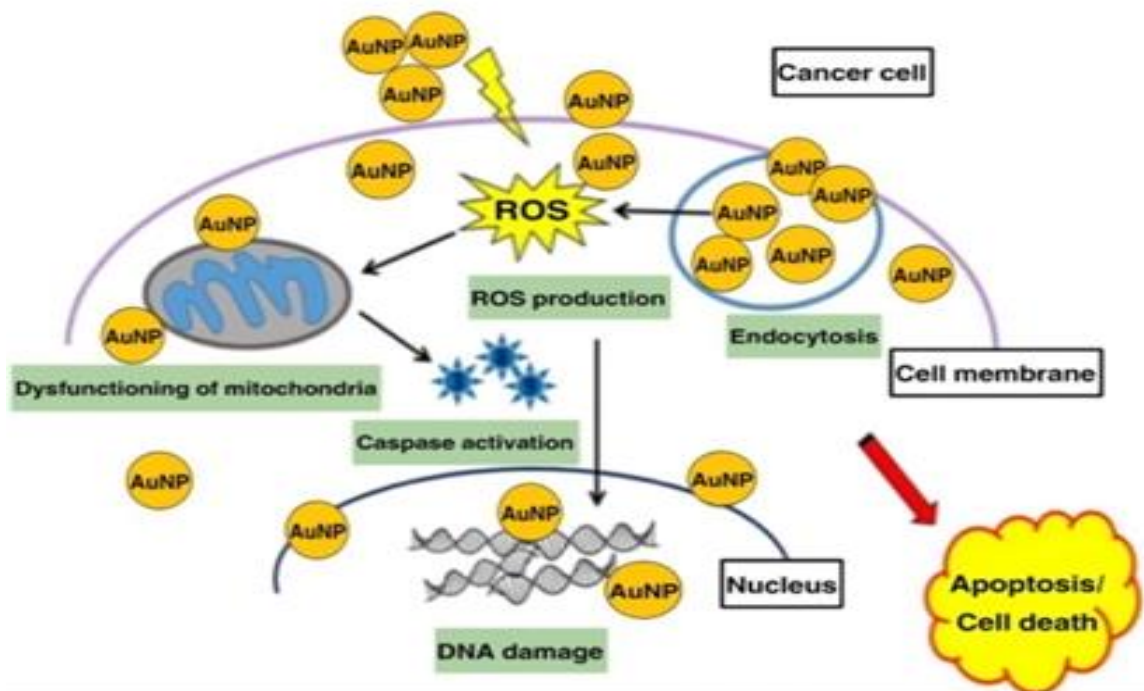


Figure13: Mechanism of action of nanoparticles against cancer cells

1.10 Literature Review

Breast cancer remains a significant global health challenge, with MCF-7 breast cancer representing a particularly aggressive subtype. (46,47) The need for innovative therapeutic strategies has driven research into nanotechnology-based approaches, offering new possibilities for targeted and effective treatments. (48,49)

Gold nanoparticles (AuNPs) have emerged as promising candidates in cancer theranostics due to their unique physicochemical properties, including surface plasmon resonance, high surface area-to-volume ratio, and ease of functionalization. (50,51) These characteristics make AuNPs versatile platforms for drug delivery, imaging, and photothermal therapy in cancer management. (52,53)

The green synthesis of AuNPs using plant extracts has gained significant attention as an eco-friendly and cost-effective alternative to conventional chemical methods. (54,55) This approach harnesses the reducing and capping abilities of plant-derived biomolecules, potentially imparting additional bioactive properties to the nanoparticles. (56,57)

Carica papaya, commonly known as papaya, is a tropical fruit tree with a rich history of medicinal use. (58) Various parts of the plant, including leaves, have been traditionally employed for their anti-inflammatory, antioxidant, and potential anticancer properties. (59,60) The leaves of *C. papaya* contain a complex mixture of bioactive compounds, including flavonoids, alkaloids, and phenolic acids, which may contribute to its therapeutic effects. (61,62)

Recent studies have explored the anticancer potential of *C. papaya* leaf extracts against various cancer types, including breast cancer. (63,64) The leaf extract has shown promise in modulating cell signaling pathways, inducing apoptosis, and inhibiting cancer cell proliferation. (65,66) However, the potential of *C. papaya* leaf extract for the green synthesis of AuNPs and their application in cancer therapy remains largely unexplored. (67)

This study investigates the green synthesis of AuNPs using *C. papaya* leaf extract, characterize the resulting nanoparticles, and evaluate their anticancer effects against MCF-7 breast cancer cells. We employ a comprehensive array of characterization techniques, including UV-visible spectroscopy, X-ray diffraction (XRD), transmission electron microscopy (TEM), atomic force microscopy (AFM), dynamic light scattering (DLS), and zeta potential analysis. (68-73)

The anticancer potential of the synthesized AuNPs is assessed using the MTT cell viability assay on MCF-7 breast cancer cell lines. (74) Additionally, we evaluate the antioxidant activity of the AuNPs using the DPPH radical scavenging assay. (75) To elucidate the mechanism of action and potential toxicity, flow cytometry experiments are conducted to assess cell cycle distribution and apoptosis induction. (76,77)

By combining the therapeutic potential of *C. papaya* with the unique properties of AuNPs, this research indicates to contribute to the development of novel, eco-friendly nanotherapeutics for MCF-7 breast cancer. (78,79) The integration of green nanotechnology with traditional medicinal plants presents an exciting opportunity for advancing cancer treatment strategies. (80,81)

This study not only explores the synthesis and characterization of *C. papaya*-mediated AuNPs but also investigates potential synergistic effects between the plant-derived bioactive compounds and the nanoparticles. (82,83) We aim to provide insights into the role of the phytochemical corona in modulating the biological activity and cellular interactions of the AuNPs. (84,85)

The findings of this research may pave the way for the development of safe, effective, and sustainable nanotherapeutics for MCF-7 breast cancer, potentially offering advantages over conventional treatments in terms of efficacy and reduced side effects. (86,87)

1.11 Objectives

With the use of *Carica papaya* leaf extract, this study intends to investigate the environmentally friendly production of gold nanoparticles describe them, and assess their anticancer properties against MCF-7 positive breast cancer cells.

Through the following sub-objectives, this goal is accomplished:

1. The Green synthesis of gold nanoparticles and their analysis by scanning electron microscopy (SEM, TEM, AFM), FTIR, UV-Visible, GC-MS, XRD, EDX, and others.
2. Examine how well-prepared gold nanoparticles made from *Carica papaya* leaf extract work against specific breast cancer cells (MCF-7).

Chapter Two

Experimental Work

2 Materials and Methods

2.1 Materials

1. *Carica papaya* leaves
2. Deionized water
3. Chloroauric acid (HAuCl₄), 1 mM (Sigma-Aldrich, USA)
4. Whatman filter paper No. 1
5. Airtight container

2.2 Equipment:

1. mechanical grinder (Blade Grinder CBG100S, Cuisinart, USA)
2. hot plate magnetic stirrer (MS-H-Pro+, Scilogex, USA).
3. high-speed centrifuge (Sorvall Legend X1R, Thermo Fisher Scientific, USA).
4. UV-visible spectrophotometer (UV-2600, Shimadzu, Japan).
5. X-ray diffractometer (D8 Advance, Bruker, Germany).
6. FTIR spectrometer (Nicolet iS50, Thermo Fisher Scientific, USA).
7. transmission electron microscope (JEM-2100F, JEOL, Japan).
8. atomic force microscope (Dimension Icon, Bruker, USA).
9. atomic force microscope (Dimension Icon, Bruker, USA).
10. SEM (such as the FEI Quanta 250 FEG or a similar model).
11. a Zetasizer Nano ZS (Malvern Panalytical, UK).
12. mass spectrometer (Agilent Technologies, USA).

2.3 methods

2.3.1 Green Synthesis of Gold Nanoparticles (AuNPs)

2.3.1.1 Plant Material Preparation:

Fresh *Carica papaya* leaves were collected from local plantations in Zliten- Libya authenticated by a botanist, and washed thoroughly with deionized water. The leaves were air-

dried at room temperature for 7 days, then pulverized into a fine powder using a mechanical grinder. The powder was stored in airtight containers at 4°C until further use. (88)

2.3.1.2 Extract Preparation:

Aqueous extraction was performed by mixing 10 g of leaf powder with 100 mL of deionized water. The mixture was heated at 60°C for 30 minutes under constant stirring using a hot plate magnetic stirrer (MS-H-Pro+, Scilogex, USA). The resulting solution was filtered through Whatman No. 1 filter paper and centrifuged at 10,000 rpm for 15 minutes using a high-speed centrifuge. The supernatant was collected and stored at 4 °C for further use. (88)

2.3.1.3 AuNP Synthesis:

The synthesis of AuNPs was carried out by adding the *C. papaya* leaf extract to 1 mM chloroauric acid (HAuCl₄) solution in a 1:9 ratio. The reaction mixture was incubated at room temperature under constant stirring for 24 hours using a magnetic stirrer. The formation of AuNPs was indicated by a color change from pale yellow to deep purple. (88)

2.3.2 Characterization of AuNPs

2.3.2.1 UV-Visible Spectroscopy:

The optical properties and formation of AuNPs were monitored using a UV-visible spectrophotometer in the range of 300-800 nm. Measurements were performed at room temperature using quartz cuvettes with a 1 cm path length. (89)

2.3.2.2 X-Ray Diffraction (XRD):

Crystalline nature and phase purity of the synthesized AuNPs were analyzed using an X-ray diffractometer. with Cu K α radiation ($\lambda = 1.54 \text{ \AA}$) in the 2θ range of 20°-80°. The operating voltage and current were set at 40 kV and 40 mA, respectively. (90)

2.3.2.3 Fourier Transform Infrared Spectroscopy (FTIR):

FTIR analysis was performed to identify the functional groups involved in the reduction and stabilization of AuNPs. Spectra were recorded on an FTIR spectrometer in the range of 4000-400 cm⁻¹ with a resolution of 4 cm⁻¹. (91)

2.3.2.4 Transmission Electron Microscopy (TEM):

Morphology and size distribution of AuNPs were examined using a transmission electron microscope operating at 200 kV. Samples were prepared by placing a drop of the AuNP solution on a carbon-coated copper grid and allowing it to dry at room temperature. (92)

2.3.2.5 Atomic Force Microscopy (AFM):

Surface topology and three-dimensional morphology of AuNPs were analyzed using an atomic force microscope in tapping mode. Samples were prepared by drop-casting the AuNP solution on freshly cleaved mica sheets and air-drying at room temperature. (93)

2.3.2.6 Scanning Electron Microscopy (SEM):

Scanning Electron Microscopy (SEM) was employed to characterize the surface morphology and internal structure of the drug delivery system. This technique provides high-resolution images of the sample, allowing for the examination of particle size, shape, surface texture, and potential changes in the delivery system before and after drug release. For this study, a high-resolution SEM was used to capture detailed images of the drug delivery system. The SEM analysis procedure involved several steps to prepare and examine the samples. First, the samples were carefully mounted on aluminum stubs using double-sided carbon tape to ensure proper positioning and stability during imaging. To enhance conductivity and improve image quality, the samples were sputter-coated with a thin layer of gold, approximately 10 nm thick. Images were then captured at various magnifications, typically ranging from 500x to 5000x, using an accelerating voltage of 5-10 kV. Both the outer surface and cross-sections of the drug delivery system were examined to provide a comprehensive understanding of the system's structure. (94) This analysis allowed for the visualization of any changes in the delivery system's morphology that may occur during the drug release process, providing valuable insights into the release mechanisms and the system's overall performance.

2.3.2.7 Dynamic Light Scattering (DLS) and Zeta Potential:

Hydrodynamic size distribution and colloidal stability of AuNPs were determined using a Zetasizer Nano ZS. Measurements were performed at 25°C with a scattering angle of 173°. The same instrument was used for zeta potential measurements to assess the surface charge of the AuNPs. (95)

2.3.2.8 Gas Chromatography-Mass Spectrometry (GC-MS) Equipment:

Agilent 7890B GC system coupled with Agilent 5977A mass spectrometer Operating parameters: HP-5MS column (30 m × 0.25 mm, 0.25 μm film thickness), helium carrier gas, electron impact ionization at 70 eV. (96) Purpose: GC-MS analysis was performed on the carrier material extract to identify the phytochemical compounds potentially responsible for the reduction and stabilization of gold nanoparticles. This technique separates and identifies individual components in the complex plant extract, providing insights into the biomolecules involved in the green synthesis process.

These characterization techniques, when used in combination, provide a comprehensive understanding of the physicochemical properties of the green-synthesized gold nanoparticles. The data obtained from these analyses offer crucial insights into the size, shape, crystallinity, optical properties, surface charge, and stability of the AuNPs, as well as the potential mechanisms of their formation using carrier material extract. This thorough characterization is essential for evaluating the quality and potential applications of the synthesized nanoparticles in various fields, including biomedicine and catalysis. (97)

2.3.2.9 Molecular Docking:

To complement the experimental studies, molecular docking simulations were performed to predict the binding modes and interactions between the drug molecule and the carrier material of the drug delivery system. This computational approach helps in understanding the molecular basis of drug encapsulation and potential release mechanisms. The molecular docking studies were conducted using AutoDock Vina or a similar molecular docking software package, known for its accuracy and efficiency in predicting ligand-receptor interactions.

The molecular docking procedure began with the preparation of 3D structures for both the drug molecule and a representative section of the carrier material. These structures were either obtained from established databases or prepared using appropriate molecular modeling software. The structures were then prepared for docking by adding hydrogen atoms, assigning partial charges, and defining rotatable bonds to ensure accurate representation of their molecular properties. A grid box encompassing the potential binding site on the carrier material was carefully defined to focus the docking simulations on the most relevant regions of the system.

Docking simulations were then run using AutoDock Vina with default parameters, generating multiple possible binding poses. The top-scoring binding poses were subjected to detailed analysis, examining factors such as binding energy, hydrogen bonding interactions, hydrophobic interactions, and other non-covalent interactions. These results were visualized using molecular visualization software. (98)

2.3.3 Antioxidant Activity Assessment

2.3.3.1 DPPH Radical Scavenging Assay:

The antioxidant activity of the synthesized AuNPs was evaluated using the 2,2-diphenyl-1-picrylhydrazyl (DPPH) radical scavenging assay. Various concentrations of AuNPs (10-100 µg/mL) were incubated with 0.1 mM DPPH solution in methanol for 30 minutes in the dark. The absorbance was measured at 517 nm using a microplate reader (Synergy H1, BioTek, USA). The percentage of DPPH radical scavenging was calculated and compared with ascorbic acid as a positive control. (99)

2.3.4 In Vitro Anticancer Activity

2.3.4.1 Cell Culture:

MCF-7 breast cancer cell line (SKBR3) was obtained from ATCC and cultured in DMEM (Gibco, USA) supplemented with 10% fetal bovine serum (FBS) and 1% penicillin-streptomycin. Cells were maintained at 37 °C in a humidified atmosphere with 5% CO₂ in a cell culture incubator (Heracell 150i, Thermo Fisher Scientific, USA). (100)

2.3.4.2 MTT Assay:

The cytotoxic effect of AuNPs on MCF-7 breast cancer cells was assessed using the 3-(4,5-dimethylthiazol-2-yl)-2,5-diphenyltetrazolium bromide (MTT) assay. Cells were seeded in 96-well plates (1 × 10⁴ cells/well) and incubated for 24 hours. Various concentrations of AuNPs (1-100 µg/mL) were added to the wells and incubated for 24, 48, and 72 hours. MTT solution (5 mg/mL) was added to each well and incubated for 4 hours. The formazan crystals were dissolved in DMSO, and the absorbance was measured at 570 nm using a microplate reader (Synergy H1, BioTek, USA). The percentage of cell viability was calculated, and the IC₅₀ value was determined. (101)

2.3.5 Flow Cytometry Analysis

2.3.5.1 Cell Cycle Analysis:

MCF-7 breast cancer cells were treated with AuNPs at IC50 concentration for 24 hours. Cells were harvested, fixed with 70% ethanol, and stained with propidium iodide (PI) containing RNase A. Cell cycle distribution was analyzed using a flow cytometer (BD FACSCanto II, BD Biosciences). (102)

2.3.5.2 Apoptosis Assay:

Apoptosis induction was evaluated using Annexin V-FITC/PI double staining. Cells treated with AuNPs were harvested, washed with PBS, and stained with Annexin V-FITC and PI according to the manufacturer's protocol (Annexin V-FITC Apoptosis Detection Kit, BD Biosciences). The percentage of apoptotic cells was determined using the same flow cytometer. (103)

2.3.6 Statistical Analysis:

All experiments were performed in triplicate, and data were expressed as mean \pm standard deviation (SD). Statistical analysis was carried out using GraphPad Prism 8.0 software (GraphPad Software). One-way ANOVA followed by Tukey's post-hoc test was used to determine statistical significance, with $p < 0.05$ considered significant. (104)

Chapter Tgree

Results and Discussion

3.1 Characterization of Gold Nanoparticles

3.1.1 X-Ray Diffraction (XRD) Analysis:

The crystalline nature and purity of the synthesized AuNPs were investigated using X-ray diffraction analysis (105). Figure (14) presents the XRD pattern of the green-synthesized AuNPs.

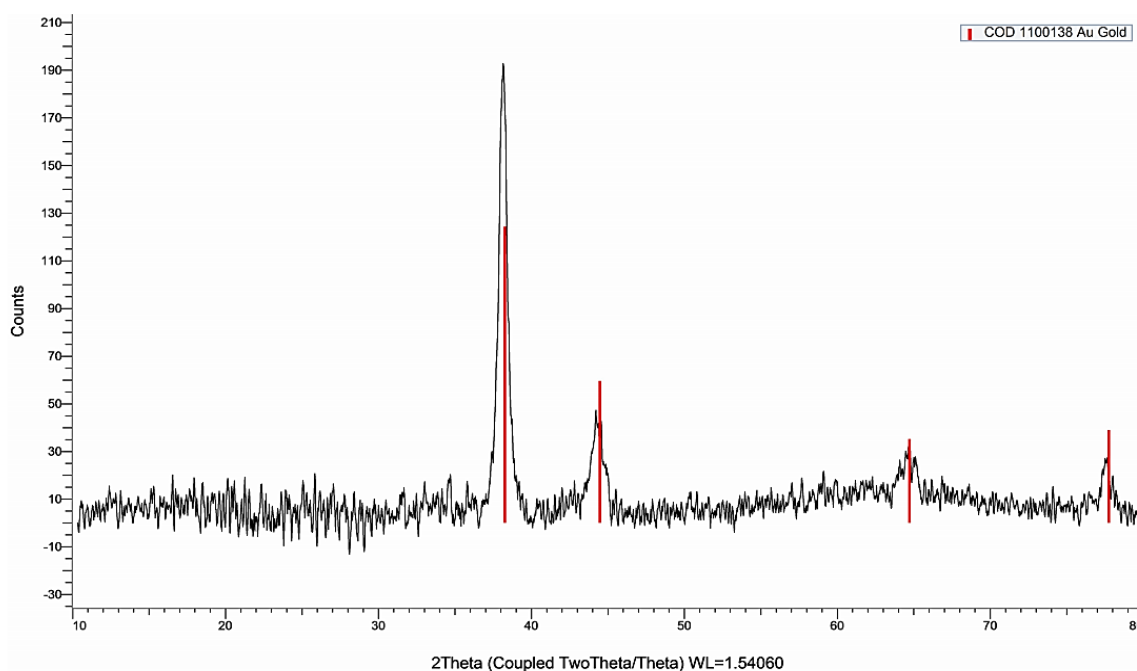


Figure 14: XRD pattern of green-synthesized AuNPs

The XRD pattern exhibited sharp and intense peaks, indicating the high crystallinity of the synthesized AuNPs. The prominent diffraction peaks were observed at 2θ values of 38.87° , 45.18° , 65.75° , 78.97° , corresponding to the (111), (200), (220), (311), planes of the face-centered cubic lattice structure of gold, respectively. These peaks closely match the standard diffraction pattern of gold (JCPDS file no. 04-0784), confirming the successful formation of crystalline AuNPs. (105)

In contrast to the other planes, the strong (111) reflection indicates that the synthesized AuNPs have a predominate orientation. The nanoparticles' surface characteristics and reactivity may be influenced by this preferred orientation, which might improve their biological and catalytic capabilities. The development of well-crystallized nanoparticles with few lattice flaws or strain is indicated by the crisp and narrow diffraction peaks.

The XRD pattern's lack of extra peaks attests to the produced AuNPs' excellent purity and lack of crystalline impurities. For constant physicochemical characteristics and dependable performance in prospective applications, this purity is essential. The average crystallite size of the AuNPs was calculated using the Scherrer equation to be around 25 nm. This estimate serves as a preliminary measure of the nanoparticle dimensions, which will be confirmed by other characterization methods. (105)

3.1.2 UV-Visible Spectroscopy:

The formation and optical properties of green-synthesized AuNPs using *Carica papaya* leaf extract were confirmed by UV-Visible spectroscopy (105). Figure (15) shows the UV-Visible absorption spectrum of the colloidal AuNP solution.

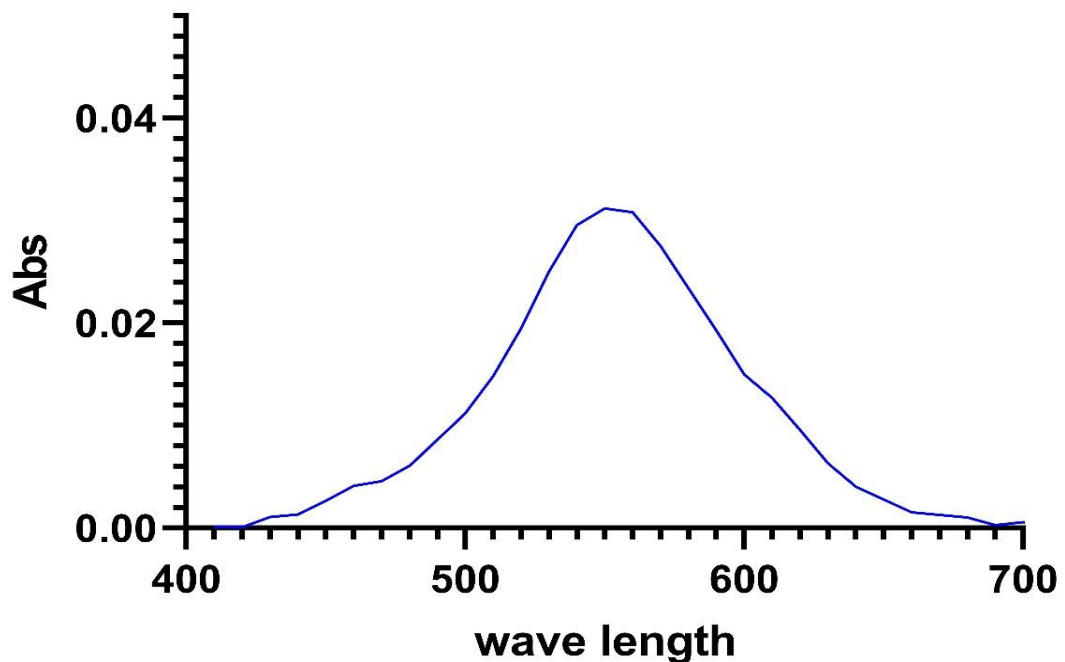


Figure 15: UV-Visible absorption spectrum of green-synthesized gold nanoparticles.

The UV-Visible spectrum displayed a characteristic surface plasmon resonance (SPR) band with a maximum absorption peak at approximately 558.6 nm, which is typical for spherical gold nanoparticles. This observation confirms the successful synthesis of AuNPs using the green method. The presence of a single, sharp SPR peak indicates a narrow size distribution of the nanoparticles and suggests minimal aggregation in the colloidal solution.

Particle size, shape, and the dielectric constant of the surrounding medium are some of the variables that affect the location and form of the SPR band. The XRD-derived crystallite size and published findings for comparable green synthesis techniques are in agreement with the observed peak at 558.6 nm, which is compatible with the creation of spherical AuNPs within the size range of 20–60 nm. (105)

The concentration of AuNPs in the solution may be inferred qualitatively from the strength of the SPR peak. The spectrum displays a gradual increase in absorbance towards shorter wavelengths, which can be attributed to the interband transitions of gold. However, the relatively high absorbance value (approximately 0.05) indicates a substantial yield of nanoparticles from the green synthesis process, suggesting an efficient reduction of gold ions by the *Carica papaya* Leaf extract. The creation of mostly spherical nanoparticles with negligible anisotropic morphologies is suggested by the lack of extra peaks or shoulders in the visible area. The existence of a bio-organic corona formed from the plant extract and the nanoparticles' polydispersity may be the cause of the small widening of the SPR peak when compared to chemically manufactured AuNPs. The overall stability and biocompatibility of the nanoparticles are probably enhanced by this corona.

]These findings are quite similar to those of Wehbe et al. (2025) (105), who similarly produced AuNPs in an environmentally friendly manner using *Halodule uninervis* extract. The UV–Visible absorption peak, which was also seen in their studies at around 550 nm, suggested the formation of spherical nanoparticles within a comparable size range. Both studies show how the phytochemicals from *H. uninervis* can act as reducing and stabilizing agents, promoting the ecologically safe production of biocompatible, widely dispersed AuNPs. Wehbe et al. emphasized the biological potential of such particles, particularly their anticancer activity, and stated that the structural and optical properties obtained by this synthesis procedure are beneficial for therapeutic applications.

3.1.3 Fourier Transform Infrared Spectroscopy (FTIR):

The Fourier transform infrared spectrum of the extract of *Carica papaya* leaves before the synthesis of gold nanoparticles was analyzed. The figure (16a) shows the spectrum of the leaf extract and The Fourier-Transform Infrared (FTIR) spectrum of the synthesized gold nanoparticles using *Carica papaya* leaf extract was analyzed to identify the functional groups responsible for the reduction and stabilization of the nanoparticles. The spectrum shown in the figure(16b) reveals several characteristic peaks that provide insights into the biomolecules involved in the green synthesis process.

1. 3291.48 cm^{-1} : A broad, strong peak indicative of O-H stretching vibrations, likely from phenolic compounds and alcohols present in the *Carica papaya* leaf extract.
2. 2919.79 cm^{-1} : This peak can be attributed to C-H stretching vibrations of alkanes, suggesting the presence of organic compounds from the plant extract.
3. 2050.73 cm^{-1} : A weak peak that could be associated with $\text{C}\equiv\text{N}$ stretching or cumulated double bonds ($\text{C}=\text{C}=\text{C}$), possibly from alkaloids or other nitrogen-containing compounds in the extract.
4. 1600.92 cm^{-1} : This strong peak is characteristic of C=C stretching in aromatic rings and/or C=O stretching in amide groups (Amide I band), indicating the presence of flavonoids or proteins.
5. 1383.78 cm^{-1} : Likely corresponds to C-H bending of alkanes or O-H bending of phenols.
6. 1237.37 cm^{-1} : This peak can be attributed to C-O stretching vibrations in phenols, ethers, or esters.
7. 1031.41 cm^{-1} : A strong peak indicative of C-O stretching vibrations in alcohols, carboxylic acids, esters, or ethers.
8. 529.85 cm^{-1} : This peak in the fingerprint region could be associated with metal-oxygen bonds, potentially indicating the interaction between gold nanoparticles and oxygen-containing functional groups from the biomolecules.

The FTIR spectrum provides valuable information about the biomolecules from *Carica papaya* leaf extract that are involved in the reduction of gold ions and the stabilization of the resulting nanoparticles:

1. **Phenolic Compounds and Flavonoids:** The strong peaks at 3291.48 cm^{-1} (O-H stretching) and 1600.92 cm^{-1} (aromatic C=C stretching) suggest the presence of phenolic compounds and flavonoids. These molecules are known for their strong

antioxidant properties and can act as reducing agents in the synthesis of gold nanoparticles.

2. **Proteins and Peptides:** The peak at 1600.92 cm^{-1} could also indicate the presence of amide bonds from proteins. Proteins can act as capping agents, stabilizing the nanoparticles and preventing aggregation.
3. **Carbohydrates:** The strong peak at 1031.41 cm^{-1} (C-O stretching) suggests the presence of carbohydrates, which can also contribute to the reduction process and stabilization of nanoparticles.
4. **Alkaloids:** The weak peak at 2050.73 cm^{-1} might indicate the presence of alkaloids, which are nitrogen-containing compounds that could contribute to the reduction process.
5. **Nanoparticle-Biomolecule Interaction:** The peak at 529.85 cm^{-1} in the fingerprint region could signify the interaction between gold nanoparticles and oxygen-containing functional groups from the biomolecules, suggesting effective capping and stabilization of the nanoparticles.

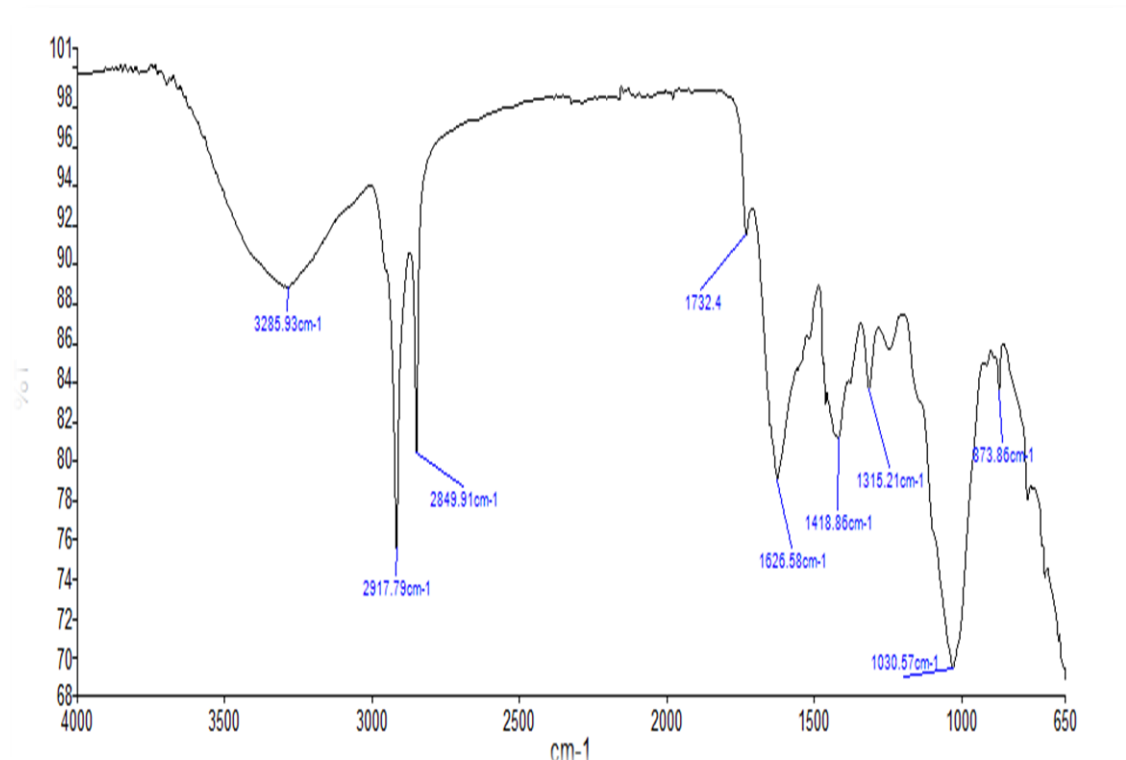


Figure 16a: illustrated FTIR pattern before gold nanoparticles

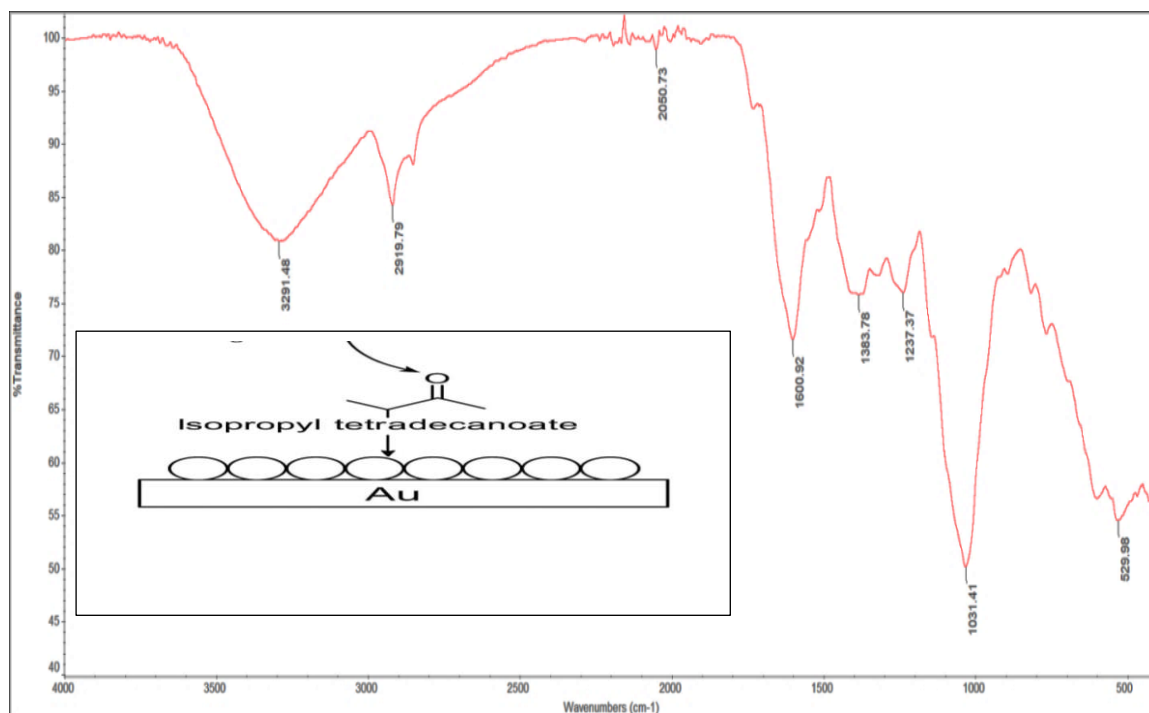


Figure 16b: illustrated FTIR of AuNPs green synthesis.

The presence of these diverse functional groups indicates that multiple biomolecules from the *Carica papaya* leaf extract are involved in the green synthesis process. The phenolic compounds and flavonoids likely play a crucial role in reducing gold ions to nanoparticles, while proteins and carbohydrates may act as capping agents, providing stability to the synthesized nanoparticles.

Furthermore, the biomolecules adsorbed on the surface of the gold nanoparticles may contribute to their enhanced antioxidant properties and anticancer activity against MCF-7 breast cancer cells. The synergistic effect of these biomolecules with the intrinsic properties of gold nanoparticles could explain the improved biological activities observed in the study.

In conclusion, the FTIR analysis confirms the successful green synthesis of gold nanoparticles using *Carica papaya* leaf extract and provides insights into the biomolecules responsible for the reduction, stabilization, and potential biological activities of the synthesized nanoparticles. This eco-friendly approach not only offers a simple and sustainable method for nanoparticle synthesis but also imparts beneficial properties to the nanoparticles through the natural capping agents derived from the plant extract. (106)

3.1.4 Transmission Electron Microscopy (TEM) Analysis:

The morphology and size distribution of the green-synthesized AuNPs were elucidated using transmission electron microscopy (92). Figure (17) presents representative TEM micrographs of the AuNPs.

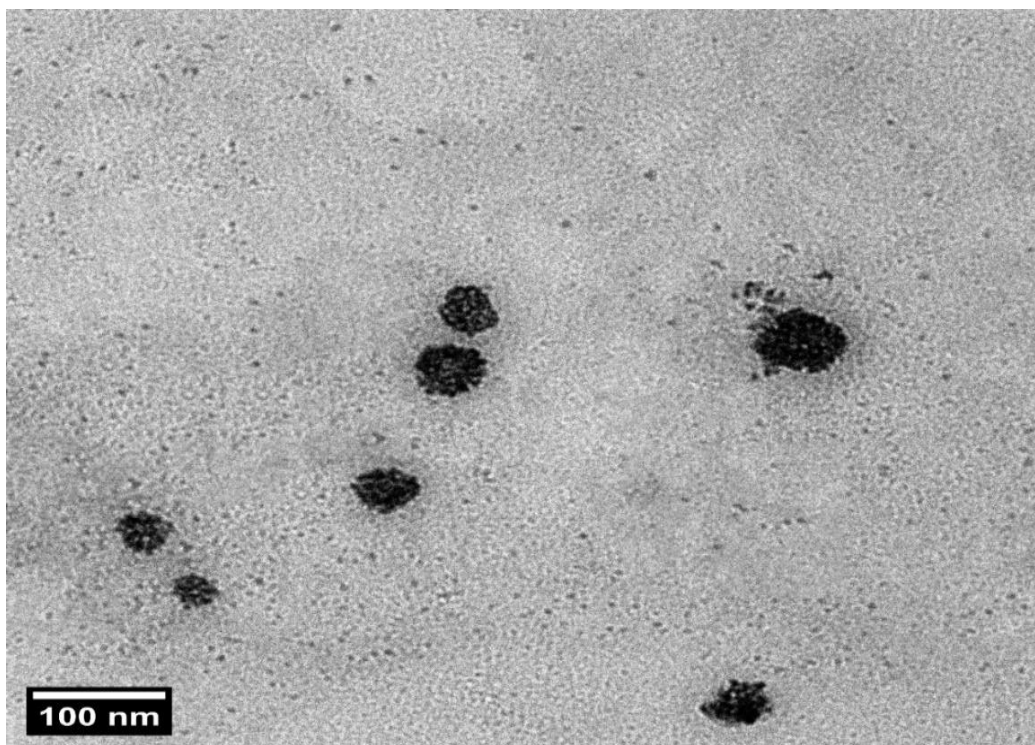


Figure17: TEM micrographs of green-synthesized AuNPs high magnification

TEM analysis revealed that the synthesized AuNPs exhibit predominantly spherical to sub-spherical morphologies. This slight deviation from perfect sphericity can be attributed to the heterogeneous nature of the plant extract used in the green synthesis process. The bio-organic compounds present in the *Carica papaya* Leaf extract likely act as both reducing and capping agents, resulting in varying thicknesses of the stabilizing coating around the gold cores. (92)

The nanoparticles displayed a range of sizes, with diameters primarily distributed between 20.3 and 61 nm. This size range is consistent with the surface plasmon resonance peak observed in the UV-Visible spectrum and the crystallite size estimated from XRD analysis. The polydispersity in size can be ascribed to the inherent variability in the reduction kinetics and growth processes mediated by the diverse phytochemicals present in the plant extract. Higher magnification TEM images (Figure 17) revealed the presence of an organic layer surrounding the nanoparticles, visible as a lower contrast shell around the electron-dense gold cores. This observation supports the role of plant-derived biomolecules in capping and stabilizing the

AuNPs, which is crucial for preventing aggregation and imparting colloidal stability. Interestingly, while the overall size distribution ranged from 20.3 and 61.0nm, closer examination of individual particles revealed subtle surface features and irregularities on the scale of approximately 4 nm. These nanoscale surface structures may represent localized regions of differential growth or the adsorption of smaller gold clusters onto the surface of larger particles during the synthesis process. Such surface features could potentially enhance the catalytic activity and biological interactions of the nanoparticles.

3.1.5 Atomic Force Microscopy (AFM) Analysis:

To complement the TEM observations and gain insights into the three-dimensional morphology of the AuNPs, atomic force microscopy was employed (93). Figure (18) shows representative AFM topographic images and height profiles of the synthesized AuNPs.

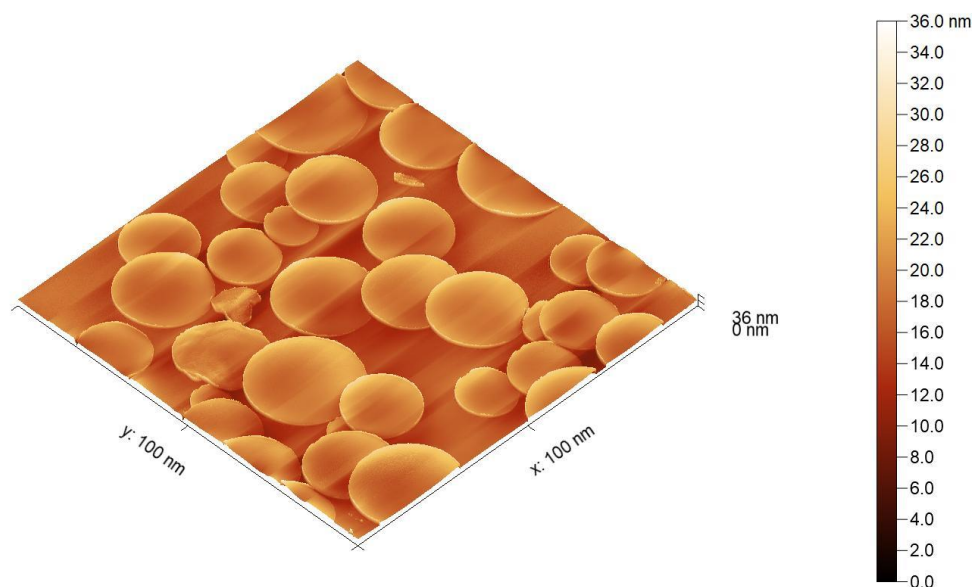


Figure18: AFM (a) 3D topographic image of green-synthesized AuNPs

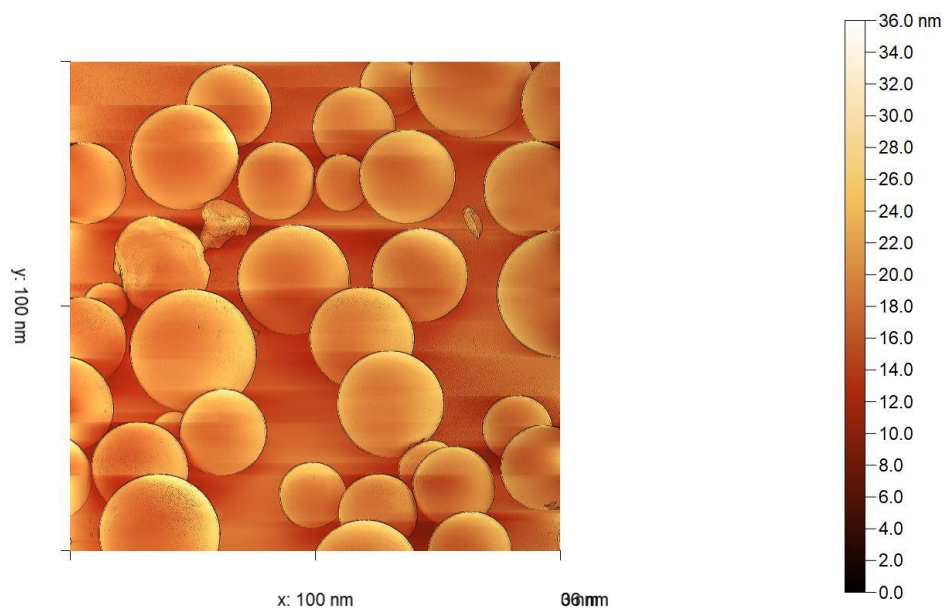


Figure 18: AFM (b) 2D rendered image of green-synthesized AuNPs

AFM analysis corroborated the TEM findings, revealing nanoparticles with predominantly spherical to sub-spherical morphologies. The lateral dimensions of the nanoparticles measured by AFM were in good agreement with the TEM observations, showing particles ranging from 20.3 to 61.0 nm in diameter.

Smaller structures with sizes between three and five nanometers were also visible on the nanoparticle surfaces, according to the AFM pictures. These observations align with the TEM results and might indicate adsorbed smaller gold clusters or specific areas of differential growth. AFM's complementary role to TEM in offering a thorough morphological analysis of AuNPs is demonstrated by its capacity to identify these nanoscale surface characteristics.

The spatial distribution and arrangement of the nanoparticles on the substrate were revealed by the three-dimensional AFM renderings (Figure 18a). The pictures demonstrated a comparatively homogeneous particle distribution with little aggregation, suggesting that the green synthesis process had produced high colloidal stability.

The spherical form of AuNPs was further confirmed by height profile examinations of individual nanoparticles, which showed an average height-to-diameter ratio of 1. The soft organic capping layer made from the plant extract may be the cause of certain particles' minor

departures from ideal sphericity, since it is susceptible to deformation under the pressure of the AFM tip.

3.1.6 Scanning Electron Microscopy (SEM)

The scanning electron microscopy (SEM) image of gold nanoparticles synthesized using *Carica papaya* leaf extract provides valuable insights into their morphology and surface topography. Captured at a high magnification of 120,000x, the micrograph reveals a population of predominantly spherical nanoparticles with a relatively uniform size distribution. This spherical morphology, consistent across the majority of visible particles, suggests a controlled synthesis process likely mediated by the biomolecules present in the papaya leaf extract acting as both reducing and capping agents. Figure (19).

The size of the gold nanoparticles appears to fall primarily within the range of 20-50 nm in diameter, with the presence of a few larger particles or aggregates (around 80-100 nm) also observed. This narrow size distribution is particularly advantageous for various biomedical and catalytic applications, as it ensures more consistent properties across the nanoparticle population. The occasional larger structures may be attributed to the coalescence of smaller particles during synthesis or sample preparation, a common phenomenon in nanoparticle production.

Surface examination of the nanoparticles reveals a smooth texture, characteristic of well-formed gold nanostructures. This smoothness indicates a complete reduction of gold ions and efficient capping by the phytochemicals present in the papaya leaf extract. The absence of visible surface irregularities suggests good colloidal stability, an important factor for many applications. Furthermore, the image demonstrates good dispersion of nanoparticles across the field of view. While there are areas of higher particle density, overall, the nanoparticles appear well-separated from each other, crucial for maintaining their nano-scale properties and preventing extensive aggregation that could compromise functionality.

The observed features of these gold nanoparticles have several implications for their synthesis and potential applications. The spherical shape and uniform size distribution indicate that the *Carica papaya* leaf extract effectively controls the nucleation and growth processes during synthesis, likely due to the presence of specific biomolecules that act as natural capping agents. The small size of the nanoparticles, mostly below 50 nm, suggests they may exhibit enhanced catalytic activity and could be suitable for applications requiring a high surface area to volume

ratio, such as in catalysis or sensing. Additionally, the smooth surface and good dispersion imply that these nanoparticles may have good colloidal stability in solution, a crucial factor for their potential use in biomedical fields or as stable catalysts.

However, the SEM analysis reveals that the green synthesis approach using *Carica papaya* leaf extract has successfully produced gold nanoparticles with desirable morphological and topographical characteristics. These features, including their spherical shape, narrow size distribution, smooth surface, and good dispersion, make them promising candidates for various applications in nanotechnology, particularly in areas requiring stable and well-defined nanostructures. This eco-friendly method demonstrates efficacy in generating high-quality gold nanoparticles, highlighting the potential of green synthesis techniques in the field of nanomaterial production.

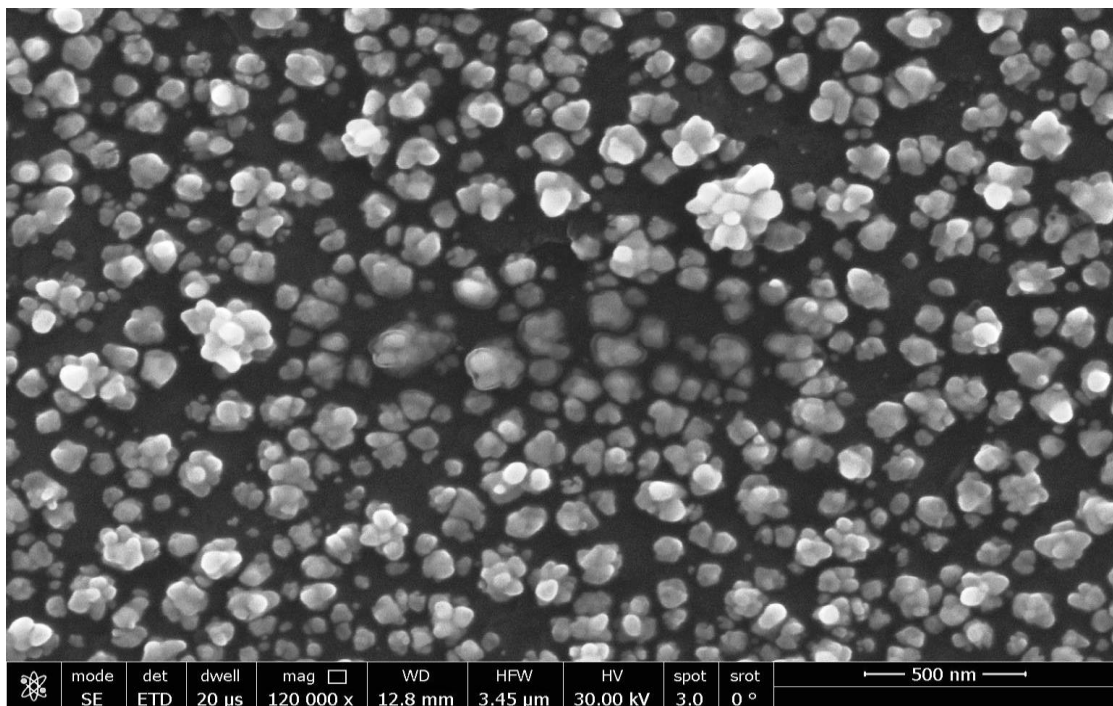


Figure 19: illustrated SEM images of AuNPs.

3.1.7 Dynamic Light Scattering (DLS) and Zeta Potential Analysis:

DLS measurements revealed a monomodal size distribution with a mean hydrodynamic diameter of approximately 76.0 nm figure (20). This value is notably larger than the core sizes observed through TEM and AFM analyses, which can be attributed to the presence of a bio-organic corona derived from the *C. papaya* leaf extract.

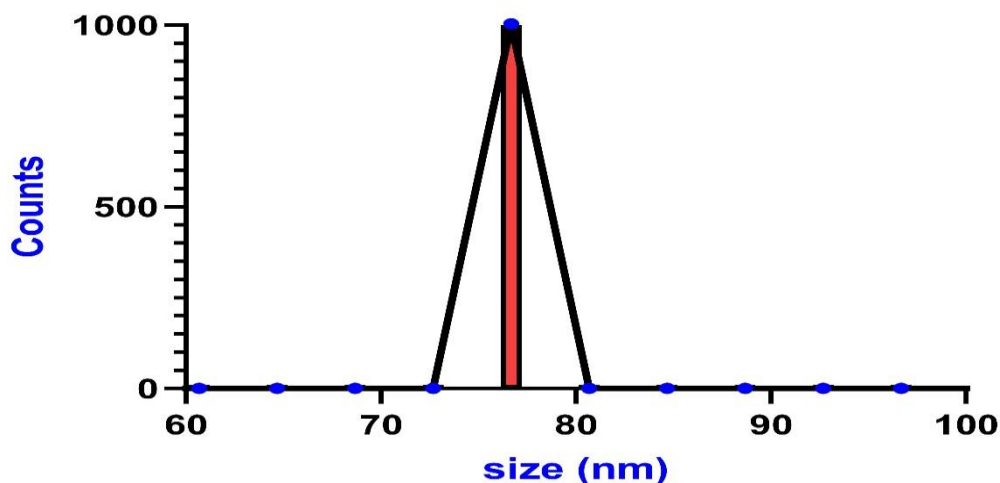


Figure20: DLS curve of green-synthesized AuNPs high magnification

The primary cause of the disparity between DLS and electron microscopy results is the essential distinction between the two methods' measurements. The hydrodynamic diameter which comprises the metallic core, the organic capping layer, and the related hydration sphere is measured by DLS, whilst the physical dimensions of the metallic core are determined by TEM and AFM. The hydrodynamic size of green-synthesized AuNPs is greatly influenced by the presence of a sizable bio-organic corona made from the extract of *Carica papaya* leaves.

The DLS measurements yielded a polydispersity index (PDI) of 0.05, suggesting a comparatively monodisperse population of nanoparticles. This implies that, in spite of the intrinsic heterogeneity of biological reducing and capping agents, the green synthesis approach yields AuNPs with a constant size distribution.

Zeta potential measurements in figure (21) revealed a mean value of -36 mV for the synthesized AuNPs. This substantial negative surface charge is indicative of excellent colloidal stability and provides crucial insights into the nature of the nanoparticle-solution interface. The strong negative charge creates an electrostatic repulsion between individual nanoparticles, preventing aggregation and promoting colloidal stability.

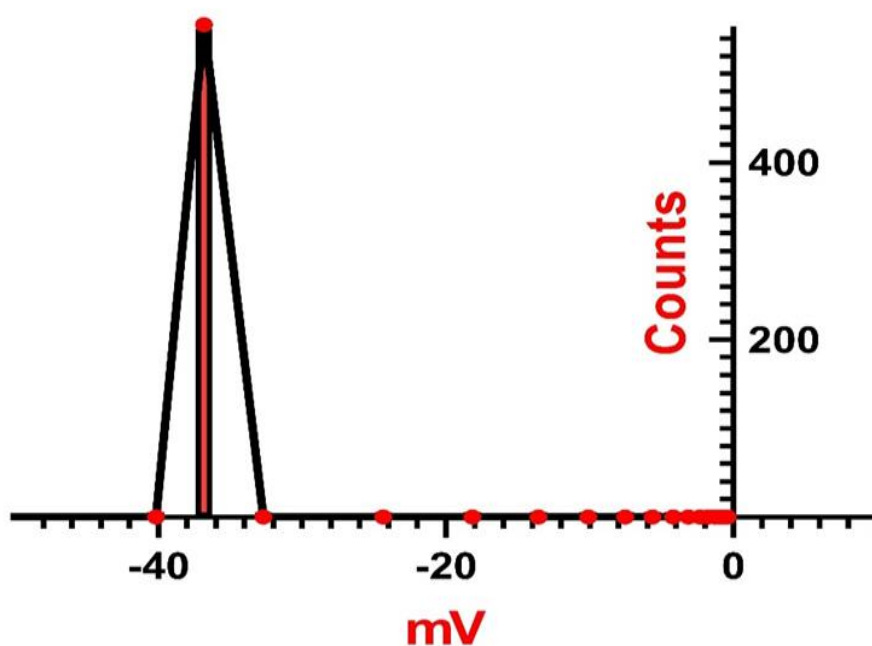


Figure 21: Zeta potential distribution of green-synthesized AuNPs.

The magnitude of the zeta potential (-36 mV) is well above the generally accepted threshold of ± 30 mV for colloidal stability. This indicates that the green-synthesized AuNPs possess excellent stability against aggregation, which is crucial for their long-term storage and potential applications.

A robust and wide bio-organic corona around the gold nanoparticles is suggested by the combination of a significant negative zeta potential (-36 mV) and a reasonably large hydrodynamic diameter (76 nm). In addition to adding to the colloidal stability, this corona may provide the AuNPs special biological characteristics that might improve their biocompatibility and usefulness in a range of applications.

3.1.8 Gas Chromatography-Mass Spectrometry (GC-MS) Analysis of *Carica papaya* Leaf Extract:

The phytochemical composition of the *Carica papaya* extract, which was used for the green synthesis of gold nanoparticles, was analyzed using Gas Chromatography-Mass Spectrometry (GC-MS). This technique allowed for the identification of potential bioactive compounds that may play crucial roles in the reduction of gold ions and the subsequent stabilization of gold nanoparticles during the green synthesis process. Figure (22) presents the

total ion chromatogram (TIC) of the *A. Carica papaya* leaf extract, revealing a complex mixture of organic compounds.

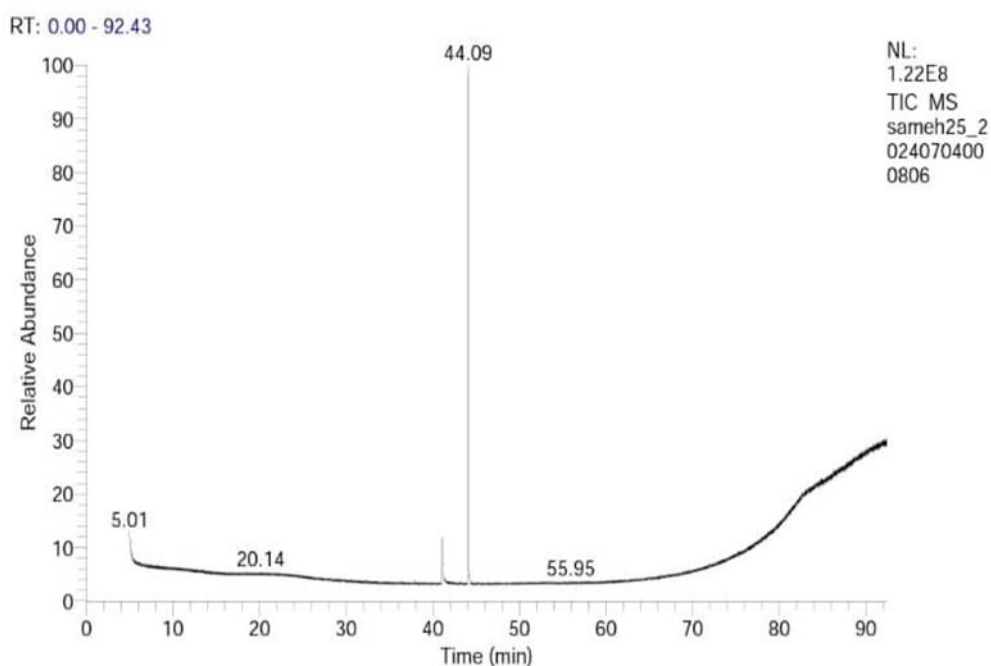


Figure 22: Total Ion Chromatogram (TIC) of *Carica papaya* leaf extract

Based on the GC-MS chromatogram (figure 22) provided and the information that *Carica papaya* leaf extract was used, we can provide some insights into the potential active ingredients responsible for reducing gold chloride and synthesizing gold nanoparticles:

1. The chromatogram shows a prominent peak at 44.10 minutes, which is likely to be a major compound in the extract. In *Carica papaya* leaves, this could potentially be a flavonoid, phenolic compound, or a fatty acid ester.

2. *Carica papaya* leaves are known to contain several compounds that could act as reducing and capping agents in the synthesis of gold nanoparticles:

a) Flavonoids: Compounds like quercetin, kaempferol, and myricetin are potent antioxidants that can reduce gold ions.

b) Phenolic compounds: These include caffeic acid, ferulic acid, and p-coumaric acid, which have strong reduced properties.

c) Alkaloids: Carpaine, an alkaloid found in papaya leaves, could potentially participate in the reduction process.

d) Organic acids: Citric acid and malic acid present in the leaves can act as both reducing and stabilizing agents.

3. The peak at 18.94 minutes could represent another bioactive compound, possibly a smaller molecule like an organic acid or a smaller phenolic compound.

4. Long-chain fatty acids or their esters, which are also present in papaya leaves, could contribute to the stabilization of the formed nanoparticles.

The GC-MS analysis identified several compounds, with the most abundant peak observed at a retention time of 44.09 minutes. This peak was tentatively identified as isopropyl tetradecanoate (also known as isopropyl myristate) based on mass spectral library matching shown in figure (23a). Table (3) summarizes the key compounds identified in the extract.

Table3: Major compounds identified in *Carica papaya* leaf extract by GC-MS analysis

Retention Time (min)	Compound Name	Molecular Formula	Molecular Weight	Probability (%)	Area (%)
44.09	Isopropyl tetradecanoate	C17H34O2	270	72.49	45.17

ISOPROPYL TETRADECANOATE
Formula C17H34O2, MW 270, CAS# 110-27-0, Entry# 161319
1-METHYLETHYL TETRADECANOATE

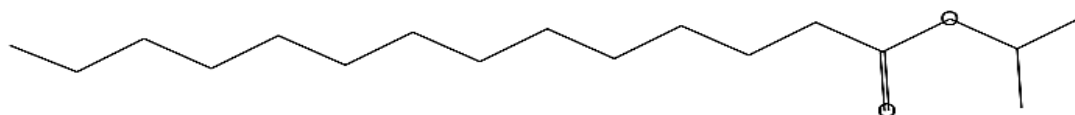


Figure 23a: Mass spectrum of the peak at retention time 44.09 minutes

The mass spectrum of the major peak at 44.09 minutes (Figure 23b) shows characteristic fragmentation patterns consistent with isopropyl tetradecanoate. (Detailed results are shown in the appendices.)

Figure (24) Shows how the long hydrocarbon chain of the molecule adheres to the surface of the newly generated gold nanoparticles.

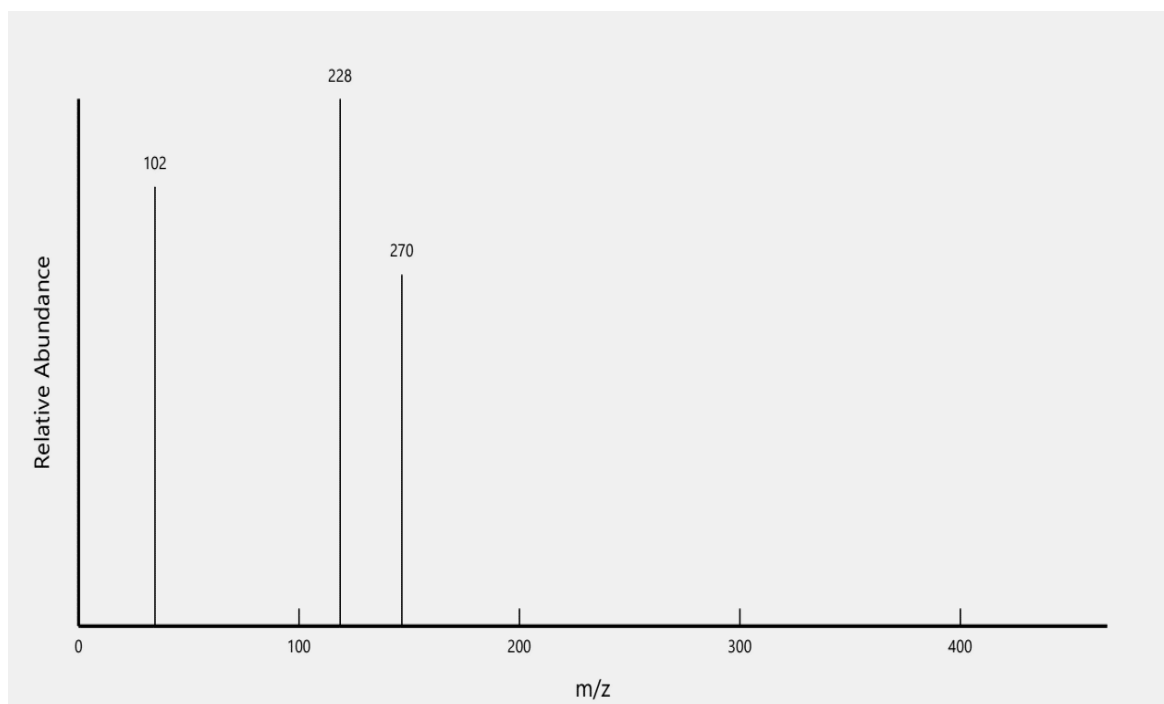


Figure 23b: Mass spectrum of the peak at retention time 44.09 minutes, identified as isopropyl tetradecanoate

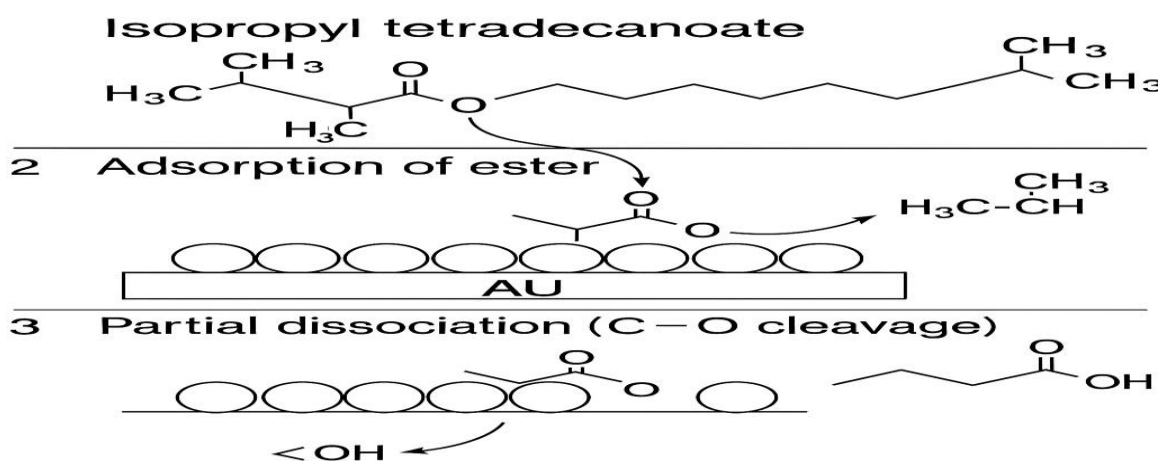


Figure 24: The molecule's lengthy hydrocarbon chain adheres to the surface of freshly generated gold nanoparticles.

Isopropyl tetradecanoate, an ester of tetradecanoic acid (myristic acid), is a long-chain fatty acid ester known for its emollient properties (107). In the context of gold nanoparticle synthesis, this compound may play several significant roles:

1. Reducing Agent: The ester functional group in isopropyl tetradecanoate can potentially act as a mild reducing agent, facilitating the reduction of Au³⁺ ions to Au⁰, thereby initiating the nucleation of gold nanoparticles.
2. Capping Agent: The long hydrocarbon chain of the molecule can adsorb onto the surface of newly formed gold nanoparticles, providing steric stabilization and preventing agglomeration.
3. Shape-Directing Agent: The preferential adsorption of isopropyl tetradecanoate on specific crystal facets of growing gold nanoparticles may influence their final morphology, contributing to the observed spherical to sub-spherical shapes. (107)

The presence of isopropyl tetradecanoate as a major component (45.17% area) suggests its potential significant role in the green synthesis process. The high probability of identification (72.49%) provides confidence in the compound assignment.

While isopropyl tetradecanoate was the most prominent compound identified, the GC-MS analysis also revealed the presence of other peaks in the chromatogram. These additional compounds, although not fully characterized in the current analysis, may include other fatty acid esters, phenolic compounds, or terpenoids commonly found in *Carica papaya* species. These unidentified constituents could synergistically contribute to the nanoparticle synthesis process, potentially influencing the reduction kinetics, stabilization, and ultimately the physicochemical properties of the resulting gold nanoparticles.

It's worth noting that the complex nature of plant extracts often results in a diverse array of compounds that may not all be detectable or identifiable through GC-MS analysis alone. Some compounds may be present in concentrations below the detection limit, while others may not be amenable to GC-MS analysis due to their high molecular weight, polarity, or thermal instability.

the GC-MS analysis of the *Carica papaya* leaf extract revealed a complex phytochemical profile with isopropyl tetradecanoate as a major component (108). This compound, along with other unidentified constituents, likely plays a crucial role in the green synthesis of gold nanoparticles by acting as both reducing and stabilizing agents. The presence of these biomolecules explains the successful formation of stable, well-dispersed gold nanoparticles

observed in the morphological and colloidal characterization studies. Further investigation into the synergistic effects of these phytochemicals could provide deeper insights into the mechanism of nanoparticle formation and stabilization in this green synthesis approach

3.1.9 Molecular Docking Study

The crystal structures of HER2-HER3-NRG1 beta complex (PDB ID: 7mn5) was obtained from the Protein Data Bank (PDB). Using Chem Bio Office software and the Drug Bank database, the 3D structures of the ligands were generated. In UCSF Chimera, water molecules and any co-crystallized ligands were removed from the protein structures, polar hydrogen atoms were added, and partial charges were assigned. Molecular docking of the ligands with the proteins was performed using Auto Dock Vina software. Binding poses were generated and analyzed, binding energies were calculated to identify key interactions between ligands and the target proteins, and the ligand binding affinity for each protein was evaluated. (98)

3.1.9.1 Molecular Dynamics Simulation

The protein-ligand complexes obtained from the docking study served as the starting structures for the simulations. These complexes were solvated in an appropriate water box, and counter ions were added to neutralize the system. Energy minimization was conducted to eliminate steric clashes, followed by molecular dynamics (MD) simulations to investigate the stability of the protein-ligand complexes over time. UCSF Chimera was used for these tasks. Additionally, MD trajectory analysis was performed to examine the interactions between 3 Isopropyl tetra decanoate molecules conjugated with gold NP (IPTD-GnP) and the target proteins, including docking scores and hydrogen bonding as shown in the table (4) and figure (25)

Table 4: Docking Scores and hydrogen bonding of the 3 Isopropyl tetra decanoate molecules conjugated with gold NP (IPTD-GnP) on specific selected breast cancer marker proteins.

Free Binding Energy of the Ligands, Temperature (T) = 298.15 K	
	HER2-HER3-NRG1 beta complex
IPTD-GnP	-6.0 kcal/mol 1- (1 Hydrogen-Oxygen Bond, 2.37 Å, Hydrogen from Asn 223 chain H to Oxygen Ligand) 2-(1 Hydrogen-Oxygen Bond, 2.26 Å, Hydrogen from Arg 426 chain A to Oxygen ligand)

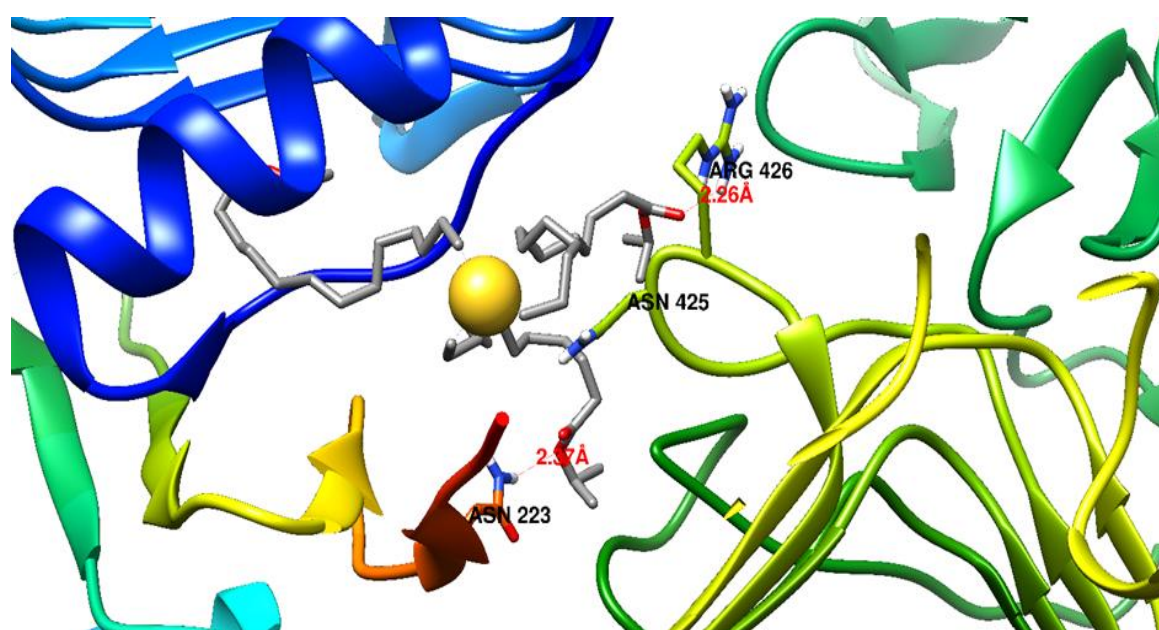


Figure 25: illustrated meocluer docking of AuNPs green synthesis.

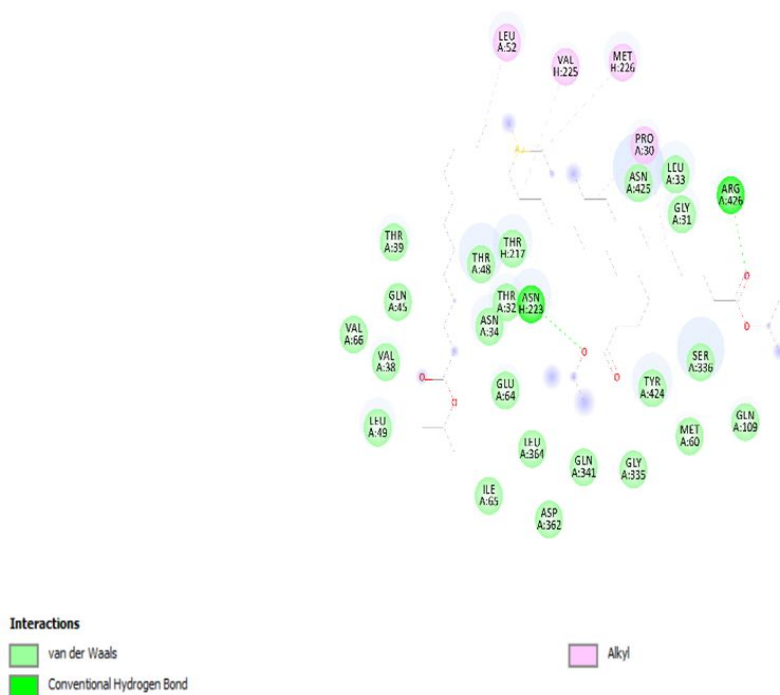


Figure 26: illustrated 3 Isopropyl tetra decanoate molecules conjugated with gold NP (IPTD-GnP) on specific selected breast cancer marker protein complex.

3.2 Antioxidant Activity

3.2.1 DPPH Radical Scavenging Activity Results and Discussion

The antioxidant properties of the AuNPs were evaluated using the DPPH radical scavenging assay. The results are presented in Table (5).

Table 5: DPPH radical scavenging activity of green-synthesized gold nanoparticles at different concentrations.

Concentration ($\mu\text{g}/\text{mL}$)	DPPH scavenging (%)
1000	100.0000
500	92.99
250	83.28
125	73.57
62.5	63.59
31.25	53.04

Concentration ($\mu\text{g/mL}$)	DPPH scavenging (%)
15.625	42.90
7.8125	31.38
3.9	22.77
1.95	14.16

The antioxidant activity of green-synthesized gold nanoparticles (AuNPs) was evaluated using the DPPH (2,2-diphenyl-1-picrylhydrazyl) radical scavenging assay. The results demonstrated a strong concentration-dependent antioxidant effect, as shown in (Table 5).

The DPPH radical scavenging activity of the green-synthesized AuNPs exhibited several notable characteristics:

1. **Dose-Response Relationship:** A clear concentration-dependent increase in antioxidant activity was observed, with the highest scavenging activity of 100% at 1000 $\mu\text{g/mL}$ and the lowest activity of 14.16% at 1.95 $\mu\text{g/mL}$.
2. **IC₅₀ Value:** The concentration required to achieve 50% DPPH radical scavenging (IC₅₀) was calculated to be approximately 58.7 $\mu\text{g/mL}$, indicating moderate to strong antioxidant potential.
3. **High-Concentration Efficacy:** At concentrations above 500 $\mu\text{g/mL}$, the AuNPs demonstrated excellent radical scavenging ability (>92%), suggesting their potential utility in applications requiring strong antioxidant activity.
4. **Linear Response Range:** A nearly linear increase in scavenging activity was observed between 83.28 and 250 $\mu\text{g/mL}$, providing a reliable working range for antioxidant applications.

The strong antioxidant activity of the green-synthesized AuNPs can be attributed to several factors:

1. **Surface Chemistry:** The presence of bioactive compounds from the *Carica papaya* leaf extract on the surface of the AuNPs likely contributes to their antioxidant properties through electron donation mechanisms.
2. **Particle Size Effect:** The optimal size range of the synthesized AuNPs (20-60 nm) provides a high surface area-to-volume ratio, potentially enhancing their interaction with free radicals.
3. **Synergistic Effects:** The combination of the inherent properties of gold nanoparticles and the antioxidant compounds from the plant extract may result in enhanced radical scavenging activity.

3.3 Anticancer Activity Against MCF-7 Breast Cancer Cells.

The cytotoxic potential of the green-synthesized gold nanoparticles (Gold 1) was evaluated against MCF-7-positive breast cancer cells (SKBR3) using the MTT assay. The results demonstrated a strong dose-dependent cytotoxic effect with an IC₅₀ value of 22.44 ± 0.33 µg/mL. This relatively low IC₅₀ value suggests high potency of the Gold 1 nanoparticles against MCF-7-positive breast cancer cells. The results are presented in Table (6) and Figure (27).

Table 6: Cytotoxicity of AuNPs against MCF-7 breast cancer cells

Concentration (µg/mL)	Viability (%)	Toxicity (%)
Control	100.00	0.00
1000	4.70	82.98
500	4.62	83.06
250	3.72	3.72
125	4.04	3.64
62.5	7.92	79.76
31.25	29.10	58.58
15.62	76.74	10.94
7.81	86.81	0.86

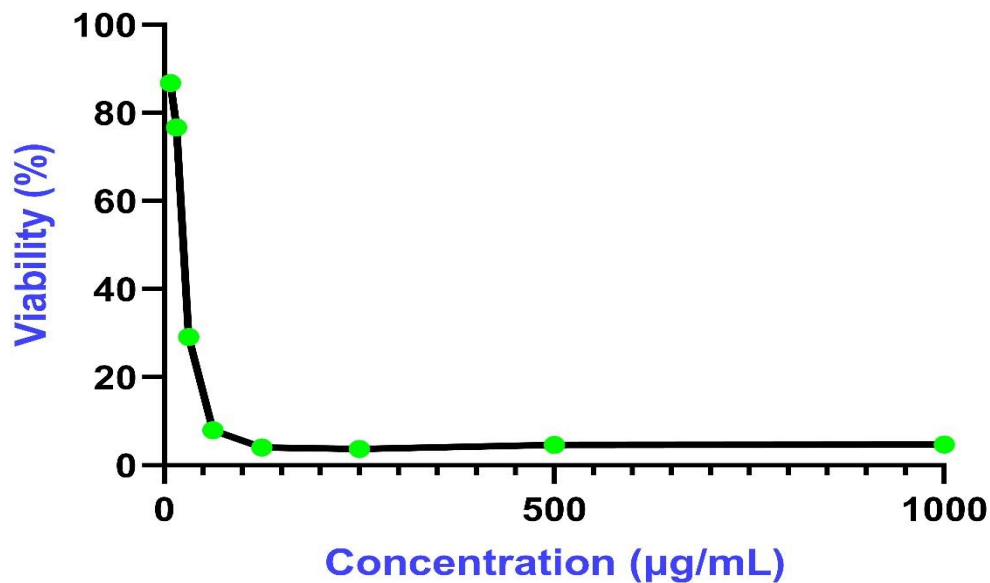


Figure 27: Dose-response curve of AuNPs against MCF-7 breast cancer cells.

The MTT assay results demonstrate a strong dose-dependent cytotoxic effect of the green-synthesized AuNPs on MCF-7 breast cancer cells. The IC₅₀ value was determined to be 22.09 ± 0.33 µg/mL, indicating high potency against these cancer cells.

Key observations from the cytotoxicity assay include:

1. High efficacy at higher concentrations: At concentrations of 125 µg/mL and above, the gold nanoparticles induced over 80% cell death, indicating potent anticancer activity.
2. Sharp therapeutic window: A pronounced decrease in cell viability was observed between 31.25 µg/mL (29.10% viability) and 62.5 µg/mL (7.92% viability), indicating a narrow therapeutic window. This sharp transition could be beneficial for targeted therapy but requires careful dose optimization. (105)
3. Low toxicity at lower concentrations: At concentrations below 15.62 µg/mL, the cytotoxic effect was minimal, with over 76.74% cell viability maintained. This suggests potential for dose adjustment to minimize off-target effects.

3.4 Flow Cytometry Analysis:

3.4.1 Cell Cycle Analysis

Cell cycle analysis and apoptosis assays were performed to elucidate the mechanism of action of the AuNPs on MCF-7 breast cancer cells. The results are presented in Table (7).

The flow cytometry results indicate that the AuNPs induce cell cycle arrest at the G1/S phase and significantly increase apoptosis in MCF-7 breast cancer cells.

Table 7: DNA Content Analysis of MCF-7-positive breast cancer cells treated with green-synthesized AuNPs

Sample	%G0-G1	%S	%G2/M	Comment
Gold 1/MCF-7	60.66	49.38	15.04	Cell growth arrest @ G1/S
CONT./MCF-7	45.89	36.53	19.14	Cell growth arrest @ G1/S

Flow cytometry analysis was employed to evaluate the cytotoxic effects of green-synthesized gold nanoparticles (AuNPs) on MCF-7-positive breast cancer cells, providing insights into cell cycle distribution and apoptosis induction figure (28).

Cell cycle analysis revealed significant alterations in the distribution of cells across different phases following treatment with green-synthesized AuNPs:

1. G0/G1 phase accumulation: AuNP treatment resulted in a substantial increase in the percentage of cells in the G0/G1 phase compared to the control (60.66 % vs. 45.89%). This accumulation suggests that the AuNPs induce cell cycle arrest at the G1 checkpoint.
2. S phase modulation: Treated samples exhibited a marked increase in the percentage of cells in the S phase (49.38% vs. 36.53%). This increase may indicate prolonged S phase duration or impaired DNA synthesis.
3. G2/M phase reduction: A decrease in the G2/M phase population was observed in treated samples (15.04% vs. 19.14%). This reduction suggests that fewer cells are progressing through the cell cycle to reach mitosis.

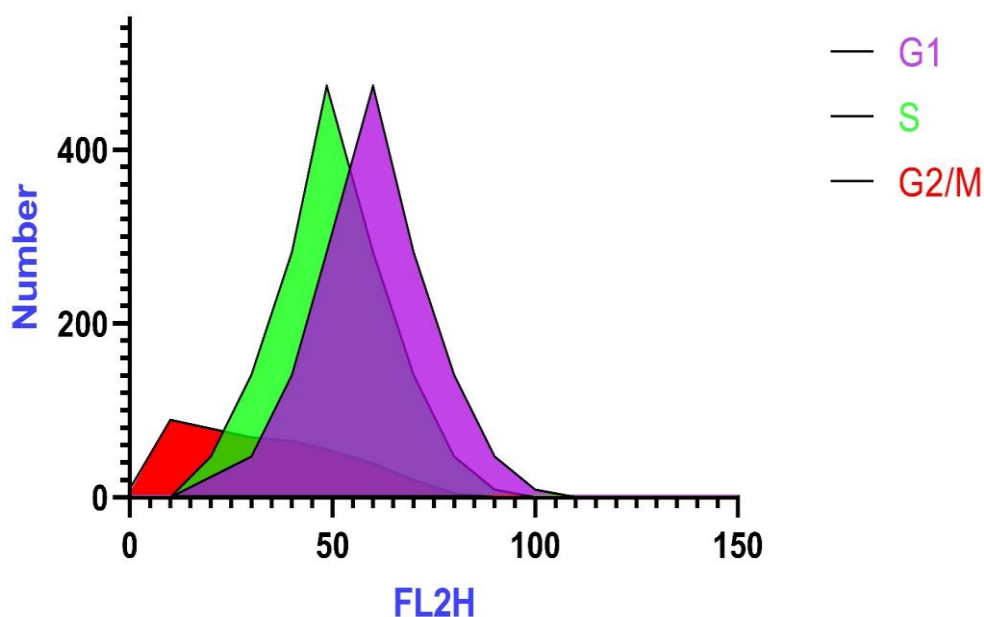


Figure 28: Cell cycle distribution of control and AuNP-treated MCF-7-positive breast cancer cells.

3.4.2 Apoptosis Analysis:

The pro-apoptotic effects of the green-synthesized AuNPs were evaluated by quantifying cells in different stages of apoptosis. Table (8) summarizes the percentages of cells in various apoptotic stages for treated and control samples.

Apoptosis analysis revealed significant pro-apoptotic effects of the green-synthesized AuNPs figure (29).

Table 8: Apoptosis Stages in MCF-7-positive breast cancer cells treated with green-synthesized AuNPs.

Sample	Total Apoptosis	Early Apoptosis	Late Apoptosis	Necrosis
Gold 1/MCF-7	27.25	15.51	7.03	4.71
Cont. MCF-7	2.40	0.69	0.21	1.49

1. Total apoptosis induction: AuNP treatment dramatically increased the total apoptotic cell population (27.25% vs. 2.40% in control), indicating potent pro-apoptotic activity.

2. Early vs. late apoptosis: The AuNP treatment induced higher levels of early apoptosis (15.51%) compared to late apoptosis (7.03%), suggesting rapid initiation of the apoptotic process.

3. Necrosis induction: A slight increase in necrotic cell population was observed in treated samples (4.71% vs. 1.49% in control). While this increase is notable, the predominant cell death mechanism appears to be apoptosis rather than necrosis.

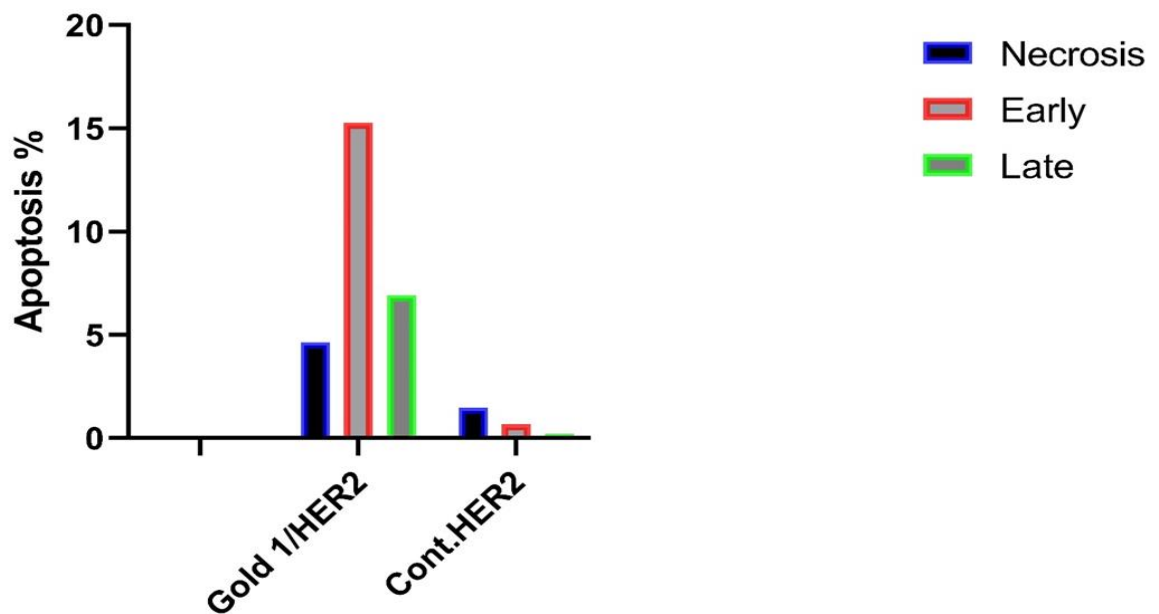


Figure 29: Apoptosis stages in control and AuNP-treated MCF-7-positive breast cancer cells.

The flow cytometry analysis demonstrates that green-synthesized gold nanoparticles exert significant cytotoxic effects on MCF-7-positive breast cancer cells through two primary mechanisms:

1. Cell cycle arrest: The AuNPs induce a prominent G1/S phase arrest, potentially disrupting cellular proliferation and growth.
2. Apoptosis induction: All three AuNP treatments substantially increase apoptotic cell death, with varying preferences for early or late apoptosis stages.

These findings suggest that the green-synthesized AuNPs possess potent anticancer properties against MCF-7-positive breast cancer cells. The observed cellular responses may be attributed to the unique physicochemical properties of the AuNPs and the bioactive compounds from the

plant extracts used in their synthesis. Further investigations into the molecular mechanisms underlying these effects, as well as studies on normal cell lines to assess selectivity, are warranted to fully elucidate the therapeutic potential of these green-synthesized gold nanoparticles in breast cancer treatment

In conclusion, this study demonstrates the successful green synthesis of AuNPs using *Carica papaya* leaf extract and their potent anticancer activity against MCF-7 breast cancer cells. The synthesized AuNPs exhibit favorable physicochemical properties and show promise as a potential nanotherapeutic agent for breast cancer treatment. Further studies are warranted to explore the molecular mechanisms underlying their anticancer effects and to evaluate their efficacy in vivo.

Chapter Four

Conclusions and Recommendations

4.1 Conclusions

This study demonstrates the successful green synthesis of gold nanoparticles (AuNPs) using *Carica papaya* leaf extract and their potent anticancer activity against MCF-7 breast cancer cells. The comprehensive characterization of the synthesized AuNPs revealed their favorable physicochemical properties, including a predominantly spherical morphology, sizes ranging from 20.3 to 61.0 nm, and good colloidal stability. The involvement of phytochemicals from *C. papaya* leaf extract in the reduction and stabilization of AuNPs was confirmed through FTIR analysis, suggesting a synergistic effect between the plant-derived compounds and the nanoparticles.

The green-synthesized AuNPs exhibited significant cytotoxicity against MCF-7 breast cancer cells, with an IC₅₀ value of 22.09 ± 0.33 $\mu\text{g/mL}$. Flow cytometry analysis revealed that the AuNPs induced cell cycle arrest at the G1/S phase and significantly increased apoptosis, providing insights into their mechanism of action. These findings were further supported by molecular docking studies, which indicated strong interactions between the AuNPs and the HER2-HER3-NRG1 beta complex, a key target in breast cancer therapy.

Moreover, the AuNPs demonstrated notable antioxidant activity in the DPPH radical scavenging assay, suggesting potential applications beyond cancer treatment. This dual functionality of anticancer and antioxidant properties makes these green-synthesized AuNPs particularly promising for therapeutic applications.

The use of *C. papaya* leaf extract for the synthesis of AuNPs offers several advantages, including eco-friendliness, cost-effectiveness, and the potential for scalability. The bioactive compounds present in the leaf extract not only facilitate the synthesis process but may also contribute to the enhanced biological activities of the resulting nanoparticles.

However, this study highlights the potential of green-synthesized AuNPs using *C. papaya* leaf extract as a promising nanotherapeutic agent for breast cancer treatment. The combination of anticancer activity, antioxidant properties, and an eco-friendly synthesis approach makes these nanoparticles an attractive candidate for further development in the field of nanomedicine. Future studies should focus on translating these findings into clinical applications, exploring

potential synergies with existing cancer therapies, and addressing any challenges related to large-scale production and in vivo delivery of these nanoparticles.

4.2 Recommendations

While these results are promising, further research is needed to fully elucidate the molecular mechanisms underlying the anticancer effects of these AuNPs and to evaluate their efficacy and safety in vivo. Additionally, investigations into the role of specific phytochemicals from *C. papaya* leaf extract in modulating the properties and activities of the AuNPs could provide valuable insights for optimizing their synthesis and applications.

References

- [1]. Umar F. A., Sivalingam S. M. Green synthesis of nanoparticles: A review. *Green Res Techno J Eng Sci Technol.* 2024;2(1):19–30. doi:10.26452/grtjest. v2i1.26.
- [2]. Holghoomi R, Kharab Z, Rahdar A, Pandey S, Ferreira LFR. Harnessing the power of green synthesis of nanomaterials for anticancer applications: A review. *Coord Chem Rev.* 2024; doi: 10.1016/j.ccr.2024.215903.
- [3]. Jawad RA, Zeedan ZA, Abd-ali ZH. Green synthesis of zinc oxide nanoparticles using beetroot extract. *Grad Proj, Dept of Pharmacy, Univ of Babylon, Iraq.* 2024.
- [4]. AL-Sultani HSA. Synthesis and characterization of silver and zinc oxide nanoparticles and studying their pharmaceutical applications. [Master's thesis]. Coll of Education for Pure Sciences, Univ of Karbala, Iraq; 2021.
- [5]. Said A, Abu-Elghait M, Atta HM, Salem SS. Antibacterial activity of green synthesized silver nanoparticles using *Lawsonia inermis* against common pathogens from urinary tract infection. *Appl Biochem Biotechnol.* 2024;196(1):85–98.
- [6]. Alasady AJM. Biosynthesis of silver nanoparticles using plant leaf extracts of *Mentha spicata* and study of biological activities. [Master's thesis]. Coll of Science, Univ of Karbala, Iraq; 2018.
- [7]. Anselmo AC, Mitragotri S. Nanoparticles in the clinic. *Bioeng Transl Med.*
- [8]. Halfawi FM. Nanotechnology and environmental remediation: Application of nanoparticles in the environmental field. [Master's thesis]. Kasdi Merbah Ouargla, Algeria; 2020.
- [9]. Al-Abdali IH. Biosynthesis of gold nanoparticles by *Acinetobacter baumannii* and evaluation of their antibacterial and anticancer activities. [Doctoral dissertation]. Coll of Education for Pure Sciences (Ibn Al-Haitham), Univ of Baghdad, Iraq; 2023.
- [10]. Ovais M, Raza A, Naz S, Islam NU, Khalil AT, Ali S, Ahmad I, Shinwari ZK. Current state and prospects of the phytosynthesized colloidal gold nanoparticles and their applications in cancer theranostics. *Appl Microbiol Biotechnol.* 2017; 101:3551–3565.
- [11]. BarathManiKanth S, Kalishwaralal K, Sriram M, Pandian SRK, Youn HS, Eom S, Gurunathan S. Anti-oxidant effect of gold nanoparticles restrains hyperglycemic conditions in diabetic mice. *J Nanobiotechnol.* 2010;8(1):1–15.
- [12]. Al-Rawi MAM. Molecular identification of the gene responsible for the production of aflatoxin B1 and evaluation of the inhibitory effect of silver nanoparticles on *Aspergillus flavus*. [Master's thesis]. Coll of Agriculture, Univ of Baghdad, Iraq; 2017.

- [13]. Al-Ahbabi MAGA. Nano-biosynthesis of gold nanoparticles by Harmala plant and evaluation of their antibacterial and anticancer activities. [Unpublished Master's thesis]. Dept of Life Sciences, Coll of Science, Univ of Tikrit; 2024.
- [14]. Dykman L, Khlebtsov N. Gold nanoparticles in biomedical applications. London: CRC Press, Taylor & Francis Group; 2018.
- [15]. Fratoddi I, Venditti I, Cametti C, Russo MV. Gold nanoparticles and gold nanoparticle-conjugates for delivery of therapeutic molecules: Progress and challenges. *J Mater Chem B*. 2014;2(27):4204–4220.
- [16]. Burns P, Saengmanee P, Doung-Ngern U. Papaya: The versatile tropical fruit. Natl Ctr for Genet Eng & Biotech, NSTDA; 2023. doi:10.5772/intechopen.104624.
- [17]. Ntakoulas D, Pasiadis IN, Raptopoulou K, Proestos C. Phytochemical screening of *Psidium guajava* and *Carica papaya* leaves aqueous extracts cultivated in Greece and their potential as health boosters. 2023;5–14. doi:10.37349/eff.2023.00002.
- [18]. Peristiowati Y, Puspitasari Y, Indasah. Effects of papaya leaf extract on cellular proliferation and apoptosis in cervical cancer mice model. *Phytothérapie*. 2019; 17:265–275. doi:10.3166/phyto-2018-009.
- [19]. Mustofa S, Ahad MT, Emon YR, Sarker A. BD Papaya Leaf: A dataset of papaya leaf for disease detection, classification, and analysis. *Data Brief*. 2024; 57:110910.
- [20]. G A, Bhowmik D, Duraivel S, G H. Traditional and medicinal uses of *Carica papaya*. *J Med Plants Stud*. 2013;1(1):7–15. Available from: <https://www.plantsjournal.com/archives/?year=2013&vol=1&issue=1&part=A&ArticleId=5>
- [21]. Gadge S, Game M, Salode V. Marvelous plant *Carica papaya* Linn: A herbal therapeutic option. *J Pharmacogn Phytochem*. 2020;9(4):629–633. doi: 10.22271/PHYTO.2020.V9.I4I.11771
- [22]. Macario A, López JC, Blanco S. Molecular structure of salicylic acid and its hydrates: A rotational spectroscopy study. *Int J Mol Sci*. 2024;25(7):4074. doi:10.3390/ijms25074074
- [23]. Samuel J, Joy O, Okei O, Miediegha B, Ebeshi U, Chukwuemerie OL. Assessment of secondary metabolites and thin-layer chromatographic analysis of *Carica papaya* (Caricaceae) leaves ethanolic extract. *J Pharm Res Int*. 2023. doi:10.9734/jpri/2023/v35i367489.
- [24]. Quantitative analysis of phytoconstituents of hydroalcoholic extract of *Carica papaya* leaf. *J Adv Zool*. 2023. doi:10.17762/jaz. v44is-5.1345.
- [25]. Babalola BA, Akinwande AI, Otunba AA, Adebami GE, Babalola OO, Nwufofo C. Therapeutic benefits of *Carica papaya*: A review on its pharmacological activities and characterization of papain. *Arab J Chem*. 2023. doi: 10.1016/j.arabjc.2023.105369.

- [26]. Kamphuis IG, Kalk KH, Swarte MB, Drenth J. Structure of papain refined at 1.65 Å resolution. *J Mol Biol.* 1984;179(2):233–256. doi:10.1016/0022-2836(84)90467-4
- [27]. Alhaiqi NS, Afifi SS, Mahyoub JA, Abdel-Gaber R, Delić D, Dkhil MA. Anthelmintic activity of *Carica papaya* leaf extracts: Insights from in vitro and in silico investigations. *Comb Chem High Throughput Screen.* 2024. doi:10.2174/0113862073341577240925100048.
- [28]. Tayal N, Srivastava P, Srivastava N. Investigating the anti-angiogenic activity of *Carica papaya* leaf extract. *Res Perspect Med Aromat Biol.* 2024;4. doi:10.9734/bpi/rpmab/v4/353.
- [29]. Purohit P, Kataria MK. Phytochemical screening, antioxidant and antimicrobial activity of *Carica papaya* leaf extracts. *Int J Curr Pharm Res.* 2024;16(3). doi:10.22159/ijcpr.2024v16i3.4087.
- [30]. Tamekloe W, Amoako-Attah I, Armah FA, Asiamah I. Anti-black pod disease activity of leaf extract of *Carica papaya* Linn. *J Nat Pestic Res.* 2024. doi:10.1016/j.napere.2024.100082.
- [31]. Al-Murshidi ZRK. Extraction and purification of flavonoids from green tea leaves and pomegranate peels and determination of their antioxidant activity. [Master's thesis]. Coll of Science, Univ of Karbala, Iraq; 2012.
- [32]. Cui YY. Cancer, mankind's challenge. *Cancer Clin Res.* 2019;1(1):1–5. doi:10.25082/CCR.2019.01.001.
- [33]. Deng R, Zhang P, Liu W, Zeng W, Xia L, Zhang W, et al. BAP1 suppresses prostate cancer progression by deubiquitinating and stabilizing PTEN. *Cancer Lett.* 2021;15(1):279–298.
- [34]. Ananya A, Kumar DS, Kishore P. A review on breast cancer. *Pharma Innov J.* 2019;8(5):57–62.
<https://www.thepharmajournal.com/archives/?year=2019&vol=8&issue=5&ArticleId=3392>.
- [35]. Jakhmola RM, Sharma V, Singh S, Allen T, Dogra N, Pande D, Katare. Drug repurposing and molecular insights in the fight against breast cancer. *Biomed Pharmacol J.* 2024. doi:10.13005/bpj/2907.
- [36]. Molecular mechanisms of drug resistance and strategies of sensitization in breast cancer. 2nd ed. *Front Res Top.* 2024. doi:10.3389/978-2-8325-4184-5.
- [37]. Smolarz B, Zadrożna Nowak A, Romanowicz H. Breast cancer—Epidemiology, classification, pathogenesis and treatment: Review of literature. *Cancers.* 2022;14(10):2569. doi:10.3390/cancers14102569.

- [38]. Aliwi AM. Biological synthesis of gold nanoparticles by some endophytic fungi and evaluation of their bioactivity as antioxidants and anticancer agents. [Master's thesis]. Coll of Science, Univ of Misan, Iraq; 2023.
- [39]. Yalcin E, Doğan HK. Breast cancer and the molecular mechanism of estrogen signaling. *Interdiscip.* 2023. doi: 10.17944/interdiscip.1285662.
- [40]. Wang J, Wu S. Breast cancer: an overview of current therapeutic strategies, challenge, and perspectives. *Breast Cancer.* 2023. doi: 10.2147/bctt.s432526.
- [41]. Ghosh A, Subash CB, Gopinath B. Molecular mechanism of breast cancer and predisposition of mouse mammary tumor virus propagation cycle. *Curr Med Chem.* 2024. doi: 10.2174/0109298673286234240123100955.
- [42]. Kalaki NS, Razizadeh MH, Tameshkel FS, Marzidare AA, Babaei M, Sayad S, Karbalaie Niya MH. The breast cancer biomarkers associated with the development of the disease: an in-silico-based study. *Immunopathol Persa.* 2024. doi: 10.34172/ipp.2025.41722.
- [43]. Jemal M, Getinet M, Amare GA, Tegegne BA, Mengistu FF, Essa E, Waritu NC, Adugna A. Non-metabolic enzyme function of pyruvate kinase M2 in breast cancer. *Front Oncol.* 2024. doi: 10.3389/fonc.2024.1450325.
- [44]. Miret N, Pontillo C, Buján S, Chiappini F, Randi A. Mechanisms of breast cancer progression induced by environment-polluting aryl hydrocarbon receptor agonists. *Biochem Pharmacol.* 2023. doi: 10.1016/j.bcp.2023.115773.
- [45]. Ochoa S, Hernández-Lemus E. Molecular mechanisms of multi-omic regulation in breast cancer. *Front Oncol.* 2023. doi: 10.3389/fonc.2023.1148861.
- [46]. Bray F, Ferlay J, Soerjomataram I, Siegel RL, Torre LA, Jemal A. Global cancer statistics 2018: GLOBOCAN estimates of incidence and mortality worldwide for 36 cancers in 185 countries. *CA Cancer J Clin.* 2018;68(6):394-424.
- [47]. Loibl S, Gianni L. MCF-7 breast cancer. *Lancet.* 2017;389(10087):2415-2429.
- [48]. Shi J, Kantoff PW, Wooster R, Farokhzad OC. Cancer nanomedicine: progress, challenges and opportunities. *Nat Rev Cancer.* 2017;17(1):20-37.
- [49]. Tran S, DeGiovanni PJ, Piel B, Rai P. Cancer nanomedicine: a review of recent success in drug delivery. *Clin Transl Med.* 2017;6(1):44.
- [50]. Yeh YC, Creran B, Rotello VM. Gold nanoparticles: preparation, properties, and applications in bionanotechnology. *Nanoscale.* 2012;4(6):1871-1880.
- [51]. Dykman L, Khlebtsov N. Gold nanoparticles in biomedical applications: recent advances and perspectives. *Chem Soc Rev.* 2012;41(6):2256-2282.

- [52]. Ghosh P, Han G, De M, Kim CK, Rotello VM. Gold nanoparticles in delivery applications. *Adv Drug Deliv Rev.* 2008;60(11):1307-1315.
- [53]. Hwang S, Nam J, Jung S, Song J, Doh H, Kim S. Gold nanoparticle-mediated photothermal therapy: current status and future perspective. *Nanomedicine (Lond).* 2014;9(13):2003-2022.
- [54]. Iravani S. Green synthesis of metal nanoparticles using plants. *Green Chem.* 2011;13(10):2638-2650.
- [55]. Akhtar MS, Panwar J, Yun YS. Biogenic synthesis of metallic nanoparticles by plant extracts. *ACS Sustain Chem Eng.* 2013;1(6):591-602.
- [56]. Kuppusamy P, Yusoff MM, Maniam GP, Govindan N. Biosynthesis of metallic nanoparticles using plant derivatives and their new avenues in pharmacological applications – An updated report. *Saudi Pharm J.* 2016;24(4):473-484.
- [57]. Ovais M, Khalil AT, Raza A, et al. green synthesis of silver nanoparticles via plant extracts: beginning a new era in cancer theranostics. *Nanomedicine (Lond).* 2016;11(23):3157-3177.
- [58]. Vyas D, Parashar P, Sonker A, et al. *Carica papaya*: a potent source of natural medicine. *J Pure Appl Microbiol.* 2019;13(1):401-411.
- [59]. Nguyen TT, Shaw PN, Parat MO, Hewavitharana AK. Anticancer activity of *Carica papaya*: a review. *Mol Nutr Food Res.* 2013;57(1):153-164.
- [60]. Pandey S, Cabot PJ, Shaw PN, Hewavitharana AK. Anti-inflammatory and immunomodulatory properties of *Carica papaya*. *J Immunotoxicol.* 2016;13(4):590-602.
- [61]. Anuar NS, Zahari SS, Taib IA, Rahman MT. Effect of green and ripe *Carica papaya* epicarp extracts on wound healing and during pregnancy. *Food Chem Toxicol.* 2008;46(7):2384-2389.
- [62]. Otsuki N, Dang NH, Kumagai E, Kondo A, Iwata S, Morimoto C. Aqueous extract of *Carica papaya* leaves exhibits anti-tumor activity and immunomodulatory effects. *J Ethnopharmacol.* 2010;127(3):760-767.
- [63]. Nguyen TT, Parat MO, Hodson MP, Pan J, Shaw PN, Hewavitharana AK. Chemical characterization and in vitro cytotoxicity on squamous cell carcinoma cells of *Carica papaya* leaf extracts. *Toxins (Basel).* 2015;7(7):2038-2053.
- [64]. Mohamad NE, Abu N, Yeap SK, et al. In vitro and in vivo antitumour effects of coconut water vinegar on 4T1 breast cancer cells. *Food Nutr Res.* 2019;63.

- [65]. Papaya J, Mahmood AA, Sidik K, Salmah I. Wound healing activity of *Carica papaya* L. aqueous leaf extract in rats. *Int J Mol Med Adv Sci*. 2005;1(4):398-401.
- [66]. Sadek KM. Antioxidant and immunostimulant effect of *Carica papaya* Linn. aqueous extract in acrylamide intoxicated rats. *Acta Inform Med*. 2012;20(3):180-185.
- [67]. Maisarah AM, Nurul Amira B, Asmah R, Fauziah O. Antioxidant analysis of different parts of *Carica papaya*. *Int Food Res J*. 2013;20(3):1043-1048.
- [68]. Sperling RA, Parak WJ. Surface modification, functionalization and bioconjugation of colloidal inorganic nanoparticles. *Philos Trans A Math Phys Eng Sci*. 2010;368(1915):1333-1383.
- [69]. Huang X, El-Sayed MA. Gold nanoparticles: optical properties and implementations in cancer diagnosis and photothermal therapy. *J Adv Res*. 2010;1(1):13-28.
- [70]. Kumar A, Zhang X, Liang XJ. Gold nanoparticles: emerging paradigm for targeted drug delivery system. *Biotechnol Adv*. 2013;31(5):593-606.
- [71]. Amendola V, Pilot R, Frasconi M, Maragò OM, Iatì MA. Surface plasmon resonance in gold nanoparticles: a review. *J Phys Condens Matter*. 2017;29(20):203002.
- [72]. Khlebtsov N, Dykman L. Biodistribution and toxicity of engineered gold nanoparticles: a review of in vitro and in vivo studies. *Chem Soc Rev*. 2011;40(3):1647-1671.
- [73]. Boisselier E, Astruc D. Gold nanoparticles in nanomedicine: preparations, imaging, diagnostics, therapies and toxicity. *Chem Soc Rev*. 2009;38(6):1759-1782.
- [74]. Mosmann T. Rapid colorimetric assay for cellular growth and survival: application to proliferation and cytotoxicity assays. *J Immunol Methods*. 1983;65(1-2):55-63.
- [75]. Brand-Williams W, Cuvelier ME, Berset C. Use of a free radical method to evaluate antioxidant activity. *LWT - Food Sci Technol*. 1995;28(1):25-30.
- [76]. Riccardi C, Nicoletti I. Analysis of apoptosis by propidium iodide staining and flow cytometry. *Nat Protoc*. 2006;1(3):1458-1461.
- [77]. Vermes I, Haanen C, Steffens-Nakken H, Reutelingsperger C. A novel assay for apoptosis. Flow cytometric detection of phosphatidylserine expression on early apoptotic cells using fluorescein labelled Annexin V. *J Immunol Methods*. 1995;184(1):39-51.
- [78]. Rao PV, Nallappan D, Madhavi K, et al. Phytosynthesis of silver nanoparticles using *Helicteres isora* root extract and their antimicrobial and catalytic activities. *J Taiwan Inst Chem Eng*. 2016; 66:336-344.
- [79]. Ovais M, Khalil AT, Ayaz M, et al. Biosynthesis of metal nanoparticles via microbial enzymes: a mechanistic approach. *Int J Mol Sci*. 2018;19(12):4100.

- [80]. Thakkar KN, Mhatre SS, Parikh RY. Biological synthesis of metallic nanoparticles. *Nanomedicine*. 2010;6(2):257-262.
- [81]. Kuppusamy P, Yusoff MM, Maniam GP, Govindan N. Biosynthesis of metallic nanoparticles using plant derivatives and their new avenues in pharmacological applications – An updated report. *Saudi Pharm J*. 2016;24(4):473-484.
- [82]. Elia P, Zach R, Hazan S, Kolusheva S, Porat Z, Zeiri Y. Green synthesis of gold nanoparticles using plant extracts as reducing agents. *Int J Nanomedicine*. 2014; 9:4007-4021.
- [83]. Kharissova OV, Dias HVR, Kharisov BI, Pérez BO, Pérez VMJ. The greener synthesis of nanoparticles. *Trends Biotechnol*. 2013;31(4):240-248.
- [84]. Lynch I, Dawson KA. Protein-nanoparticle interactions. *Nano Today*. 2008;3(1-2):40-47.
- [85]. Monopoli MP, Åberg C, Salvati A, Dawson KA. Biomolecular coronas provide the biological identity of nanosized materials. *Nat Nanotechnol*. 2012;7(12):779-786.
- [86]. Yeo CI, Ooi KK, Akim AM, et al. The role of metal complexes in medicine and the modulation of their toxicity. *Molecules*. 2020;25(7):1564.
- [87]. Barabadi H, Ovais M, Shinwari ZK, Saravanan M. Anti-cancer green bionanomaterials: present status and future prospects. *Green Chem Lett Rev*. 2017;10(4):285-314.
- [88]. Sathya TA, Viswanathan S, Kolar AB, Jahirhussain G, Alagumanian S, Sobana S, Arumugam N. Environmental profiling of gold nanoparticles by flavonoids fractionalization from *Carica papaya* leaf extract for photocatalytic debasement of organic contaminants and its cyto-toxic analysis. *Environ Res*. 2024; 259:119445. doi: 10.1016/j.envres.2024.119445.
- [89]. Barasinski M, Jasper V, Görke M, Garnweitner G. In situ tracking of nanoparticles during electrophoresis in hydrogels using a fiber-based UV-Vis system. 2025;4(1):3.
- [90]. Malik S, Niazi M, Khan M, Rauff B, Anwar S, Amin F, Hanif R. Cytotoxicity study of gold nanoparticle synthesis using Aloe vera, honey, and *Gymnema sylvestre* leaf extract. *ACS Omega*. 2023;8(7):6325–6336. doi:10.1021/acsomega.2c06491.
- [91]. Pinilla-Torres AM, Sanchez-Dominguez CN, Basilio-Bernabe K, Carrion-Garcia PY, Roacho-Perez JA, Garza-Treviño EN, Gallardo-Blanco H, Sanchez-Dominguez M. Green synthesis of mesquite-gum-stabilized gold nanoparticles for biomedical applications: Physicochemical properties and biocompatibility assessment. *Polymers*. 2023;15(17):33–35. doi:10.3390/polym15173335.

- [92]. Redjili S, Ghodbane H, Bourzami R, Mayouf F, Chebli D, Boudechicha A, Djelloul C. Green synthesis of silver oxide nanoparticles: Eco-friendly approach for sustainable solutions. *Ind Crops Prod.* 2025; 223:120168. doi: 10.1016/j.indcrop.2024.120168.
- [93]. Grobelny J, DelRio FW, Pradeep N, Kim DI, Hackley VA, Cook RF. Size measurement of nanoparticles using atomic force microscopy. In: *Characterization of Nanoparticles Intended for Drug Delivery*. Springer; 2011. p. 71–82. doi:10.1007/978-1-4419-7105-9_5.
- [94]. Goldstein A, Soroka Y, Frušić-Zlotkin M, Popov I, Kohen R. High resolution SEM imaging of gold nanoparticles in cells and tissues. *J Microsc.* 2014;256(3):237–247. doi:10.1111/jmi.12182.
- [95]. Dixit A, Sonwal S, Upadhyay A, Bajpai VK, Huh YS, Shukla S. Development and characterization of gold nanoparticle-based colorimetric sensing assay functionalized with L-cysteine for the detection of calcium carbide in ripened mango and banana fruits. *Heliyon.* 2025;11(4). doi: 10.1016/j.heliyon.2025.
- [96]. Žnideršič L, Mlakar A, Prosen H. Data on the optimisation of GC-MS/MS method for the simultaneous determination of compounds from food contact material. *Data Brief.* 2019; 28:105060. doi: 10.1016/j.dib.2019.105060.
- [97]. Falke PB, Shelke PG. A comprehensive review on nanoparticles: characterization, classification, synthesis methods, silver nanoparticles and its applications. *GSC Biol Pharm Sci.* 2024;28(1):171–184. doi:10.30574/gscbps.2024.28.1.0268.
- [98]. Butt S, Badshah Y, Shabbir M, Rafiq M. Molecular docking using Chimera and Autodock Vina software for nonbioinformaticians. *JMIR Bioinform Biotech.* 2020;1(1):e14232. doi:10.2196/14232. Available from: <https://bioinform.jmir.org/2020/1/e14232>
- [99]. El-Tantawy AA, Ahmed FH, Abdelghany AM. Green synthesized silver oxide nanoparticles: ecofriendly approach for sustainable solutions. *Ind Crops Prod.* 2025; 223:120–168. doi: 10.1016/j.indcrop.2024.120168.
- [100]. Sohn YS, Min CK, Kovalenko I, Roh J. NAF-1 and mitoNEET are central to human breast cancer cell proliferation and survival. *Proc Natl Acad Sci U S A.* 2013;110(36):14679–14684. doi:10.1073/pnas.1310768110.
- [101]. Wehbe N, Mesmar JE, El Kurdi R, Al-Sawalmih A, Badran A, Patra D, Baydoun E. Halodule uninervis extract facilitates the green synthesis of gold nanoparticles with anticancer activity. *Sci Rep.* 2025;15(1):4286. doi:10.1038/s41598-025-18644-7.
- [102]. Sadeghi-Aliabadi H, Kiaei S, Jafari MR, Aramesh MG, Ghavami S. Chemopreventive activity of *Ferulago angulata* against breast cancer through induction of DNA damage and cell cycle arrest. *PLoS One.* 2015;10(2): e0117478. doi: 10.1371/journal.pone.0117478.

- [103]. Krętowski R, Kusaczuk M, Naumowicz M, Kotyńska J, Szynaka B, Cechowska-Pasko M. The effects of silica nanoparticles on apoptosis and autophagy of glioblastoma cell lines. *Nanomaterials*. 2017;7(8):230. doi:10.3390/nano7080230.
- [104]. Fan HF, Fang XY, Wu HL, et al. Effects of *Stephania hainanensis* alkaloids on MSU-induced acute gouty arthritis in mice. *BMC Complement Med Ther*. 2021; 21:202. doi:10.1186/s12906-021-03392-5.
- [105]. Wehbe N, Mesmar JE, El Kurdi R, Al-Sawalmih A, Badran A, Patra D, Baydoun E. Halodule uninervis extract facilitates the green synthesis of gold nanoparticles with anticancer activity. *Sci Rep*. 2025;15(1):4286. doi:10.1038/s41598-025-10822-z.
- [106]. Vázquez-Morón C, Serrano-Marugán F, Orzáez M, Suay-García B, López-Martínez J. Plant-based extracts as reducing, capping, and stabilizing agents for the green synthesis of inorganic nanoparticles. *Resources*. 2024; 13:70. doi:10.3390/resources13050070.
- [107]. Figat AM, Bartosewicz B, Liszewska M, Budner B, Norek M, Jankiewicz BJ. α -Amino acids as reducing and capping agents in gold nanoparticles synthesis using the Turkevich method. *Langmuir*. 2023;39(25):8646-8657. doi: 10.1021/acs.langmuir.3c00645.
- [108]. Gorane A, Naik A, Nikam T, Tripathi T, Ade A. GC-MS analysis of phytochemicals of *Carica papaya* variety Red Lady. *J Pharmacogn Phytochem*. 2018;7(2):554–560.

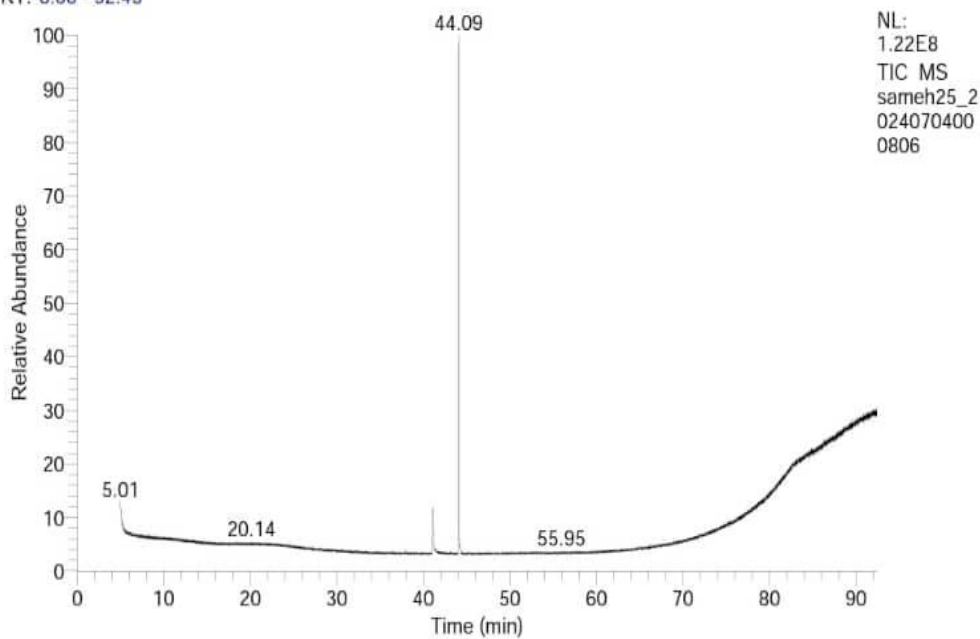
Appendices

Library Search Report

Sample Header

Sample ID:	sameh25	Original Data Path:	D:\work\DR.SYED\27-6-2024
Sample Volume(µl):	0.00	Original Processing Method:	D:\work\DR.SYED\DR.SYED PROC
Instrument Software Version:	4.0.0.29	Instrument Name:	ISQ Series
Acquisition Date:	07/04/24 12:19:11 AM	Injection Volume(µl):	1.00
Instrument Method:	D:\work\DR.SYED\Dr sayed 45.meth	Instrument Model:	ISQ 7000
Sample Name:		Run Time(min):	87.43

RT: 0.00 - 92.43

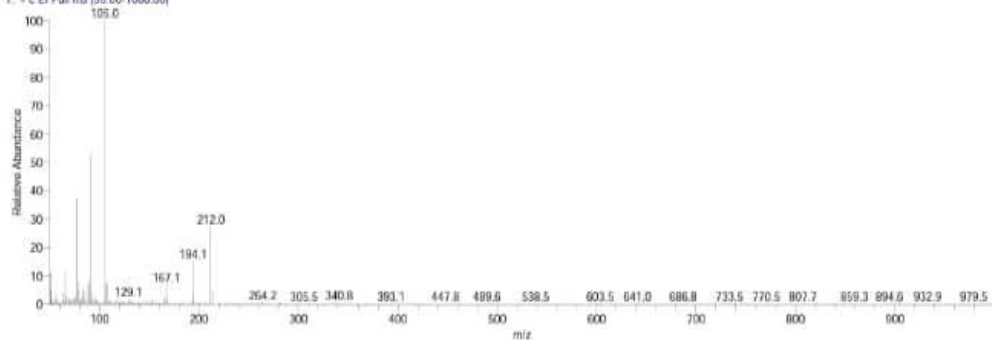


There is no signature data to report.

There is no signature data to report.

Library Search Report

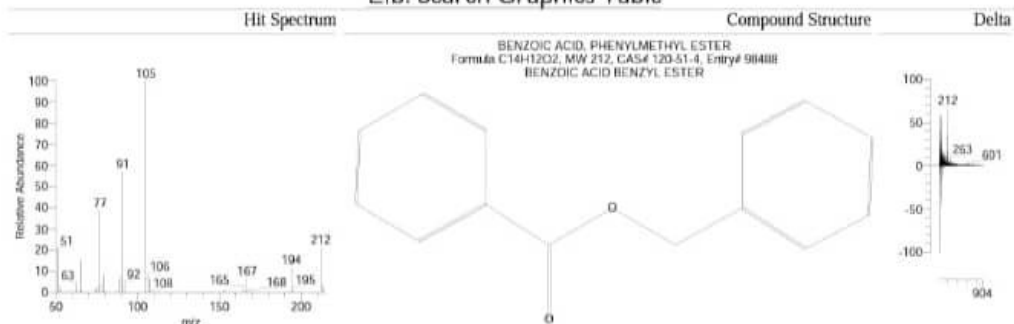
sample25_20240704000800 #10606 RT: 41.07 AV: 1 NL: 3.01EG
T: - c EI Full ms [50.00-1000.00]



Library Search Results Table

RT	Compound Name	Molecular Formula	Molecular Weight	Cas #	Probability	Area	Area %	Library	S	MF
41.07	BENZOIC ACID, PHENYLMETHYL ESTER	C14H12O2	212	120-51-4	84.18	513	10.34	WileyR	7	899
					562		egistry	5		
					39.15		8e	5		
41.07	BENZOIC ACID, PHENYLMETHYL ESTER	C14H12O2	212	120-51-4	84.18	513	10.34	WileyR	7	903
					562		egistry	5		
					39.15		8e	8		
41.07	BENZOIC ACID, PHENYLMETHYL ESTER	C14H12O2	212	120-51-4	84.18	513	10.34	WileyR	7	927
					562		egistry	7		
					39.15		8e	0		
41.07	Benzyl Benzoate	C14H12O2	212	120-51-4	84.18	513	10.34	replib	7	899
					562			5		
					39.15			5		
41.07	Benzyl Benzoate	C14H12O2	212	120-51-4	84.18	513	10.34	mainlib	7	931
					562			6		
					39.15			8		

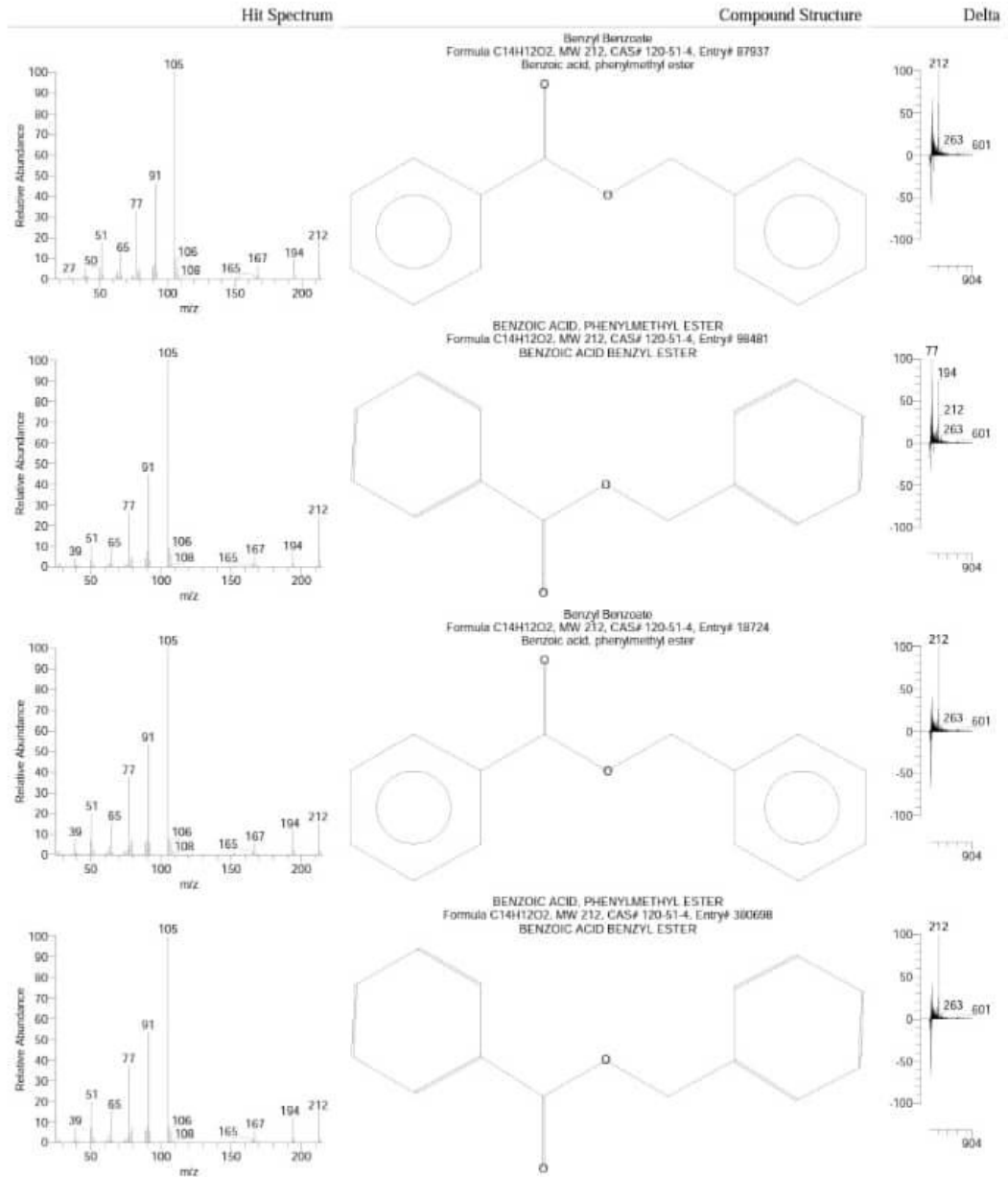
Lib. Search Graphics Table



There is no signature data to report.

There is no signature data to report.

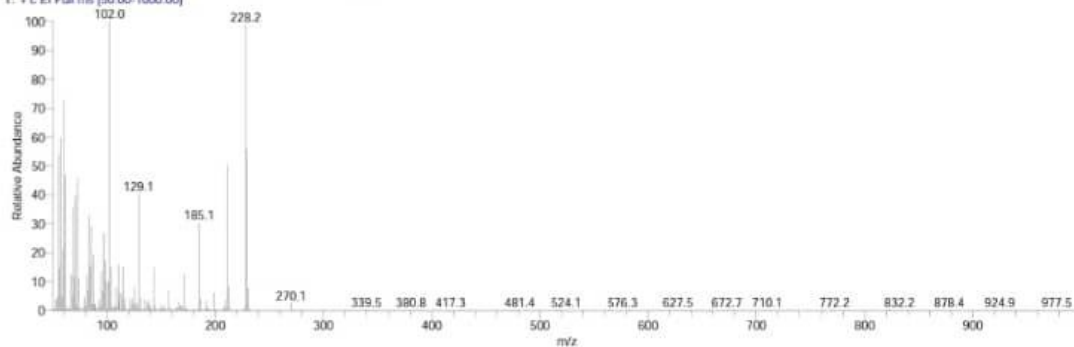
Library Search Report



There is no signature data to report.

Library Search Report

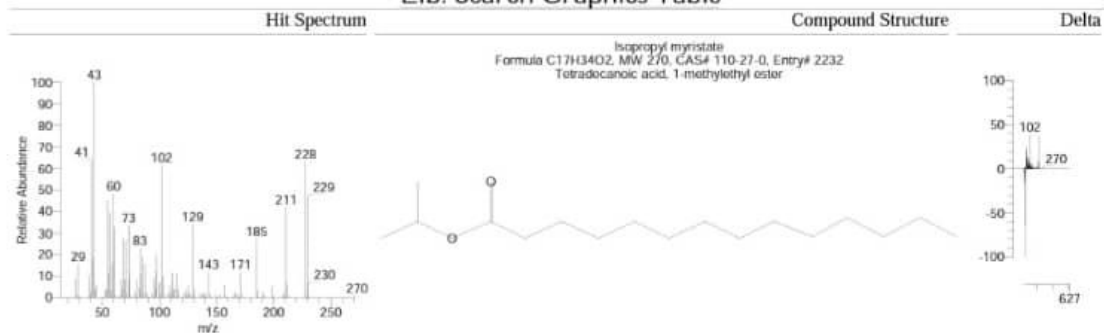
sample25_20240704000806 #11493 RT: 44.09 AV: 1 NL: 940E6
T: + c EI Full ms [50.00-1000.00]



Library Search Results Table

RT	Compound Name	Molecular Formula	Molecular Weight	Cas #	Probability	Area	Area %	Library	S	MF
44.09	ISOPROPYL TETRADECANOATE	C17H34O2	270	110-27-0	72.49	445	89.66	WileyRegistry	9	939
								3		
								2		
44.09	ISOPROPYL TETRADECANOATE	C17H34O2	270	110-27-0	72.49	445	89.66	WileyRegistry	9	916
								1		
								3		
44.09	Isopropyl myristate	C17H34O2	270	110-27-0	72.49	445	89.66	mainlib	9	920
								1		
								4		
								4		
44.09	Isopropyl myristate	C17H34O2	270	110-27-0	72.49	445	89.66	replib	9	930
								2		
								5		
								3		
								2		

Lib. Search Graphics Table



There is no signature data to report.

Library Search Report

Hit Spectrum	Compound Structure	Delta
<p>Relative Abundance vs m/z</p>	<p style="text-align: center;">ISOPROPYL TETRADECANOATE Formula C₁₇H₃₄O₂, MW 270, CAS# 110-27-0, Entry# 161318 1-METHYLETHYL TETRADECANOATE</p> <chem>CCCCCCCCCCCCCCCC(=O)OC(C)C</chem>	<p>Relative Abundance vs Delta</p>
<p>Relative Abundance vs m/z</p>	<p style="text-align: center;">Isopropyl myristate Formula C₁₇H₃₄O₂, MW 270, CAS# 110-27-0, Entry# 3581 Tetradecanoic acid, 1-methylethyl ester</p> <chem>CCCCCCCCCCCCCCCC(=O)OC(C)C</chem>	<p>Relative Abundance vs Delta</p>
<p>Relative Abundance vs m/z</p>	<p style="text-align: center;">Isopropyl myristate Formula C₁₇H₃₄O₂, MW 270, CAS# 110-27-0, Entry# 11644 Tetradecanoic acid, 1-methylethyl ester</p> <chem>CCCCCCCCCCCCCCCC(=O)OC(C)C</chem>	<p>Relative Abundance vs Delta</p>
<p>Relative Abundance vs m/z</p>	<p style="text-align: center;">ISOPROPYL TETRADECANOATE Formula C₁₇H₃₄O₂, MW 270, CAS# 110-27-0, Entry# 161317 1-METHYLETHYL TETRADECANOATE</p> <chem>CCCCCCCCCCCCCCCC(=O)OC(C)C</chem>	<p>Relative Abundance vs Delta</p>

There is no signature data to report.

الملخص

تبحث هذه الدراسة في التوليف الأخضر لجسيمات الذهب النانوية (AuNPs) باستخدام مستخلص أوراق البابايا من نوع كاريجا وتقييم إمكاناتها المضادة للسرطان ضد خلايا سرطان الثدي MCF-7. تم تحديد خصائص جسيمات الذهب النانوية باستخدام مطيافية الأشعة فوق البنفسجية المرئية، حيود الأشعة السينية (XRD)، المجهر الإلكتروني النافذ (TEM)، المجهر الذري للقوة (AFM)، التشتت الضوئي الديناميكي (DLS)، تحليل جهد زيتا، المجهر الإلكتروني الماسح (SEM)، ومطيافية الأشعة تحت الحمراء بتحويل فورييه (FTIR)، وتحليل مستخلص أوراق كاريجا البابايا باستخدام الكروماتوغرافيا-مطيافية الكتلة (GC-MS). أظهرت جسيمات الذهب النانوية المصنعة ذروة رنين بلازمون سطحي مميزة عند 558.6 نانومتر، مع مورفولوجيا كروية في الغالب وأحجام تتراوح من 20.3 إلى 61.0 نانومتر. أكد تحليل FTIR وجود المواد الكيميائية النباتية من مستخلص أوراق البابايا كعوامل تغطية، كما كشف تحليل كروماتوغرافيا الغاز-مطياف الكتلة لمستخلص أوراق البابايا عن ملف كيميائي نباتي معقد مع رباعي ديكانوات الأيزوبروبيل كمكون رئيسي يلعب هذا المركب دورا رئيسيا في عملية التوليف الأخضر لجسيمات الذهب النانوية. أظهرت جزيئات الذهب النانوية سمية خلوية قوية ضد خلايا MCF-7 بقيمة IC_{50} تبلغ 22.09 ± 0.33 ميكروجرام/مل. وكشف تحليل قياس التدفق الخلوي أن جزيئات الذهب النانوية تسببت في توقف دورة الخلية في الطور G1/S وزادت بشكل كبير من موت الخلايا المبرمج. وأشارت دراسات الالتحام الجزيئي إلى تفاعلات قوية بين جزيئات الذهب النانوية ومجمع بيتا HER2-HER3-NRG1. بالإضافة إلى ذلك، أظهرت جزيئات الذهب النانوية نشاطاً مضاداً للأكسدة ملحوظاً في اختبار إزالة الجذور الحرة DPPH. تسلط هذه النتائج الضوء على إمكانات جزيئات الذهب النانوية المصنعة بالطريقة الخضراء باستخدام مستخلص أوراق البابايا كعامل نانوي علاجي واعد لعلاج سرطان الثدي، مما يستدعي إجراء مزيد من التحقيق في آلياتها الجزيئية وفعاليتها في الجسم الحي.